ADDIS ABABA UNIVERSITY

FACULTY OF TECHNOLOGY

SCHOOL OF GRADUATE STUDIES

DEPARTMENT OF MECHANICAL ENGINEERING

STRESS ANALYSIS OF A COMPOSITE MATERIAL SHELL HAVING A CRACK

ATHESIS SUBMITTED TO A SCHOOL OF GRADUATE STUDIES OF ADDIS ABABA UNIVERSITY IN PARTIAL FULFILLMENT FOR DEGREE OF MASTERS OF SCIENCE IN MECHANICAL DESIGN (MECHANICAL ENGINEERING)

BY

JIREGNA HIRKO

ADVISOR

ALEM BAZEZEW (Dr.)

DECEMBER, 2008

Addis Ababa University Faculty of Technology

Mechanical Engineering Department

Stress Analysis of a Composite Shell with Crack

By

Jiregna Hirko

Approved by Board of Examiners:

Mr. Hamsasew Moges ________________________

Chairman Department of Graduate Committee

Dr. Alem Bazezew ________________________

Advisor

Dr. Ing Tamirat Tesfaye ________________________

Internal Examiner

Acknowledgement

In the first place, I would like to take this opportunity to express my sincere gratitude to Dr. Alem Bazezew, my supervisor, for having patience to help me to work on this research and for his constant guidance and encouragement throughout the course of project. He is also greatly acknowledged for delivering his suggestion in streaming the project in the intended direction.

Thanks to my friend, Kenate Nemera, whose affection I never forget in life. He was by my side to provide me with necessary journals and reference materials.

Alemayehu Gonfa, Olkaba Woyessa and Abdulkadir Aman are also greatly acknowledged for their intimacy and cooperation in the whole period of the work.

My love also goes to my wife Amelework and my son Sifan at the moral expense of which I am here to accomplish this study.

Finally, I would like to express my deepest appreciation to the staffs of departments of Mechanical Engineering of BDU and AAU for facilitating my study and arranging everything for me to accomplish this achievement.

Table of Content

List of Figures

Abstract

Composite materials are artificially made materials used in various mechanical applications like shells and plates. A composite material cylindrical shell is one of the components used in weight sensitive areas like aeronautics and marine environments. In these applications, the weight of the components is much more related to cost and the mechanical properties of the structural material are of great importance to hinder the damage that could result as a result of failure. On the other hand, strength and stiffness are very important parameters to prevent the associated serious failures. So, in order to prevent failure and save weight composite materials were evolved with currently emerging technology. Composite materials are nowadays commonly used in the aviation industry and marine applications in the form of vessels or shells.

In this work, what is targeted at is the carrying out the stress variation analysis of composite material cylindrical shell. The analysis was performed by studying the properties of composites, their areas of application, anisotropic elasticity relations, fracture mechanics approach for composites, and finally finite element method application is applied to investigate the stress distribution at the crack tip in the composite material shell.

Mathematical modeling and finite element simulation of the cracked shell was performed and the problem was at the end solved using ANSYS finite element analysis package. Consequently, results were obtained in the post processing stage of ANSYS. The main results obtained were the mode of stress and strain variation, the profile of the cracked surface, and the localized critical stress and strain regions at the crack front which could be cold shielded damaged zone. Ultimately, the stress and strain variation, the crack propagation schemes were compared to isotropic material shell to draw conclusion on the advantages of composites compared to conventional materials with regard to crack advancement.

Key words: Composite materials, anisotropic stress-strain relationship, laminate, finite element model, crack simulation, classical shell theory.

DECLARATION

I hereby declare that the work which is being presented in this thesis entitled" Stress Analysis of a Composite Shell with Crack" is original work of my own, has not been presented for a degree of any other university and all resources of materials used for this thesis have been duly acknowledged.

________________________ _________________________

Jiregna Hirko Date

(Candidate)

This is to certify that the above declaration made by the candidate is correct to the best of my knowledge.

___________________________________ ____________________

Dr. Alem Bazezew Date

(Thesis Supervisor)

CHAPTER ONE
THE PROBLEM STATEMENT

1.1 Introduction

Fracture is one of the main causes of catastrophic failure in structural materials, like shells and plates, which are the basic element of all natural and man-made structures. Figuratively speaking, material materializes the structural concepts [3].

In many practical applications, using composites is more efficient. For example, in highly competitive airline markets, one is continuously looking for ways to lower the overall mass of the aircraft without decreasing the stiffness and strength of its components. This is possible by replacing conventional metal alloys with composite materials. Even if the composite material costs may be higher, the reduction in the number of parts in an assembly and the savings in the fuel costs make them more profitable [1]. Depending on whether the structural design is strength-critical or stiffness-critical, the material used should therefore have a high strength-to-weight ratio (or specific weight) or a high stiffness-to-weight ratio or specific stiffness [30].

A shell is an initially curved plate defined by a middle surface, about which a constant or variable thickness is symmetrically situated. Atypical ratio of a shell thickness to its radius is of the order 1:20 [2]. Shells are generally subjected to in-plane loading and to the forces and couples normal to the surfaces, which are called here lateral loading [2]. This nature of loading implies that the common mode of failure of shell structures is either in buckling or fracture (burst) of its walls. However, surface irregularities and micro cracks can be imparted to materials for various reasons. This could be while a joint is made, during manufacturing, assembly, etc. Hence, it is very important to analyze how the stress varies in the vicinity of crack in composite structures.

The classical design criterion considers strength and stiffness parameters of a material to be with in allowable limits for the safety of the design. In case of discontinuities, however, a sufficient safety margin and stress concentration factor is considered to prevent the ultimate failure of a component. Modern engineering design includes fracture toughness of materials to strength and stiffness considerations. The interaction of material properties such as fracture toughness, with a design stress and crack size controls the conditions for the growth of fracture in a component.

Composite shell structures are commonly used in several engineering applications such as, nuclear power plants, power stations, aerospace industries, pressure vessels, artillery equipment, pharmaceutical industries, boilers, ships and other areas in which special properties of improved strength, stiffness, fatigue, impact resistance properties, thermal conductivity, corrosion resistance, etc. are of primary demand. However, due to the nature of the areas of their applications, the structures need to be carefully designed using modern techniques like fracture mechanics approach for the reliability of the design. [16] Shells are commonly subjected to either high internal pressure or surface traction and mainly fail due to fracture or buckling. Thus, the fracture-stress interface in a shell structures should be thoroughly analyzed to prevent catastrophic failure of the high cost components aforementioned.

In composites shell structures like shells, the mechanics of fracture is not as simple. First, cracks can grow in the form of fiber breaks, matrix breaks, debonding between fibers and matrix, and debonding between layers. Second, there are no single critical stress intensity factors and strain energy release rates to determine the fracture mechanics process [1]. Consequently, fracture mechanics in composites is still open field as there are several mechanisms of failure and developing a uniform criterion for the materials is quite impossible.

1.2 Justification of the Problem

A shell is, in essence, a structure that can be derived from a plate by initially forming the middle surface as a singly (or doubly) curved surface. The way in which the shell supports external loads is quite different from that of a flat plate. The stress resultants acting on the middle surface of the shell have both tangential and normal components which carry a major part of the load, a fact that explains the economy of shells as load-carrying structures and their well-deserved popularity [31]. The derivation of detailed governing equations for a curved shell problem presents many difficulties and, in fact, leads to many alternative formulations, each depending on the approximations introduced.

In the finite element treatment of shell problems, difficulties referred to above are eliminated, at the expense of introducing a further approximation. This approximation is of a physical, rather than mathematical, nature. In this, it is assumed that the behaviour of a continuously curved surface can be adequately represented by the behaviour of a surface built up of small flat elements. Intuitively, as the size of the subdivision decreases it would seem that convergence must occur and indeed experience indicates such a convergence [31].

Moreover, the nonlinearity imparted by material properties and geometric variations are also the contributing factors for the structural analysis of composite shells. The limitation in the analytical relation development for composite materials in general is also another important factor that compels us to use the finite element method of stress analysis in the vicinity of a cracked composite structure. Hence, in the current work, the main problem to be handled is the analysis of the effect of crack on the stress level in a composite shell. This analysis will focus on the flaws introduced into a cylindrical shell structure to investigate how the stress varies at the crack tip or crack front. The work is conducted by using finite element simulation of the model of the composite shell.

CHAPTER TWO
LITERATURE SURVEY

2.1 Literature Review

Composite shell structures are finding applications in a variety of systems; including aircraft and submarine structures, space structures, automobiles, sport equipment, medical prosthetic devices and electronic circuit boards. They are most suitable in applications that require high strength-to-weight ratio, high stiffness-to- weight ratios.

Despite careful design, practically every structure contains stress risers due to the presence of inclusions, holes and cracks. Bolt holes and rivet holes are necessary components for structural joints. It is not surprising; therefore, the majority of the service cracks nucleate in the vicinity of a stress riser [17]. This situation of containing stress risers is significantly more complex in the case high-performance laminated composite Materials. According to Folia [17] description, the presence of a hole or a crack of in the laminate introduces significant stress contributions in the third dimension which create a very complicated three dimensional stress state in the vicinity of such discontinuities. Moreover, the complex state of stress may depend on the stacking sequence of the laminate, the fibre orientation of each lamina as well as the material properties of the fibre and the matrix. In general Folia described such damaged process to be characterized as (i) debonding along fibre-matrix interfaces, (ii) matrix cracking parallel to the fibres, (iii) matrix cracking between fibres, (iv) delamination along the interface of two adjacent laminae with different fibre orientations, and (v) fibre breakage.

Solid materials can be anisotropic and inhomogeneous. Examples of such solids are Composite materials and rock strata. Furthermore, such solid materials can contain flaws or imperfections. The theoretical capability to predict and evaluate the responses of those complicated solids under external loading is extremely important since they can be used for important structural components or they are responsible for failures. Therefore, over the last few decades, a large number of researchers have devoted their time and effort to enhance our theoretical capability for the prediction and evaluation. A brief account of the relevant publication in open literature is given in the ensuring it [6].

For instance, [6] had carried out the analysis of elliptical cracks perpendicular to the interface of two joined transversely isotropic solids using boundary element method (BEM). Shang Xin-chnn [7] has done on an analytical solution of free vibration of composite shell structure-hermetic capsule. In his analysis, he used the basic equations on axisymmetric vibration based on the Love classical thin shell theory and derived for shells of revolution with arbitrary meridian shape. He forwarded his exact solutions for validating approximate methods of analysis in composite structures.

Mahdi *et al.* [8] examined the effects of the material and structural geometry on the crushing behavior, energy absorption, failure mechanism and failure mode of circular conical composite shell. In the paper, the static crushing behavior of circular conical composite shell under uniform axial compressive load has been investigated experimentally using a cone with vertex angles 0, 6, 12 and 18 degrees. And the vertical length and bottom outer diameter were kept for all the cases as 100 and 110 mm, respectively. Failure modes were examined using several photographs taken during the crushing stages for each specimen. Results obtained from the investigation showed that the initial failure was dominated by the interfacial and shear failure, while the delamination and eventually fibre fracture were dominated the failure mechanism after the initial failure. It had also been found, from the analysis, that the static crushing behaviour of the circular conical shell is very sensitive to the change in the vertex angle and the energy absorption capacity of circular conical and cylindrical shell to be greatly affected by the type of reinforcement.

Orthotropic materials such as composites are widely used in different branches of engineering and structural systems like those in aerospace and automobile industries, power plants, etc. Since the ratio of strength to weight and stiffness of such materials in many cases is higher than other conventional engineering materials, applications of these orthotropic materials have been widely expanded according to Mohammadi [10]. The major type of defect that is most likely to take place in these structures is cracking. Cracks can be initiated under different circumstances, such as initial weakness in material strength, fatigue, yielding and imperfection in production procedure. As a result, properties related to fracture mechanics of these types of material are highly prominent; reviving greatly the research efforts in this area. The elastic stress and displacement distribution around cracks in anisotropic media has important applications in the fracture behaviour of composite materials [9]. Hence, we need to investigate develop solutions to some basic plane problems of anisotropic materials containing cracks.

As discussed in concept of fracture mechanics, a crack can be regarded as the limiting case of an elliptical cavity as one axis is reduced to zero [16]. Thus, in some cases the solution to the crack problem can be determined from a corresponding elliptical cavity problem. There exists, however, more direct methods for solving crack problems in anisotropic materials.

The stress analysis of anisotropic laminated structures received due attention over the past decades. Ruddock and Spencer (1997) proposed a new numerical method, which determines numerical solutions of the 3D elasticity equations without recourse to any thin shell or plate approximations, for determination of the stress and deformation in laminated and inhomogeneous, anisotropic, elastic plates and shells.

One of the theoretical and practical problems of solid mechanics whose solution gave rise to a large research area in the 20th century is the theory of inhomogeneous structural systems such as laminated plates and shells that had origin in air craft industry [11].

Pinskunov and Rasskazov [11] also stated the challenging nature of the stress-strain analysis of the structures and indicated the evolution of some theoretical models for certain classes of laminated shells and plates.

In the paper of evolution of theory of laminated plates and shells, Pinskunov and Rasskazov [11], stated was the important feature of laminated plates and shells to be the strong effect of transverse shear stress on the deformation of the structures. Consequently, the classical theory based on the Kirhhoff-Love hypothesis limitation for full application was disclosed. The mentioned limitation of the classical theory in modelling the stress-strain state of laminated systems resulted in two basic approaches were developed: application of the three-dimensional theory of elasticity and the equations derived by reducing three-dimensional elastic to two-dimensional one, Pinskunov and Rasskazov [11].

Moreover, Pinskunov and Rasskazov [11] also stated the development of different approaches such as direct structural theories of laminated plates and shells, continuous structural theories of laminated plates and shells, development of generalized nonclassical models of the theory of laminated plates and shells. Ultimately, the authors indicated the arise of the need to combine the theory of laminated plates and shells with the most efficient and universal modern numerical methods of solid mechanics (stress-strain analysis) called finite-element method (FEM). The capability of FEM to describe the lamination of the structures across the thickness and its piecewise-heterogeneity over the surface (in plan) was considered as the fundamental advantage; and further verification of the different theories developed against experimental results was also reflected in the general trend analysis stress-strain relations in the laminated structures.

Zenkour [12] studied on the stress analysis of axisymmetric shear deformable cross-ply laminated circular cylindrical shells by using the Maupertuis-Lagrange (M-L) mixed variational formula and formulated the governing equations of circular cylindrical shells laminated by orthotropic layers. Using the variational approach, he presented analytical solutions for symmetric and antisymmetric laminated circular cylindrical shells under sinusoidal loads and subjected arbitrary boundary conditions. In the analysis, the results of both numerical and analytical solution were presented and the disparity that sufficiently agrees with each other was obtained for different boundary conditions.

Numerical modelling of non-linear deformation and buckling of composite plate-shell structures under pulsed loading was studied by Abrosimov [13]. The kinematic model of deformation of the structural element was based on Timoshenko-type hypotheses, which is oriented to the calculation of nonstationary deformation processes in composite structures under small deformations but large displacements and rotational angles. The equations of motion of a composite shell structure were derived based on the principle of virtual displacements with some additional conditions allowed for some structural elements. To solve the initial boundary-value problem formulated, an efficient numerical method was developed based on the finite-difference discretization of variational equations of motion in space variables and an explicit second order time integration scheme.

More recently studies are becoming widely undertaken by different researchers in the areas of stress analysis of composite structures (shell/plates) having cutouts and cracks. For instance, Lee *et al.* [14] had studied the strain distribution around the unstiffened and stiffened circular cutout of the isotropic stainless steel (ANSI type 304) and the GFRP laminated composite cylindrical shells subjected to axial compression experimentally and numerically-by finite element method. The experimental results obtained were compared with the numerical analysis. In the experiment, the strain was measured around the circular cutout by strain measuring system under uniform axial compression loading and the numerical of Lee *et al*. [14] was performed by the commercial finite element code ANSYS. The stress concentration factor (SCF) was defined to investigate the stress concentration around the circular cutout. The SCF of the stainless still cylindrical shell with stiffened cutout was found to be decreased by 39% in experiment and 50% in numerical analysis. On the other hand, the SCF of GFRP laminated composite cylindrical shell was observed to be decreased by 22% in experiment and 31% in numerical analysis.

From the experiment, the authors concluded that the SCF could be reduced effectively by stiffening cutout on the stainless still and GFRP laminated composite cylindrical shell. So, this comparative analysis was among those analyses performed on damaged composite structures.

Furthermore, Gerasimov *et al.* [15] studied ductile fracture nature of composite shells in axial compression based on an analysis of kinematically permissible strain rate fields and determined upper boundary of the limiting load for three different types of shells and compared the result with empirical data. Accordingly, satisfactory correspondence between theoretical and experimental data was investigated.

The stress distribution around the equilateral triangular hole in an elastic isotropic equilateral triangular hole in an elastic isotropic plate was studied, by Theocaris and Petrou [19] singular points are observed near the sharp corners. Daoust and Hoa [20] developed an analytical solution to determine the stress distribution around a triangular hole in an infinite anisotropic plate. The important feature of this solution is that, the mapping function considered will account for different rations of the base length to height of the triangle and also different degrees of straightness of the sides. This solution has considered only single layered plate with uni-directional 0˚fibers.

Rybicki and Schmueser [21] investigated the stress behaviour around a circular hole in a laminated plate using a three-dimensional finite element (used iso-parametric compatible displacement element) stress analysis. First computed results for the tangential strain distribution around a circular hole for a [0˚/±45˚/0˚]s laminate under uni-axial loading are compared with laboratory data to provide a level of confidence in the analysis. Next attention is focused on the interlaminar normal stress distribution around the free edge of the circular hole and the effect of changes in stacking sequence and lay-up angle.

Sekhar and Srinivas [18], studied on dynamic analysis of cracked hollow composite shafts by modelling them based on first order shear deformation theory using finite element method with shell elements. The influences of crack parameters, fibre orientation (stacking sequences) and material properties on the vibration characteristics of composite shafts have been studied. The characteristic difference of cracked composite rotor mode shape with that of uncracked composite rotor was observed. According to the study, when crack depth increases, the eigen frequencies were found to be decreasing at a faster rate as compared to other stacking sequences for all the materials studied. Thus stacking sequence highly sensitive to crack was investigated.

The present study aims at the stress analysis of a cracked composite shell. The composite shell will been modelled based on first order shear deformation theory using finite element method with shell elements. Materials such as, carbon–epoxy have be tried for various stacking sequences. The influences of crack parameters, fibre orientation (stacking sequences) and material properties on the stress characteristics of composite shells will be studied.

2.2 Motivation

The survey of literature highlighted that most of the analytical solutions are for infinite length plate and for each shape of hole a new solution has to be derived all together. It is very difficult to find analytical solutions for complicated shapes. So the only alternative in such cases as we conclude form the review is finite element method which can give good results for a variety of cracks, holes and ranges of loadings. Even the application of the concept of fracture mechanics approach to anisotropic material structures is very limited.

Many of the works done by the various researchers in the past to recent reveals that there are some Finite Element and few analytical solutions available for shells with holes. Most of these solutions deals with regular shapes of holes, for example, circular, elliptical, triangle etc. In the modern era of space technology, however, the need for composite materials is increasing rapidly, and for the practical purposes various shapes of holes are made in it, which makes designers to find out the stresses around holes for the safe design of the space vehicles or any structure. However, the production of these different features (cut-outs), manufacturing processes or assembly can further induce flaws or cracks in the structures. Hence, the researcher is motivated to conduct the analysis of such material structures by considering modern design concept-fracture mechanics to analyze the mode of variation of stress in a cracked shell structure. Thus, the concept fracture mechanics could be integrated in the early such product development stage.

3.3 Scope of the Work

The aim of the present work is to demonstrate the mode of stress variation in the vicinity of a crack tip of a composite cylindrical shell structure or laminate by using finite element method. The laminate is subjected to inplane loading or biaxial stresses or loadings at any arbitrary orientation. Solutions are to be found for different crack orientations with respect to the axis of the cylinder/shell.

The scope of the work is limited to the mathematical modelling of the cracked cylindrical composite shell structure under in-plane loading and simulating it in ANSYS environment to investigate the stress state variation at the crack tip.

CHAPTER THREE

BACKGROUND OF THE STUDY

3.1 COMPOSITE MATERIALS AND THEIR APPLICATIONS

3.1.1. Introduction to Composite Materials

The word "composite" in composite material signifies that two or more materials are combined on a macroscopic scale to form a useful material. The key is the macroscopic examination of a material. Different materials can be combined on a microscopic scale, such as in alloying, but the resulting material is macroscopically homogeneous [4].

A composite is a structural material which consists of combining two or more constituents. The constituents are combined at a microscopic level and are not soluble in each other. One constituent is called the reinforcing phase and the one in which it is embedded is called matrix. The function of the matrix is to support and protect the fibres and to provide a means of distributing load among and transmitting load between the fibres.

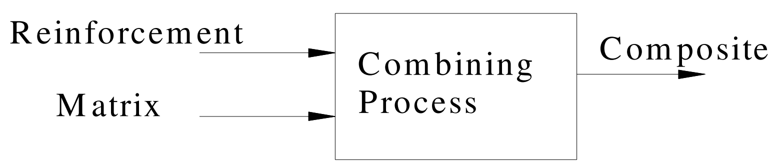

Figure 3.1.1 Composite material production principles

The reinforcing phase material may be in the form of fibers, particle or flakes; the matrix phase materials are generally continuous. Composite materials can be natural or artificial. Example of naturally found composites includes wood where the lognon matrix is reinforced with cellulose fibers. The man made composite category includes the family of polymer composites and others (epoxy, graphite etc…).

Advanced composites are composite materials which are traditionally used in the aerospace industries. These composites have high performance reinforcements of a thin diameter in matrix material such as epoxy and aluminium. The advantage of composites is that they usually exhibit the best qualities of their constituents and often some qualities that neither constituent possesses. The properties that can be improved by forming a composite material include: fatigue life, temperature-dependent behaviour, thermal insulation, thermal conductivity, acoustical insulation, strength, stiffness, corrosion resistance, wear resistance, attractiveness and weight.

The engineering of modern composite materials has had a significant impact on design and construction. By combining two or more materials together, it is now possible to tailor-make advanced composite materials man has ever used. The history of man-made composite materials can be dated back to ancient Egyptians, Chinese, and Israelites. It is interesting to note that they all made bricks by mixing straw and clay. In Ethiopia also, there are different types of construction materials traditionally made in the form of composites. It was recognized that by gluing thin veneers together, the strength of wood was enhanced and the possibility of swelling and shrinkage minimized.

The principle of composite materials can be found in numerous naturally occurring substances. For instance, wood, cellulose, and bone are among the naturally existing composites. Where as the best example of man-made composite materials is concrete.

Since 1970s, application of composites has widely increased due to the development of new fibers such as carbon, boron, and aramids, and new composite systems with matrices made of metals and ceramics [1].

According to Kaw [1], a composite is a structural material which consists of two or more constituents. The constituents are combined at a microscopic level and are not soluble in each other. One constituent is called the reinforcing phase (fibre) and the one in which it is embedded is called the matrix. Most composites are made up of just two materials. One material (the matrix or binder) surrounds and binds together a cluster of fibers or fragments of a much stronger material (the reinforcement). For instance, in the case of mud bricks, the two roles are taken by the mud and the straw; in concrete, by the cement and the aggregate; in a piece of wood, by the cellulose and the lignin. In fiber glass, the reinforcement is provided by fine threads or fibers of glass, often woven into a sort of cloth, and the matrix is a plastic.

Over recent decades many new composites have been developed, some with very valuable properties. By carefully choosing the reinforcement, the matrix, and the manufacturing process that brings them together, engineers can tailor the properties to meet specific requirements. They can, for example, make the composite sheet very strong in one direction by aligning the fibres that way, but weaker in another direction where strength is not so important. They can also select properties such as resistance to heat, chemicals, and weathering by choosing an appropriate matrix material.

Choosing materials for the matrix

For the matrix, many modern composites use thermosetting or Thermosoftening plastics (also called resins). The plastics are polymers that hold the reinforcement together and help to determine the physical properties of the end product.

Thermosetting plastics are liquid when prepared but harden and become rigid (i.e., they cure) when they are heated. The setting process is irreversible, so that these materials do not become soft under high temperatures. These plastics also resist wear and attack by chemicals making them very durable, even when exposed to extreme environments.

Thermosoftening plastics, as the name implies, are hard at low temperatures but soften when they are heated. Although they are less commonly used than thermosetting plastics they do have some advantages, such as greater fracture toughness, long shelf life of the raw material, capacity for recycling and a cleaner, safer workplace because organic solvents are not needed for the hardening process.
Ceramics, carbon and metals are used as the matrix for some highly specialized purposes. For example, ceramics are used when the material is going to be exposed to high temperatures (eg, heat exchangers) and carbon is used for products that are exposed to friction and wear (eg, bearings and gears).

Choosing materials for the reinforcement

Although glass fibers are by far the most common reinforcement, many advanced composites now use fine fibers of pure carbon. Carbon fibers are much stronger than glass fibers, but are also more expensive to produce. Carbon fiber composites are light as well as strong. They are used in aircraft structures and in sporting goods (such as golf clubs), and increasingly are used instead of metals to repair or replace damaged bones. Polymers are not only used for the matrix, they also make a good reinforcement material in composites. For example, Kevlar is a polymer fiber that is immensely strong and adds toughness to a composite. It is used as the reinforcement in composite products that require lightweight and reliable construction (eg, structural body parts of an aircraft).

The reinforcement fibers are immersed in a matrix to form a single layer known as lamina. A lamina is a flat arrangement of unidirectional fibers or woven fibers in a matrix. It is the basic building block in fiber-reinforced composite laminates. A lamina or ply is a plane or curved layer of unidirectional fibers or woven fabric in a matrix. It is unidirectional lamina or ply, which is an orthotropic material in its principal directions. A laminate is made up of two or more unidirectional lamina or plies stacked together at various orientations.

Laminated composites consist of layers of at least two different materials that are bonded together. The properties that can be emphasized by lamination are strength, stiffness, low weight, corrosion resistance, wear resistance, beauty or attractiveness, thermal insulation, acoustical insulation. In a composite structural design, laminates are used. As stated here, the laminates could of special arrangement to simplify the mathematical analysis of the structure. The mathematical analysis of a laminate is different from that of the isotropic materials. Moreover, the manufacturing process and failure prediction techniques also involve some mathematical complexity as presented in the body of this report.

3.1.2. Classification of composites

Composites are classified by the geometry of the reinforcement, as in figures 3.1.2, 3.1.3 and 3.1.4, particulate, flake and fibres, or by the type of matrix; polymer, metal, ceramics and carbon. Particulate composites consist of particles immersed in materials such as alloys and ceramics. They are usually isotopic since the particles are added randomly.

Particulate composites have the advantages such as improved strength, increased operating temperature and oxidation resistance etc. Typical examples include use of aluminium particles in rubber, silicon carbide particles in aluminium, and gravel, sand and cement to make concrete.

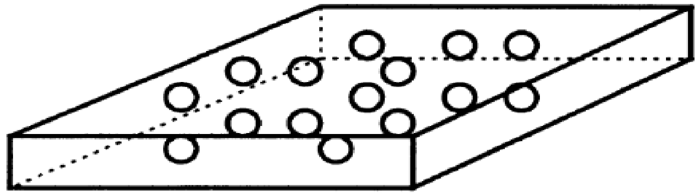

Figure 3.1.2 Particulate composite

Flake composites consist of flat reinforcements of materials. Typical flake materials are glass, mica, aluminium and silver. Flake composite provide advantages such as high out-of plane flexural modulus, higher strength, and low cost. However, flakes can not be oriented easily and only a limited number of materials are available for use.

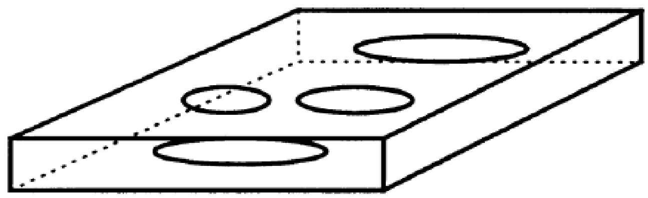

Figure 3.1.3 Flake composites

Fibre composite consist of materials reinforced by short (discontinuous) or long (continuous) fibre. Fibres are generally anisotropic and examples include carbon and aramids. The fundamental units of continuous fibre matrix composite are unidirectional or woven fibre laminas. Laminas are staked on top of each other at various angles to form a multidirectional laminate.

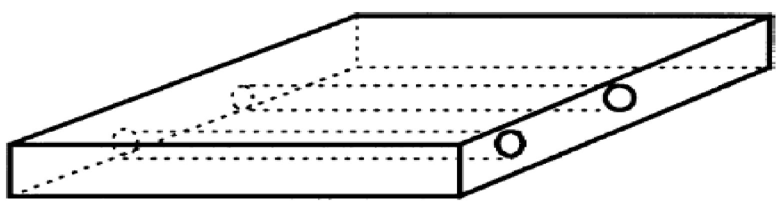

Figure 3.1.4 Fiber composites

Polymer matrix composites

The most common advanced composites are polymer matrix composites (PMC). These polymers consist of a polymer (example epoxy, polyester, urethane) reinforced by thin diameter fibres (e. g. graphite, aramids, boron, carbon). For example, graphite epoxy composites are approximately five times stronger than steel on a weighted-to-weighted basis. The reasons why they are the most common composites include their low cost, high strength, and simple manufacturing principles. The main drawbacks of

PMCs include low operating temperatures, high coefficient of thermal and moisture expansion, and law elastic properties in certain directions.

Metal matrix composites

Metal matrix composites (MMCs) as the name implies, have a metal matrix. Examples of matrices in such composites include aluminium, magnesium and titanium. Typical fibres include carbon and silicon carbide. Metals are mainly reinforced to increase or decrease their properties to suit the needs of the design. For example, the elastic stiffness and strength of metals can be increased while large coefficients of thermal expansion and thermal and electrical conductivities of metals can be reduced by the addition of fibres such as silicon carbide.

MMCs are mainly used to provide advantages over monolithic metals such as steel and aluminium. These advantages include higher specific strength and modulus by reinforcing low density metals such as aluminium and titanium; lower coefficient of thermal expansion by reinforcing with fibres with low coefficients of thermal expansion such as graphite and maintaining properties such as strength at high temperatures.

MMCs have several advantages over polymer matrix composites. These include higher elastic properties, higher service temperature, insensitivity to moisture, higher electrical and thermal conductivities, and better wear, fatigue and flaw resistances. The drawbacks of MMCs over PMCs include higher processing temperatures and higher densities.

Some of the areas of applications of MMCs include the following:

- **Space**: the space shuttle uses boron/ aluminium tubes to support its fuselage frame.
- **Military**: precision components of missile guidance systems demand dimensional stability, that is, the geometries of the components can not change during use. MMCs such as SiC/aluminium composites satisfy these requirements since they have high micro-yield strength.
- **Transportation**: MMCs are finding use now in automotive engines which are lighter than their metal counter parts. Also MMCs are the material of choice for gas turbine engines for their high strength and low weight.

Ceramic Matrix Composites (CMC)

Ceramic Matrix Composites have a ceramic matrix such as alumina, calcium, aluminium silicate reinforced by fibres such as carbon and silicon carbide.

Advantages of CMCs include high strength, hardness, high service temperature, chemical inertness, and low density. However, ceramics by themselves have low fracture toughness. Under tensile or impact loading, they fail catastrophically. Reinforced ceramics with fibres, such as silicon carbide or carbon, increases their fracture toughness because it causes gradual failure of the composite. This combination of a fibre ceramic matrix composite make more attractive for application where both high mechanical properties and extreme service temperatures are desired.

Application of CMCs

CMCs are finding increased application in high temperature areas where MMCs cannot be used. Typical applications include cutting tool inserts in oxidizing and high temperature environments.

Carbon- Carbon composites:

Carbon- carbon composites use carbon fibers in a carbon matrix. Carbon- carbon composites are used in very high temperature environments of up to 6000 ^{0}F (3315 ^{0}C), and are 20 times stronger and 30% lighter than graphite fibers. Carbon by itself is brittle and flaw sensitive like ceramics. Reinforcement of a carbon matrix allows the composite to fail gradually and also gives advantages such as ability to withstand high temperatures, low creep at high temperatures, low density, good tensile and comprehensive strengths, high fatigue resistance, high thermal conductivity, and high coefficient of friction. Drawbacks include high cost, low sheer strength, and susceptibility to oxidations at high temperatures.

Applications

The main uses of carbon-carbon composites are the following:

- Space shuttle nose cones
- Aircraft brakes
- Mechanical fasteners – fasteners needed for high temperature applications are made of carbon-carbon composites, as they lose little strength at high temperatures.

3.1.3. Mechanical Behaviour of Composite Materials

Composite materials have many characteristics that are different from conventional engineering materials. Some characteristics are merely modifications of conventional behaviour; others are totally new and require new analytical and experimental procedures. Most common engineering materials are homogen*eous* and *isotropic*.

A *homogeneous* body has, uniform properties throughout, i.e., the properties are not a function of *position* in the body. An *isotropic* body has material properties that are the same in every direction at a point in the body, i.e., the properties are not *a* function of *orientation* at a point in the body. In contrast, composite materials are often both *inhomogeneous* and *nonisotropic* (orthotropic or, more generally, anisotropic). An *inhomogeneous* body has non-uniform properties over the body, i.e., the properties are *a* function of *position* in the body [1].

An *orthotropic* body has material, properties that are different in three mutually perpendicular directions at a point in the body and, further, have three mutually perpendicular planes of material symmetry. Thus, the properties are a function of orientation at a point in the body. An *anisotropic* body has material properties that are different in all directions at a point in the body. There are no planes of material property symmetry. Again, the properties are a function of orientation at a point in the body.

Because of the inherent heterogeneous nature of composite materials, they are conveniently studied from two points of view: micromechanics and macro mechanics in the paragraphs to follow see figure 1.4. Micromechanics - is the study of composite material behaviour wherein the interaction of the constituent materials is examined on a microscopic scale. This is particularly concerned with the composition of the composites in their early fabrication process. Macromechanics - is the study of composite material behaviour where in the material is presumed homogeneous and the effects of the constituent materials are detected, only as averaged apparent properties of the composite.

Basic Assumptions

The basic assumptions made in material science approach model of fibre reinforced composites are [1]:

- The bond between fibres and matrix is perfect
- The fibres are continuous and parallelly aligned in each. They are packed regularly; i. e. the space between fibres is uniform.
- Fibre and matrix materials are linear elastic, they follow approximately Hooke's law and each elastic model is constant.
- The composite is free of voids.

3.1.4. Application of composite materials in Ethiopia

In Ethiopia, there is no science and technology of composite materials. The different manufacturing industries are using conventional materials as raw materials. Moreover, the materials science aspects of the engineering educations are also not commonly focusing on composite materials. However, the world is advancing taking the lead of nature by substituting conventional engineering materials by modern advanced composites in the way of striving for light weight, higher strength, higher stiffness, and durability. Modern aviation industrial components of the developed countries are using composite based materials as in put in manufacturing of aeronautic materials. The Ethiopian aviation and military industry are the major buy-strategy based institutions. As a result, nowadays deferent equipments and machines are imported from the developed countries; but their maintenance and reconditioning needs knowledge of composites. Therefore, the one can perceive that the technology of composites is vital for the country's industrial sector development and further enhancement.

3.1.5. Advantages and Disadvantages of Using Composites

The greatest advantage of composite materials is strength and stiffness combined with lightness. By choosing an appropriate combination of reinforcement and matrix material, it is possible to produce properties that exactly fit the requirements for a particular structure for a particular purpose [1]. The Airbus A380, has been overweight to four to five tons initially, however the weight requirement is met by the use of composites in the body and internal parts figures 3.1.5 and 3.1.6

Figure 3.1.5 Body parts of airbus A380 made of advanced composites.

Modern aviation, both military and civil, is a prime example. It would be much less efficient without composites. In fact, the demands made by that industry for materials that are both light and strong has been the main force driving the development of composites. It is common now to find wing and tail sections, propellers and rotor blades made from advanced composites, along with much of the internal structure and fittings. The airframes of some smaller aircraft are made entirely from composites, as are the wing, tail and body panels of large commercial aircraft.

In thinking about planes, it is worth remembering that composites are less likely than metals (such as aluminum) to break up completely under stress. A small crack in a piece of metal can spread very rapidly with very serious consequences (especially in the case of aircraft). However, the fibers in composites act to block the widening of any small crack and to share the stress around [1].

The right composites also stand up well to heat and corrosion. This makes them ideal for use in products that are exposed to extreme environments such as boats, chemical-handling equipment and spacecraft. Another advantage of composite materials is that they provide design flexibility. Composites can be moulded into complex shapes-a great asset when producing something like a surfboard or a boat hull.

Figure 3.1.6 Internal body parts if airbus A380 made of advanced composites.

What are the limitations of composites?

The downside of composites is usually the cost. Although manufacturing processes are often more efficient when composites are used, the raw materials are expensive. Composites will never totally replace traditional materials like steel, but in many cases they are just what we need. And no doubt new uses will be found as the technology evolves. We haven't yet seen all that composites can do.

In general, disadvantage of composites can be summarized as follows:

- high cost of fabrication
- complex mechanical characterization
- difficulty to repair
- Composites do not have a high combination of strength and fracture toughness as compared to metals.
- Composites do not necessarily give higher performance in all properties used for material selection.

Bearing in mind the aforementioned concepts of composites, it is now possible to go into detail analysis of related works and ultimately study the stress and strain variation in a composite shell with crack by specifying the problem.

3.2. OVERVIEW OF MECHANICS OF COMPOSITES

3.2.1. Anisotropic Stress-Strain Relationship

At a point in an anisotropic material, material properties are different in all directions. These types of materials which have different material properties in different directions are called anisotropic materials.

How is a composite structure analyzed mechanically?

A composite material consists of two or more materials or constituents and hence the analysis and design of such materials are different from the conventional materials such as steel. The approach followed to analyze the mechanical behaviour of a composite structure is as given in figure 3.2.1.

First, find the average properties of a composite ply from the individual properties of the constituents' properties include stiffness, strength, and thermal and moisture expansion coefficients. Note that the average properties are derived by considering the ply to be homogeneous. At this level, one can optimize for the stiffness and strength requirements of a lamina. This is called micromechanics of a lamina. This case is related to synthesis of composite materials; but our focus here is on the analysis of a laminated composite used in the building of structural material-shell.

Second, develop the stress-strain relationship for a unidirectional or bidirectional lamina. Loads may be applied along the principal directions of the symmetry of a lamina or off-axis. Also one can develop relationships for stiffness, thermal and moisture expansion coefficients and strengths of angle plies. Failure theories of a lamina are based on the stress in the lamina and strength properties of a lamina. This is called Macromechanics of a lamina [1].

A structure made of composite materials is generally a laminate structure made of various laminas stacked on top of each other. Knowing the macromechanics of a lamina, it is possible to develop the mechanics of a laminate. Stiffness, strength and thermal and moisture expansion coefficients can be found for the whole laminate. Laminate failure is based on stresses and application of failure theories to each ply. This knowledge of analysis of composites can then eventually form the basis for the mechanical design of structures made of composites.

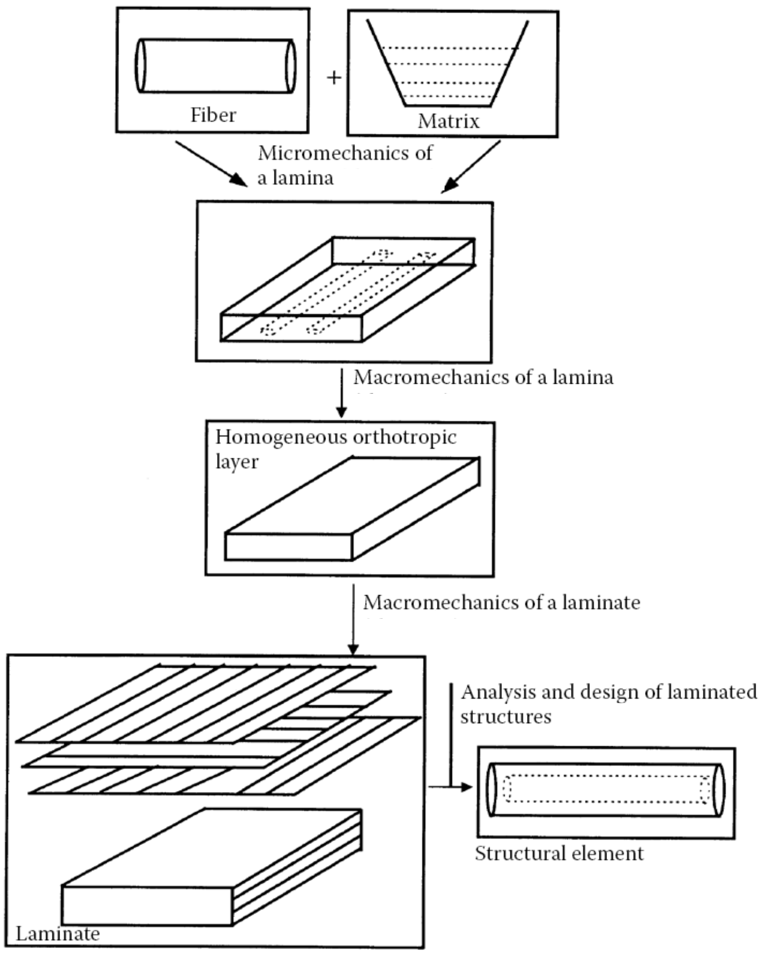

Figure 3.2.1 Schematic analysis of laminated composites [1]

Definition of stress

Stress is the intensity of force per unit area (Fig.3.2.2). It is given by

$$\sigma = \lim_{dA \to 0} \frac{P}{dA} \tag{3.1}$$

Where $\vec{P} = P_x i + P_y j + P_z k$ in its rectangular components

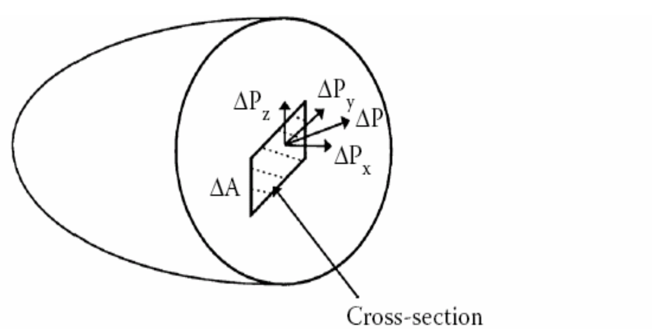

Figure 3.2.2 Forces on an infinitesimal area on the y-z plane

Definition of strain

Let $u = u$ (x,y,z) = is the displacement along the x axis at appoint (x,y,z)

v = v(x,y,z)=is the displacement along the y-axis at appoint (x,y,z)

$\omega = (x, y, z)$ = the displacement along the z –axis at appoint (x,y,z)

And the corresponding strain components of the above mentioned displacements are respectively $\varepsilon_x, \varepsilon_y, and\ \varepsilon_z$. Then we have the following relationship between the strain components and the corresponding displacements as follows:

$$\varepsilon_x = \frac{\partial u}{\partial x},\ \varepsilon_y = \frac{\partial v}{\partial y}, and\ \varepsilon_z = \frac{\partial \omega}{\partial z} \tag{3.2}$$

$$\gamma_{xy} = \frac{\partial u}{\partial y} + \frac{\partial v}{\partial x},\ \gamma_{xz} = \frac{\partial \omega}{\partial x} + \frac{\partial u}{\partial z}, and\ \gamma_{yz} = \frac{\partial \omega}{\partial y} + \frac{\partial v}{\partial z} \tag{3.3}$$

3.2.2. Stress-strain relations for different materials planes of symmetry

Material reactions under stresses can be described by a set of constitutive equations. The stress and the corresponding strain are related to each other by the relation in compliance form is [1]

$$\begin{Bmatrix} \varepsilon_{xx} \\ \varepsilon_{yy} \\ \varepsilon_{zz} \\ \gamma_{xy} \\ \gamma_{xz} \\ \gamma_{yz} \end{Bmatrix} = \begin{bmatrix} S_{11} & S_{12} & S_{13} & S_{14} & S_{15} & S_{16} \\ S_{21} & S_{22} & S_{23} & S_{24} & S_{25} & S_{26} \\ S_{31} & S_{32} & S_{33} & S_{34} & S_{35} & S_{36} \\ S_{41} & S_{42} & S_{43} & S_{44} & S_{45} & S_{46} \\ S_{51} & S_{52} & S_{53} & S_{54} & S_{55} & S_{56} \\ S_{61} & S_{62} & S_{63} & S_{64} & S_{65} & S_{66} \end{bmatrix} \begin{Bmatrix} \sigma_{xx} \\ \sigma_{yy} \\ \sigma_{zz} \\ \tau_{xy} \\ \tau_{xz} \\ \tau_{yz} \end{Bmatrix} \tag{3.4}$$

In stiffness form

$$\{\sigma_i\} = \lfloor C_{ij} \rfloor \{\varepsilon_j\} \tag{3.5}$$

The conversion is that the symbol S is used for compliance and the symbol C is used for stiffness. In most general case, the strain and stress with the subscript ij is not the same as the one with ji. The [C] and the [S] would each be a nine by nine matrix. But because of the definition of shear stress and shear strain on orthogonal planes, it will reduce to six by six non equal terms inside. This would imply that there is a need for 36 constants to describe the stress-strain behaviour of any generic material. i.e.,

$$\begin{Bmatrix} \sigma_{xx} \\ \sigma_{yy} \\ \sigma_{zz} \\ \tau_{xy} \\ \tau_{xz} \\ \tau_{yz} \end{Bmatrix} = \begin{bmatrix} C_{11} & C_{12} & C_{13} & C_{14} & C_{15} & C_{16} \\ C_{21} & C_{22} & C_{23} & C_{24} & C_{25} & C_{26} \\ C_{31} & C_{32} & C_{33} & C_{34} & C_{35} & C_{36} \\ C_{41} & C_{42} & C_{43} & C_{44} & C_{45} & S_{46} \\ C_{51} & C_{52} & C_{53} & C_{56} & C_{55} & C_{56} \\ C_{61} & C_{62} & C_{63} & C_{64} & C_{65} & C_{66} \end{bmatrix} \begin{Bmatrix} \varepsilon_{xx} \\ \varepsilon_{yy} \\ \varepsilon_{zz} \\ \gamma_{xy} \\ \gamma_{xz} \\ \gamma_{yz} \end{Bmatrix} \tag{3.6}$$

In the constitutive equation (3.6), 36 constants are needed to determine the stress-strain relation.

Invoking compatibility conditions, where no two materials may occupy the same space, the stiffness matrix [C] and the compliance matrix [S] should be symmetric. This leads to the first set of constitutive equations describing material behaviour. For anisotropic material having no plane of symmetry, a total of 21 elastic constants are needed to determine the stress-strain relation. In general form for triclinic materials we have the stress-strain relation to take the form

$$\begin{Bmatrix} \sigma_{xx} \\ \sigma_{yy} \\ \sigma_{zz} \\ \tau_{xy} \\ \tau_{xz} \\ \tau_{yz} \end{Bmatrix} = \begin{bmatrix} C_{11} & C_{12} & C_{13} & C_{14} & C_{15} & C_{16} \\ & C_{22} & C_{23} & C_{24} & C_{25} & C_{26} \\ & & C_{33} & C_{34} & C_{35} & C_{36} \\ & & & C_{44} & C_{45} & C_{46} \\ & 0 & & & C_{55} & C_{56} \\ & & & & & C_{66} \end{bmatrix} \begin{Bmatrix} \varepsilon_{xx} \\ \varepsilon_{yy} \\ \varepsilon_{zz} \\ \gamma_{xy} \\ \gamma_{xz} \\ \gamma_{yz} \end{Bmatrix} \tag{3.7}$$

In case of monotonic materials, materials which have only one plane of material symmetry, the number of independent elastic constants needed to describe the stress-strain relation will reduce to 13. The stiffness matrix entry will be

$$\begin{Bmatrix} \sigma_{xx} \\ \sigma_{yy} \\ \sigma_{zz} \\ \tau_{xy} \\ \tau_{xz} \\ \tau_{yz} \end{Bmatrix} = \begin{bmatrix} C_{11} & C_{12} & C_{13} & 0 & 0 & C_{16} \\ & C_{22} & C_{23} & 0 & 0 & C_{26} \\ & & C_{33} & 0 & 0 & C_{36} \\ & & & C_{44} & C_{45} & 0 \\ & 0 & & & C_{55} & 0 \\ & & & & & C_{66} \end{bmatrix} \begin{Bmatrix} \varepsilon_{xx} \\ \varepsilon_{yy} \\ \varepsilon_{zz} \\ \gamma_{xy} \\ \gamma_{xz} \\ \gamma_{yz} \end{Bmatrix} \tag{3.8}$$

If a material has three mutually perpendicular planes of material symmetry, then the stiffness matrix contains 9 independent elastic material constants and is given as

$$\begin{Bmatrix} \sigma_{xx} \\ \sigma_{yy} \\ \sigma_{zz} \\ \tau_{xy} \\ \tau_{xz} \\ \tau_{yz} \end{Bmatrix} = \begin{bmatrix} C_{11} & C_{12} & C_{13} & 0 & 0 & 0 \\ & C_{22} & C_{23} & 0 & 0 & 0 \\ & & C_{33} & 0 & 0 & 0 \\ & & & C_{44} & 0 & 0 \\ & 0 & & & C_{55} & 0 \\ & & & & & C_{66} \end{bmatrix} \begin{Bmatrix} \varepsilon_{xx} \\ \varepsilon_{yy} \\ \varepsilon_{zz} \\ \gamma_{xy} \\ \gamma_{xz} \\ \gamma_{yz} \end{Bmatrix} \tag{3.9}$$

Three mutually perpendicular planes of material symmetry also imply that there are three mutually perpendicular planes of elastic symmetry. Moreover, there are nine independent elastic constants. This is a common material symmetry unlike anisotropic and monoclinic materials. Examples of an orthotropic material include a single lamina of continuous fibre, composite arranged in a rectangular array as in figure 3.2.3.

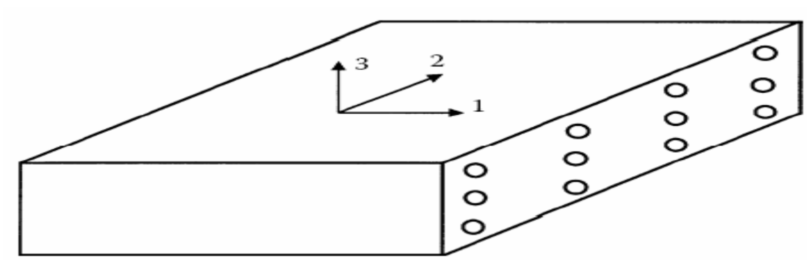

Figure 3.2.3 A unidirectional lamina as a monoclinic material

Unidirectional fibre composites can be regarded as orthotropic materials which possess three mutually orthogonal planes of symmetry. The directions perpendicular these planes are called the material principal directions.

In general, we can summarize the number of independent elastic constants for various types of materials:

- Anisotropic: 21
- Monoclinic: 13
- Orthotropic: 9
- Transversely isotropic: 5
- Isotropic: 2

3.2.3. Reduction of the Constitutive Equation

For a three-dimensional body constitutive equation in (3.4) can be equivocally expressed in 1-2-3 orthogonal Cartesian coordinate system

$$\begin{Bmatrix} \varepsilon_1 \\ \varepsilon_2 \\ \varepsilon_3 \\ \gamma_{23} \\ \gamma_{31} \\ \gamma_{12} \end{Bmatrix} = \begin{bmatrix} S_{11} & S_{12} & S_{13} & S_{14} & S_{15} & S_{16} \\ S_{21} & S_{22} & S_{23} & S_{24} & S_{25} & S_{26} \\ S_{31} & S_{32} & S_{33} & S_{34} & S_{35} & S_{36} \\ S_{41} & S_{42} & S_{43} & S_{44} & S_{45} & S_{46} \\ S_{51} & S_{52} & S_{53} & S_{54} & S_{55} & S_{56} \\ S_{61} & S_{62} & S_{63} & S_{64} & S_{65} & S_{66} \end{bmatrix} \begin{Bmatrix} \sigma_1 \\ \sigma_2 \\ \sigma_3 \\ \tau_{23} \\ \tau_{31} \\ \tau_{12} \end{Bmatrix} \tag{3.10}$$

A unidirectional lamina falls under the orthotropic material category. If the lamina is thin and does not carry any out-of-plane loads, one can assume plane stress conditions for the lamina. Therefore, taking Equation (3.10) and inverse of Equation (3.9) and assuming $\sigma_3 = 0$, $\tau_{23} = 0$, and $\tau_{31} = 0$, then

$\varepsilon_3 = S_{13}\sigma_1 + S_{23}\sigma_2$, $\gamma_{23} = \gamma_{31} = 0$.

The normal strain, ε_3, is not an independent strain because it is a function of the other two normal strains, ε_1 and ε_2. Therefore, the normal strain, ε_3, can be omitted from the stress–strain relationship (3.10) or its inverse. Also, the shearing strains, γ_{23} and γ_{31}, can be omitted because they are zero. Inverting Equation (3.9) for an orthotropic plane stress problem, it can then be written as

$$\begin{Bmatrix} \varepsilon_1 \\ \varepsilon_2 \\ \gamma_{12} \end{Bmatrix} = \begin{bmatrix} S_{11} & S_{12} & 0 \\ S_{21} & S_{22} & 0 \\ 0 & 0 & S_{66} \end{bmatrix} \begin{Bmatrix} \sigma_1 \\ \sigma_2 \\ \tau_{12} \end{Bmatrix} \tag{3.11}$$

Where, S_{ij} are the elements of the compliance matrix. Note the four independent compliance elements in the matrix.

Inverting Equation (3.11) gives the stress–strain relationship as in Lee [14] relation for moderate thin shell,

$$\begin{Bmatrix} \sigma_1 \\ \sigma_2 \\ \tau_{12} \end{Bmatrix} = \begin{bmatrix} Q_{11} & Q_{12} & 0 \\ Q_{21} & Q_{22} & 0 \\ 0 & 0 & Q_{66} \end{bmatrix} \begin{Bmatrix} \varepsilon_1 \\ \varepsilon_2 \\ \gamma_{12} \end{Bmatrix} \tag{3.12}$$

Where, Q_{ij} are the reduced stiffness coefficients. Which are related to the compliance coefficients as

$$Q_{11} = \frac{S_{11}}{S_{11}S_{22} - S^2{}_{12}} = \frac{E_1}{1 - v_{12}v_{21}} \tag{3.13}$$

$$Q_{12} = \frac{S_{12}}{S_{11}S_{22} - S^2{}_{12}} = \frac{v_{12}E_2}{1 - v_{12}v_{21}} = Q_{21} \tag{3.15}$$

$$Q_{22} = \frac{S_{11}}{S_{11}S_{22} - S^2{}_{12}} = \frac{E_2}{1 - v_{12}v_{21}} \tag{3.16}$$

$$Q_6 = \frac{1}{S_{66}} = G_{12} \tag{3.17}$$

Where,

E_1 = longitudinal young's modulus (in direction 1)

E_2= transverse young's modulus (in direction 1)

v_{12} = Major poison's ratio, where the general poison's ratio, v_{ij}, is defined as the ratio of the negative of the normal strain in direction 'j' to the normal strain in direction 'i', when the only normal load is applied in direction 'i'

G_{12} = in-plane shear modulus (in plane 1–2)

3.2.4. Hooke's Law for a Two-Dimensional Angle Lamina

Generally, a laminate does not consist only of unidirectional laminae because of their low stiffness and strength properties in the transverse direction. Therefore, in most laminates, some laminae are placed at an angle. It is thus necessary to develop the stress–strain relationship for an angle lamina.

The coordinate system used for showing an angle lamina is as given in Figure 3.2.3. The axes in the 1–2 coordinate systems are called the local axes or the material axes. The direction 1 is parallel to the fibers and the direction 2 is perpendicular to the fibers. The axes in the x–y coordinate system are called the global axes or the off-axes. The angle between the two axes is denoted by an angle θ. The global and local stresses in an angle lamina are related to each other through the angle of the lamina, θ

$$\begin{Bmatrix} \sigma_x \\ \sigma_y \\ \tau_{xy} \end{Bmatrix} = [T]^{-1} \begin{Bmatrix} \sigma_1 \\ \sigma_2 \\ \tau_{12} \end{Bmatrix} \tag{3.18}$$

where [*T*] is called the transformation matrix and is defined as

$$[T]^{-1} = \begin{bmatrix} c^2 & s^2 & -2sc \\ s^2 & c^2 & 2sc \\ sc & -sc & c^2 - s^2 \end{bmatrix} \text{ and } [T] = \begin{bmatrix} c^2 & s^2 & 2sc \\ s^2 & c^2 & -2sc \\ -sc & sc & c^2 - s^2 \end{bmatrix} \quad (3.19)$$

$c = \cos(\theta), \quad s = \sin(\theta)$

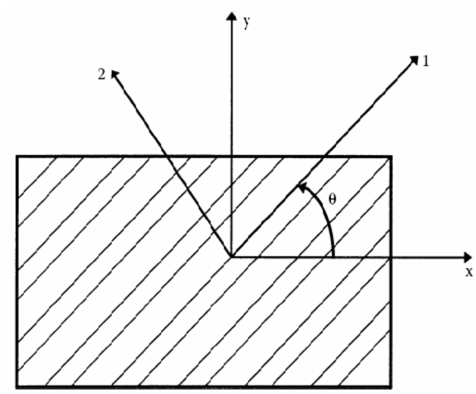

Figure 3.2.4 Local and global axes of an angle lamina

The global and local strains are also related through the transformation matrix

$$\begin{Bmatrix} \varepsilon_1 \\ \varepsilon_2 \\ \gamma_{12}/2 \end{Bmatrix} = [T] \begin{Bmatrix} \varepsilon_x \\ \varepsilon_y \\ \gamma_{xy}/2 \end{Bmatrix} \quad (3.20)$$

3.2.5. Stress-Strain Relationship in a Laminate

A lamina (also called a ply or layer) is a single flat layer of unidirectional fibers or woven fibers arranged in a matrix. It is the building block of a laminate. A laminate is a stack of plies of composites. Each layer can be laid at various orientations and can be made up of different material systems. The stiffness, strengths, and hygrothermal properties of a laminate will depend on:

- Elastic moduli
- The staking position
- Thickness
- Angle of orientation
- Coefficients of thermal expansion
- Coefficients of moisture expansion of each individual lamina

3.2.5.1 Laminate Code

Each layer in a laminate is identified by:

- its location in a laminate
- its material
- its angle of orientation with respect to ref axes

Each lamina is represented by the angle of ply and separated from other plies by slash sign. The first ply is the top of the laminate.

0
–45
90
60
30

[0/-45/90/60/30] denotes the code for the above laminate. It consists of five plies, each of which has different angle to the reference x-axis. A slash separates each lamina. The above code also implies that each ply is made of the same material and is of the same thickness.

3.2.5.2. Strain-Displacement Relationship

The following assumptions are made in the classical lamination theory to develop the relationships:

- Each lamina is orthotropic.
- Each lamina is homogeneous.
- A line straight and perpendicular to the middle surface remains
- Straight and perpendicular to the middle surface during deformation($\gamma_{xz}=\gamma_{yz}= 0$).
- The laminate is thin and is loaded only in its plane ($\sigma_z=\tau_{xz}=\tau_{yz}= 0$).
- Displacements are continuous and small throughout the laminate
- Each lamina is elastic.
- No slip occurs between the lamina interfaces.

At any point other than the midplane, the two displacements in the *x–y* plane will depend on the axial location of the point and the slope of the laminate midplane with the *x* and *y*-directions. For example, as shown in Figure 3.2.5,

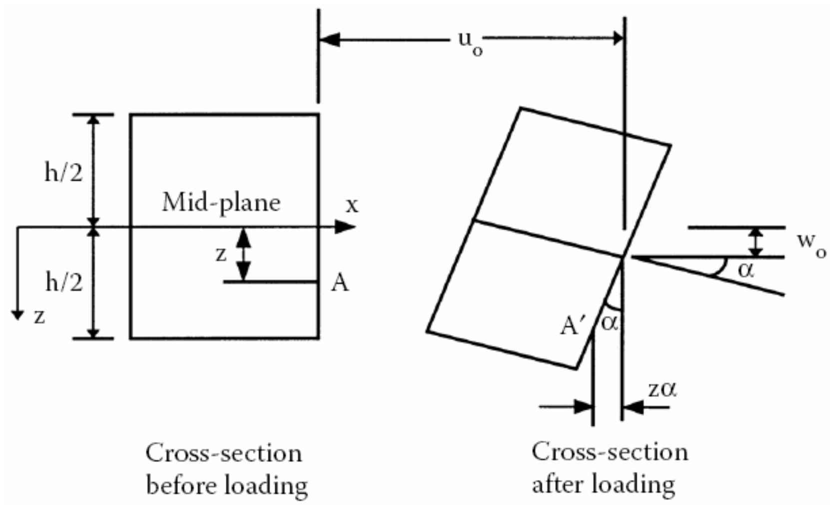

Figure 3.2.5 Relationship between mid-plane displacements and curvatures [1]

$u = u_o - z\alpha$ where, z-is the location from the mid-plane

$$\alpha = \frac{\partial w_o}{\partial x}$$

$$\frac{\partial u}{\partial x} = \frac{\partial u_o}{\partial x} - z\frac{\partial^2 w_o}{\partial x^2}$$

$$\varepsilon_x = \frac{\partial u_o}{\partial x} - z\frac{\partial^2 w_o}{\partial x^2} \tag{3.21}$$

$$\varepsilon_y = \frac{\partial v_o}{\partial y} - z\frac{\partial^2 w_0}{\partial y^2} \tag{3.22}$$

$$\gamma_x = \frac{\partial u}{\partial y} + \frac{\partial v}{\partial x} = \frac{\partial u_0}{\partial y} + \frac{\partial v_0}{\partial x} - \partial z\frac{\partial^2 w_o}{\partial x \partial y} \tag{3.23}$$

From (3.21), (3.22) and (3.23) the strain displacement equation in matrix form becomes:

$$\begin{Bmatrix} \varepsilon_x \\ \varepsilon_y \\ \gamma xy \end{Bmatrix} = \underbrace{\begin{Bmatrix} \dfrac{\partial u_o}{\partial x} \\ \dfrac{\partial v_o}{\partial y} \\ \dfrac{\partial u_o}{\partial y} + \dfrac{\partial v_o}{\partial x} \end{Bmatrix}}_{\substack{\textit{midplane} \\ \textit{strain}}} + Z \underbrace{\begin{Bmatrix} -\dfrac{\partial^2 w_o}{\partial x^2} \\ -\dfrac{\partial^2 w_o}{\partial y^2} \\ -2\dfrac{\partial^2 w_o}{\partial x \partial y} \end{Bmatrix}}_{\substack{\textit{midplane} \\ \textit{curvature}}} \tag{3.24}$$

Laminate strain can be written as:

$$\begin{Bmatrix} \varepsilon_x \\ \varepsilon_y \\ \gamma_{xy} \end{Bmatrix} = \begin{Bmatrix} \varepsilon^o{}_x \\ \varepsilon^o{}_y \\ \gamma^o{}_{xy} \end{Bmatrix} + Z \begin{Bmatrix} \kappa_x \\ \kappa_y \\ \kappa_{xy} \end{Bmatrix} \tag{3.25}$$

Equation (3.25) shows linear relation between strains in the laminate to the curvatures of the laminate

where z= the distance from the mid-plane of the point in the laminate (figure 3.2.5).

3.2.5.3. Stress and strain in a laminate

$$\begin{Bmatrix} \sigma_x \\ \sigma_y \\ \tau_{xy} \end{Bmatrix} = \begin{bmatrix} \overline{Q}_{11} & \overline{Q}_{12} & \overline{Q}_{16} \\ \overline{Q}_{12} & \overline{Q}_{22} & \overline{Q}_{26} \\ Q_{16} & \overline{Q}_{26} & Q_{66} \end{bmatrix} \begin{Bmatrix} \varepsilon_x \\ \varepsilon_y \\ \gamma_{xy} \end{Bmatrix} \tag{3.26}$$

Where $\left[\overline{Q}\right]$= the reduced transformed stiffness corresponds to that of the ply located at the point along the thickness of the laminate.

Substituting equation (3.25) in to (3.26) we obtain

$$\begin{Bmatrix} \sigma_x \\ \sigma_y \\ \tau_{xy} \end{Bmatrix} = \begin{bmatrix} \overline{Q}_{11} & \overline{Q}_{12} & \overline{Q}_{16} \\ \overline{Q}_{12} & \overline{Q}_{22} & \overline{Q}_{26} \\ Q_{16} & \overline{Q}_{26} & Q_{66} \end{bmatrix} \begin{Bmatrix} \varepsilon^o{}_x \\ \varepsilon^o{}_y \\ \gamma^o{}_{xy} \end{Bmatrix} + Z \begin{bmatrix} Q_{11} & Q_{12} & Q_{16} \\ Q_{12} & Q_{22} & Q_{26} \\ Q_{16} & Q_{26} & Q_{66} \end{bmatrix} \begin{Bmatrix} \kappa_x \\ \kappa_y \\ \kappa_{xy} \end{Bmatrix} \tag{3.27}$$

From (3.27) the stresses linearly vary along the thickness only.

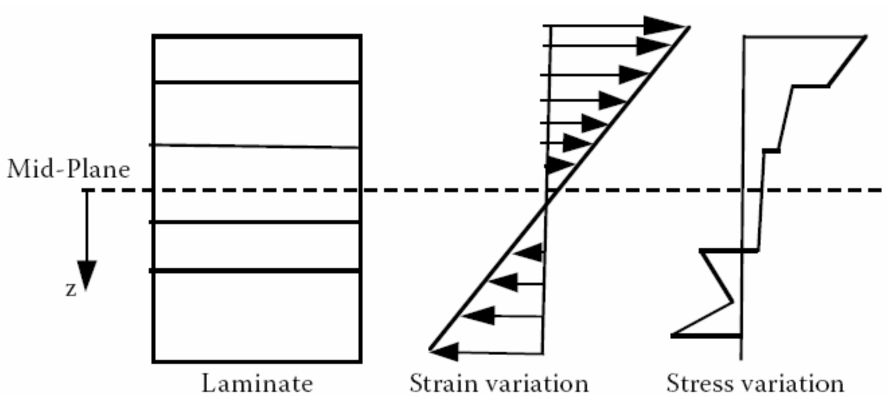

Fig 3.2.6 Strain and stress variation through the thickness of the laminate [1]

3.2.5.4 Loads related to mid plane strain and curvatures

The mid-plane strains and shell curvatures in Equation (3.25) are the unknowns for finding the lamina strains and stresses. However, Equation (3.27) gives the stresses in each lamina in terms of these unknowns. The stresses in each lamina can be integrated through the laminate thickness to give resultant forces and moments (or applied forces and moments) as shown in figure 3.2.7. The forces and moments applied to a laminate will be known, so the mid-plane strains and shell curvatures can then be found. This relationship between the applied loads and the mid-plane strains and curvatures is developed in this section.

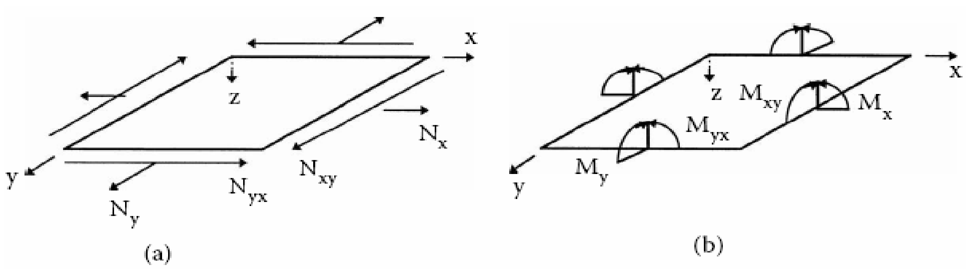

Figure 3.2.7 Resultant forces and moments on a laminate [1]

Consider a laminate made of 'n' plies shown in fig. 3.2.8, each ply has a thickness of t_k. then the total thickness of the laminate 'h' is

$$h = \sum_{k=1}^{n} t_k \tag{3.28}$$

Then, the location of the midplane is *h*/2 from the top or the bottom surface of the laminate. The *z*-coordinate of each ply '*k*' surface (top and bottom) is given by

Ply 1: $h_o = -\frac{h}{2}$ (for top surface)

Ply 2: $h_1 = -\frac{h}{2} + k_1$ (for bottom surface)

Ply κ : (κ : $(\kappa = 4, 3 ... \text{n} - 1)_i$

$$h_{k-1} = -\frac{h}{2} + \sum_{l=1}^{k-1} t_l = -\frac{h}{2} + \sum_{l=1}^{k-1} t_l \quad \text{(for top surface)}$$

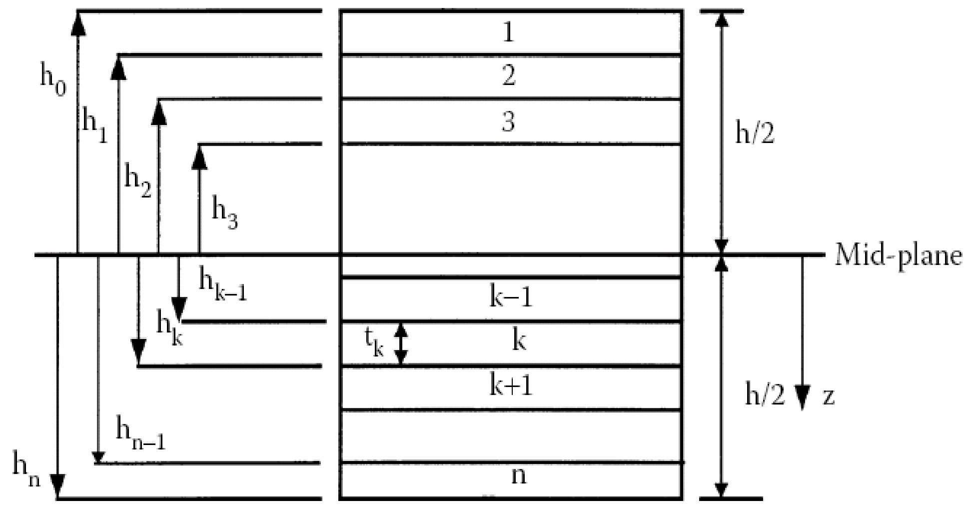

Figure 3.2.8 Coordinate locations of plies in a laminate [1]

$$h_k = -\frac{h}{2} + \sum_{l=1}^{k} t_k \quad \text{(Bottom surface)}$$

$$\text{Ply n: } h_{n-1} = \frac{h}{2} - t_n \quad \text{(Bottom surface)} \tag{3.29a}$$

$$h_n = \frac{h}{2} \quad \text{(Bottom surface)} \tag{3.29b}$$

Integrating the global stresses in each lamina give the resultant forces per unit length in x-y plane through the laminate thickness.

$$N_x = \int_{-\frac{h}{2}}^{\frac{h}{2}} \sigma_x dz \tag{3.30}$$

Where N_x, N_y - normal forces per unit length

$$N_y = \int_{-\frac{h}{2}}^{\frac{h}{2}} \sigma_y dz \tag{3.31}$$

Where N_{xy} shear force per unit length

$$N_{xy} = \int_{-\frac{h}{2}}^{\frac{h}{2}} \tau_{xy} dz \tag{3.32}$$

Where, $\frac{h}{2}$ is half thickness of the laminate

Similarly, the resultant moment will be (xy plane)

$$M_x = \int_{-\frac{h}{2}}^{\frac{h}{2}} \sigma_x Z dz \tag{3.33}$$

Where M_x, M_y - Bending moment per unit length

$$M_y = \int_{-\frac{h}{2}}^{\frac{h}{2}} \sigma_y z dz \tag{3.34}$$

M_{xy} - Twisting moment per unit length

$$M_{xy} = \int_{-\frac{h}{2}}^{\frac{h}{2}} \tau_{xt} z dz \tag{3.35}$$

Equations from (3.30) through (3.35) for a laminate can be written in a matrix form

$$\begin{bmatrix} N_x \\ N_y \\ N_{xy} \end{bmatrix} = \int_{-\frac{h}{2}}^{\frac{h}{2}} \begin{bmatrix} \sigma_x \\ \sigma_y \\ \tau_{xy} \end{bmatrix} dz \tag{3.36}$$

$$\begin{bmatrix} M_x \\ M_y \\ M_{xy} \end{bmatrix} = \int_{-\frac{h}{2}}^{\frac{h}{2}} \begin{bmatrix} \sigma_x \\ \sigma_y \\ \tau_{xy} \end{bmatrix} Z dz \tag{3.37}$$

This gives

$$\begin{bmatrix} N_x \\ N_y \\ N_{xy} \end{bmatrix} = \sum_{k=1}^{n} \int_{h_{k-1}}^{h_k} \begin{bmatrix} \sigma_x \\ \sigma_y \\ \tau_{xy} \end{bmatrix} d_z \tag{3.38}$$

$$\begin{bmatrix} M_x \\ M_y \\ M_{xy} \end{bmatrix} = \sum_{k=1}^{n} \int_{h_{k-1}}^{h_k} \begin{bmatrix} \sigma_x \\ \sigma_y \\ \tau_{xy} \end{bmatrix} Z dz \tag{3.39}$$

Substituting Equation (3.29) in equation (3.39), the resultant forces and moments can be written in terms of the mid-plane strains and curvatures.

$$\begin{Bmatrix} N_x \\ N_y \\ N_{zy} \end{Bmatrix} = \sum_{k=1}^{n} \int_{h_{k-1}}^{h_k} \begin{bmatrix} \overline{Q_{11}} & \overline{Q_{12}} & \overline{Q_{16}} \\ \overline{Q_{12}} & \overline{Q_{22}} & \overline{Q_{26}} \\ \overline{Q_{16}} & \overline{Q_{26}} & \overline{Q_{66}} \end{bmatrix} \begin{Bmatrix} \varepsilon^o{}_x \\ \varepsilon^o{}_y \\ \gamma^o{}_{xy} \end{Bmatrix} d_z + \sum_{k=1}^{n} \int_{h_{k-1}}^{h_k} \begin{bmatrix} \overline{Q_{11}} & \overline{Q_{12}} & \overline{Q_{16}} \\ \overline{Q_{12}} & \overline{Q_{22}} & \overline{Q_{26}} \\ \overline{Q_{16}} & \overline{Q_{26}} & \overline{Q_{66}} \end{bmatrix} \begin{Bmatrix} \kappa_x \\ \kappa_y \\ \kappa_{xy} \end{Bmatrix} Zd_z \qquad (3.40)$$

Similarly,

$$\begin{Bmatrix} M_x \\ M_y \\ M_{zy} \end{Bmatrix} = \sum_{k=1}^{n} \int_{h_{k-1}}^{h_k} \begin{bmatrix} \overline{Q_{11}} & \overline{Q_{12}} & \overline{Q_{16}} \\ \overline{Q_{12}} & \overline{Q_{22}} & \overline{Q_{26}} \\ \overline{Q_{16}} & \overline{Q_{26}} & \overline{Q_{66}} \end{bmatrix} \begin{Bmatrix} \varepsilon^o{}_x \\ \varepsilon^o{}_y \\ \gamma^o{}_{xy} \end{Bmatrix} dz + \sum_{k=1}^{n} \int_{h_{k-1}}^{h_k} \begin{bmatrix} \overline{Q_{11}} & \overline{Q_{12}} & \overline{Q_{16}} \\ \overline{Q_{12}} & \overline{Q_{22}} & \overline{Q_{26}} \\ \overline{Q_{16}} & \overline{Q_{26}} & \overline{Q_{66}} \end{bmatrix} \begin{Bmatrix} \kappa_x \\ \kappa_y \\ \kappa_{xy} \end{Bmatrix} z^2 dz \qquad (3.41)$$

In Equations (3.40) and (3.41), mid-plane strains and plate curvatures are independent for 'Z' coordinates and also $[\overline{Q}]_k$ is constant for each ply. Hence, Equations (3.40) and (3.41) can be written as

$$\begin{Bmatrix} N_x \\ N_y \\ N_{zy} \end{Bmatrix} = \left\{ \sum_{k=1}^{n} \begin{bmatrix} \overline{Q_{11}} & \overline{Q_{12}} & \overline{Q_{16}} \\ \overline{Q_{12}} & \overline{Q_{22}} & \overline{Q_{26}} \\ \overline{Q_{16}} & \overline{Q_{26}} & \overline{Q_{66}} \end{bmatrix}_k \int_{h_{k-1}}^{h_k} dz \right\} \begin{Bmatrix} \varepsilon^o{}_x \\ \varepsilon^o{}_y \\ \gamma^o{}_{xy} \end{Bmatrix} + \left\{ \sum_{k=1}^{n} \begin{bmatrix} \overline{Q_{11}} & \overline{Q_{12}} & \overline{Q_{16}} \\ \overline{Q_{12}} & \overline{Q_{22}} & \overline{Q_{26}} \\ \overline{Q_{16}} & \overline{Q_{26}} & \overline{Q_{66}} \end{bmatrix}_k \int_{h_{k-1}}^{h_k} Zdz \begin{Bmatrix} \kappa_x \\ \kappa_y \\ \kappa_{xy} \end{Bmatrix} \right\} \qquad (3.42)$$

$$\begin{Bmatrix} M_x \\ M_y \\ M_{xy} \end{Bmatrix} = \left\{ \sum_{k=1}^{n} \begin{bmatrix} \overline{Q_{11}} & \overline{Q_{12}} & \overline{Q_{16}} \\ \overline{Q_{12}} & \overline{Q_{22}} & \overline{Q_{26}} \\ \overline{Q_{16}} & \overline{Q_{26}} & \overline{Q_{66}} \end{bmatrix}_k \int_{h_{k-1}}^{h_k} Zdz \begin{Bmatrix} \varepsilon^o{}_x \\ \varepsilon^o{}_y \\ \gamma^o{}_{xy} \end{Bmatrix} \right\} + \left\{ \sum_{k=1}^{n} \begin{bmatrix} \overline{Q_{11}} & \overline{Q_{12}} & \overline{Q_{16}} \\ \overline{Q_{12}} & \overline{Q_{22}} & \overline{Q_{26}} \\ \overline{Q_{16}} & \overline{Q_{26}} & \overline{Q_{66}} \end{bmatrix}_k \int_{h_{k-1}}^{h_k} Z^2 dz \begin{Bmatrix} \kappa_x \\ \kappa_y \\ \kappa_{xy} \end{Bmatrix} \right\} \qquad (3.43)$$

Knowing that $\int_{h_{ky}}^{h_k} dz = h_k - h_{k-1}$, $\int_{h_{k-1}}^{h_k} Zdz = h_k^2 - h_{k-1}^2$, $\int_{h_{k-1}}^{h_k} Z^2 dz = \frac{1}{3}\left(h_k^3 - h_{k-1}^3\right)$

and substituting in Equations (3.42) and (3.43) gives

$$\begin{bmatrix} N_x \\ N_y \\ N_{xy} \end{bmatrix} = \begin{bmatrix} A_{11} & A_{12} & A_{16} \\ A_{12} & A_{22} & A_{26} \\ A_{16} & A_{26} & A_{66} \end{bmatrix} \begin{Bmatrix} \varepsilon^{o}{}_{x} \\ \varepsilon^{o}_{y} \\ \gamma^{o}_{xy} \end{Bmatrix} + \begin{bmatrix} B_{11} & B_{12} & B_{16} \\ B_{12} & B_{22} & B_{26} \\ B_{16} & B_{26} & B_{66} \end{bmatrix} \begin{Bmatrix} \kappa_x \\ \kappa_y \\ \kappa_{xy} \end{Bmatrix}$$

$$\begin{bmatrix} M_x \\ M_y \\ M_{xy} \end{bmatrix} = \begin{bmatrix} B_{11} & B_{12} & B_{16} \\ B_{12} & B_{22} & B_{26} \\ B_{16} & B_{26} & B_{66} \end{bmatrix} \begin{Bmatrix} \varepsilon^{o}_{x} \\ \varepsilon^{o}_{y} \\ \gamma^{o}_{xy} \end{Bmatrix} + \begin{bmatrix} D_{11} & D_{12} & D_{16} \\ D_{12} & D_{22} & D_{26} \\ D_{16} & D_{26} & D_{66} \end{bmatrix} \begin{Bmatrix} \kappa_x \\ \kappa_y \\ \kappa_{xy} \end{Bmatrix} \qquad (3.44)$$

Where

$$A_{ij} = \sum_{k=1}^{n} \left[\left(\overline{Q_{ij}}\right)\right]_k \left(h_k - h_{k-1}\right) \qquad \text{i = 1, 2, 3; j = 1, 2, 3} \qquad (3.45)$$

$$B_{ij} = \frac{1}{2} \sum_{k=1}^{n} \left[\left(\overline{Q_{ij}}\right)\right]_k \left(h_k^2 - h_{k-1}^2\right) \qquad \text{i = 1, 2, 3; j = 1, 2, 3} \qquad (3.46)$$

$$D_{ij} = \frac{1}{3} \sum_{k=1}^{n} \left[\left(\overline{Q_{ij}}\right)\right]_k \left(h_k^3 - h_{k-1}^3\right) \qquad \text{i = 1, 2, 3; j = 1, 2, 3} \qquad (3.47)$$

The [A], [B], and [D] matrices are called the extensional, coupling, and bending stiffness matrices, respectively. Combining Equations in (3.44) gives six simultaneous equations and six unknowns

$$\begin{bmatrix} N_x \\ N_y \\ N_{xy} \\ M_x \\ M_y \\ M_{xy} \end{bmatrix} = \begin{bmatrix} A_{11} & A_{12} & A_{16} & B_{11} & B_{12} & B_{16} \\ A_{12} & A_{22} & A_{26} & B_{12} & B_{22} & B_{26} \\ A_{16} & A_{26} & A_{66} & B_{16} & B_{26} & B_{66} \\ B_{11} & B_{12} & B_{16} & D_{11} & D_{12} & D_{16} \\ B_{12} & B_{22} & B_{26} & D_{12} & D_{22} & D_{26} \\ B_{16} & B_{22} & B_{66} & D_{16} & D_{26} & D_{66} \end{bmatrix} \begin{Bmatrix} \varepsilon^{o}_{x} \\ \varepsilon^{o}_{y} \\ \gamma^{o}_{xy} \\ \kappa_x \\ \kappa_y \\ \kappa_{xy} \end{Bmatrix} \qquad (3.48)$$

The extensional stiffness matrix [A] relates the resultant in-plane forces to the in-plane strains, and the bending stiffness matrix [D] relates the resultant bending moments to the plate curvatures. The coupling stiffness matrix [B] couples the force and moment terms to the mid-plane strains and mid-plane curvatures.

The following are the steps for analyzing a laminated composite structure subjected to the applied forces and moments:

1. Find $[Q]$ for each ply using: $E_1, E_2, V_{12}, V_{21}, G_{xy}$ as

$$Q_{11} = \frac{E_1}{1 - V_{12}V_{22}} \qquad Q_{12} = \frac{V_{12}E_2}{1 - V_{12}V_{21}}$$

$$Q_{22} = \frac{E_2}{1 - V_{12}V_{21}} \qquad Q_{66} = G_{12}$$

2. Find the value of the transformed reduced stiffness matrix [$\bar{Q}$] for each ply using the [Q] matrix calculated in step 1 and the angle of the ply as follows

$$\bar{Q}_{11} = Q_{11}C^4 + Q_{22}S^4 + 2(Q_{12} + 2Q_{66})S^2C^2$$

$$\bar{Q}_{12} = (Q_{11} + Q_{22} - 4Q_{66})S^2C^2 + Q_{12}\left(S^4 + C^4\right)$$

$$\bar{Q}_{22} = Q_{11}S^4 + Q_{22}C^4 + 2(Q_{12} + 2Q_{66})S^2C^2$$

$$\bar{Q}_{16} = (Q_{11} - Q_{22} - 2Q_{66})SC^3 - (Q_{22} - Q_{12} - 2Q_{66})S^3C$$

$$\bar{Q}_{26} = (Q_{11} - Q_{12} - 2Q_{66})S^3C - (Q_{22} - Q_{12} - 2Q_{66})C^3S$$

$$\bar{Q}_{66} = (Q_{11} + Q_{12} - 2Q_{12} - 2Q_{66})S^2C^2 + Q_{66}\left(C^2 + S^2\right)$$

Where $C = Cos\ \theta$ $S = \sin\ \theta$ θ – is ply angle.

3. Knowing the thickness t_k of each ply, find the coordinate of the top and bottom surface, h_i, i = 1…, n, of each ply, using Equation (3.29 a & b).

4. Use the $\left[\bar{Q}\right]$ matrices from step 2 and the location of each ply from step 3 to find the three stiffness matrices [A], [B], and [D] from Equation (3.44), (3.45) and (3.46).

5. Substitute the stiffness matrix values found in step 4 and the applied forces and moments in Equation (3.48).

6. Solve the six simultaneous equations (3.48) to find the mid-plane strains and curvatures.

7. Now that the location of each ply is known, find the global strains in each ply using Equation (3.25).

8. For finding the global stresses, use the stress–strain Equation

$$\begin{bmatrix} \sigma_x \\ \sigma_y \\ \tau_{xy} \end{bmatrix} = \begin{bmatrix} \bar{Q}_{11} & \bar{Q}_{12} & \bar{Q}_{16} \\ \bar{Q}_{12} & \bar{Q}_{22} & \bar{Q}_{26} \\ \bar{Q}_{16} & \bar{Q}_{26} & \bar{Q}_{66} \end{bmatrix} \begin{bmatrix} \varepsilon_x \\ \varepsilon_y \\ \gamma_{xy} \end{bmatrix},$$

9. For finding the local strains, use the transformation Equation

$$\begin{bmatrix} \varepsilon_1 \\ \varepsilon_2 \\ \gamma_{12}/2 \end{bmatrix} = [\mathrm{T}] \begin{Bmatrix} \varepsilon_x \\ \varepsilon_y \\ \gamma_{xy}/2 \end{Bmatrix}, \text{Where}$$

$$[T]^{-1} = \begin{bmatrix} c^2 & s^2 & -2sc \\ s^2 & c^2 & 2sc \\ sc & -sc & c^2 - s^2 \end{bmatrix} \text{ and } [T] = \begin{bmatrix} c^2 & s^2 & 2sc \\ s^2 & c^2 & -2sc \\ -sc & sc & c^2 - s^2 \end{bmatrix}$$

$$c = \cos(\theta), \quad s = \sin(\theta)$$

10. For finding the global stresses, use the transformation Equation

$$\begin{Bmatrix} \sigma_x \\ \sigma_y \\ \tau_{xy} \end{Bmatrix} = [T]^{-1} \begin{Bmatrix} \sigma_1 \\ \sigma_2 \\ \tau_{12} \end{Bmatrix}$$

11. Check failure condition of the laminate using one of the failure theories (for instance Tsai-Hill theory) [1]

$$\left[\frac{\sigma_1}{(\sigma_1^T)_{ult}}\right]^2 - \left[\frac{\sigma_1 \sigma_2}{(\sigma_1^T)_{ult}^2}\right] + \left[\frac{\sigma_2}{(\sigma_2^T)_{ult}}\right]^2 + \left[\frac{\tau_{12}}{(\tau_{12})_{ult}}\right]^2 < 1$$

3.2.5.5 Special types laminates

Symmetric Laminates

A laminate is called symmetric if the material, angle, and thickness of plies are the same above and below the mid-plane. An example of symmetric laminates is:

0°
90°
0°
90°
0°

Symmetric Laminate

For symmetric laminates from the definition of [B] matrix, it can be proved that [B] = 0. Thus, Equation (3.48) can be decoupled to give

$$\begin{bmatrix} N_x \\ N_y \\ N_{xy} \end{bmatrix} = \begin{bmatrix} A_{11} & A_{12} & A_{16} \\ A_{12} & A_{22} & A_{26} \\ A_{16} & A_{26} & A_{66} \end{bmatrix} \begin{Bmatrix} \varepsilon_x^o \\ \varepsilon_y^o \\ \gamma_{xy}^o \end{Bmatrix} \tag{3.49}$$

$$\begin{bmatrix} M_x \\ M_y \\ M_{xy} \end{bmatrix} = \begin{bmatrix} D_{11} & D_{12} & D_{16} \\ D_{12} & D_{22} & D_{26} \\ D_{16} & D_{26} & D_{66} \end{bmatrix} \begin{Bmatrix} \kappa_x \\ \kappa_y \\ \kappa_{xy} \end{Bmatrix} \tag{3.50}$$

This shows that the force and the moment terms are uncoupled. Thus, if a laminate is subjected to only forces, it will have zero mid-plane curvatures. Similarly, if it is subjected only to moments, it will have zero mid-plane strains.

The uncoupling between extension and bending in symmetric laminates makes analyzing such laminates simpler. It also prevents a laminate from twisting due to thermal loads, such as cooling down from processing temperatures and temperature fluctuations during use such as in a space shuttle, etc.

Cross-Ply Laminates

A laminate is called a cross-ply laminate (also called laminates with specially orthotropic layers) if only 0 and 90° plies were used to make a laminate. An example of a cross ply laminate is a $[0/90/0/90/0]_s$ laminate:

0º
90º
0º
90º
0º

Cross-ply laminate

For cross-ply laminates, A_{16}= 0, A_{26}= 0, B_{16}= 0,B_{26}= 0, D_{16} = 0, and D_{26} = 0; thus, equation (3.48) can be written as

$$\begin{bmatrix} N_x \\ N_y \\ N_{xy} \\ M_x \\ M_y \\ M_{xy} \end{bmatrix} = \begin{bmatrix} A_{11} & A_{12} & 0 & B_{11} & B_{12} & 0 \\ A_{12} & A_{22} & 0 & B_{12} & B_{22} & 0 \\ 0 & 0 & A_{66} & 0 & 0 & B_{66} \\ B_{11} & B_{12} & 0 & D_{11} & D_{12} & 0 \\ B_{12} & B_{22} & 0 & D_{12} & D_{22} & 0 \\ B_{16} & B_{22} & B_{66} & 0 & 0 & D_{66} \end{bmatrix} \begin{Bmatrix} \varepsilon_x^o \\ \varepsilon_y^o \\ \gamma_{xy}^o \\ \kappa_x \\ \kappa_y \\ \kappa_{xy} \end{Bmatrix} \tag{3.51}$$

In these cases, decoupling occurs between the normal and shear forces, as well as between the bending and twisting moments. If a cross-ply laminate is also symmetric, then in addition to the preceding uncoupling, the coupling matrix [B] = 0 and no coupling takes place between the force and moment terms.

Angle Ply Laminates

A laminate is called an angle ply laminate if it has plies of the same material and thickness and only oriented at + θ and – θ directions. An example of an angle ply laminate is [–30/30/–30/30]:

-30º
30º
-30º
30º

Angle ply laminate

If a laminate has an even number of plies, then A_{16}=A_{26}= 0. However, if the number of plies is odd and it consists of alternating +θ and –θ plies, then it is symmetric, giving [B] = 0, but also A_{16}, A_{26}, D_{16}, and D_{26} also become small as the number of layers increases for the same laminate thickness. This behaviour is similar to the symmetric cross-ply laminates. However, these angle ply laminates have higher shear stiffness and shear strength properties than cross-ply laminates.

Anti-symmetric Laminates

A laminate is called antisymmetric if the material and thickness of the plies are the same above and below the mid-plane, but the ply orientations at the same distance above and below the mid-plane are negative of each other. An example of an antisymmetric laminate is:

45°
30°
-30°
-45°

Antisymmetric laminate

From Equation (3.45) and Equation (3.47), the coupling terms of the extensional stiffness matrix, A_{16}=A_{26}=0, and the coupling terms of the bending stiffness matrix, D_{16}=D_{26}= 0. Then, the equation in (3.48) becomes

$$\begin{bmatrix} N_x \\ N_y \\ N_{xy} \\ M_x \\ M_y \\ M_{xy} \end{bmatrix} = \begin{bmatrix} A_{11} & A_{12} & 0 & B_{11} & B_{12} & B_{16} \\ A_{12} & A_{22} & 0 & B_{12} & B_{22} & B_{26} \\ 0 & 0 & A_{66} & B_{16} & B_{26} & B_{66} \\ B_{11} & B_{12} & B_{16} & D_{11} & D_{12} & 0 \\ B_{12} & B_{22} & B_{26} & D_{12} & D_{22} & 0 \\ B_{16} & B_{22} & B_{66} & 0 & 0 & D_{66} \end{bmatrix} \begin{Bmatrix} \varepsilon_x^o \\ \varepsilon_y^o \\ \gamma_{xy}^o \\ \kappa_x \\ \kappa_y \\ \kappa_{xy} \end{Bmatrix} \tag{3.52}$$

Balanced Laminate

A laminate is balanced if layers at angles other than 0 and 90° occur only as plus and minus pairs of +θ and –θ. The plus and minus pairs do not need to be adjacent to each other, but the thickness and material of the plus and minus pairs need to be the same. Here, the terms A_{16}=A_{26}= 0. An example of a balanced laminate is [30/40/–30/30/–30/–40]:

30°
40°
-30°
30°
-30°
-40°

Balanced laminate

From equation (3.48),

$$\begin{bmatrix} N_x \\ N_y \\ N_{xy} \\ M_x \\ M_y \\ M_{xy} \end{bmatrix} = \begin{bmatrix} A_{11} & A_{12} & 0 & B_{11} & B_{12} & B_{16} \\ A_{12} & A_{22} & 0 & B_{12} & B_{22} & B_{26} \\ 0 & 0 & A_{66} & B_{16} & B_{26} & B_{66} \\ B_{11} & B_{12} & B_{16} & D_{11} & D_{12} & D_{16} \\ B_{12} & B_{22} & B_{26} & D_{12} & D_{22} & D_{26} \\ B_{16} & B_{22} & B_{66} & D_{16} & D_{26} & D_{66} \end{bmatrix} \begin{Bmatrix} \varepsilon_x^o \\ \varepsilon_y^o \\ \gamma_{xy}^o \\ \kappa_x \\ \kappa_y \\ \kappa_{xy} \end{Bmatrix} \tag{3.53}$$

If the number of plies in a balanced laminate is odd, it can be made symmetric. For such laminates the coupling stiffness matrix is also zero.

3.2.5.6 Failure Condition of Laminates

Like any isotropic materials there are different failure conditions for laminates. Some of these are maximum normal stress theory of failure, von misses theory of failure, normal strain theory of failure and others. This failure conditions are customized to predict failures of composite structures.

The modification of Von Misses theory, called Tsia-Hill failure theory, is one of the most commonly used theory of failure. It is based on the distortion energy failure theory of von misses for isotropic materials as applied to anisotropic materials. According to this theory failure is supposed to take place in a material only when the distortion energy is greater than the failure distortion energy of the material.

Based on the distortion energy theory; Tsia proposed that a lamina fails if

$$\left[\frac{\sigma_1}{\left(\sigma_1^T\right)_{ult}}\right]^2 - \left[\frac{\sigma_1\sigma_2}{\left(\sigma_1^T\right)_{ult}^2}\right] + \left[\frac{\sigma_2}{\left(\sigma_2^T\right)_{ult}}\right]^2 + \left[\frac{\tau_{12}}{\left(\tau_{12}\right)_{ult}}\right]^2 < 1 \tag{3.54}$$

Where σ_1 - is the applied tensile strength in the Principal direction 1

$\left(\sigma_1^T\right)_{ult}$ - is the ultimate tensile strength in the Principal direction 1

σ_2 - is the transverse tensile strength applied in the direction 2

$\left(\sigma_2^T\right)_{ult}$ - is the ultimate tensile strength in the Principal direction 2

τ_{12} - is the in plane shear stress applied (in plane 1-2)

$\left(\tau_{12}\right)_{ult}$ - is the ultimate in plane shear strength (in plane 1-2)

CHAPTER FOUR
MODELLING OF THE CYLINDERICAL SHELL STRUCTURE

4.1 Mathematical Modelling

Mathematical modelling is the activity devoted to the study of the simulation of physical phenomena by computational processes. The goal of the mathematical simulation is to predict the behaviour of some product within its environment. Mathematical modelling subsumes a number of activities, as illustrated by figure 4.1.

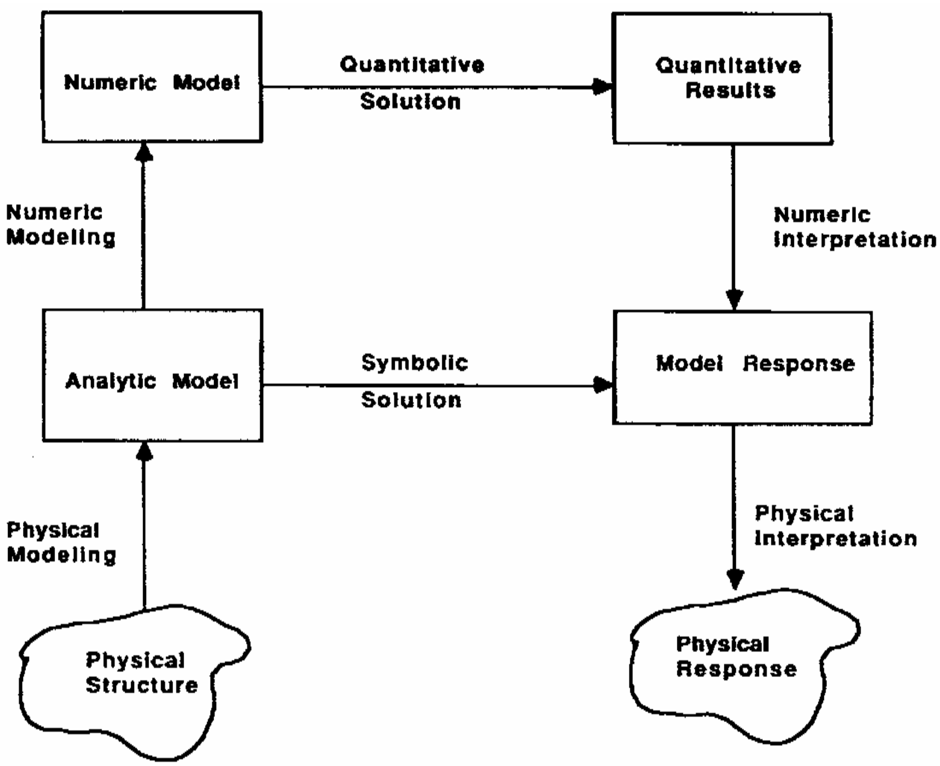

Figure 4.1 Mathematical Modelling Processes [9]

The mathematical modelling activities presented include model generation, interpretation of numerical results, and development and control of numerical algorithms as a series of interrelated activities.

All mechanical models are characterized mathematically by very complex expressions, many of which, until the advent of electronic computation, stood outside the reach of the scientific and engineering communities. Recently, the computer has made it possible to solve many problems of mechanics, dramatically expanding the capabilities for mathematical modelling [22].

We will first consider here a first order shear deformation theory applicable to laminated cylindrical shells of shallow curvature, shown in figure 4.2. The thickness and in-plane dimensions of the shell are denoted by h, a, and b, respectively. The displacements in the x, θ, and z are denoted by u, v, and w respectively. The radius, R, is assumed to be much larger than the thickness, h. In addition, transverse shear strains γ_{xz} and $\gamma_{\theta z}$ are no longer negligible, although the thickness strain ε_z is neglected.

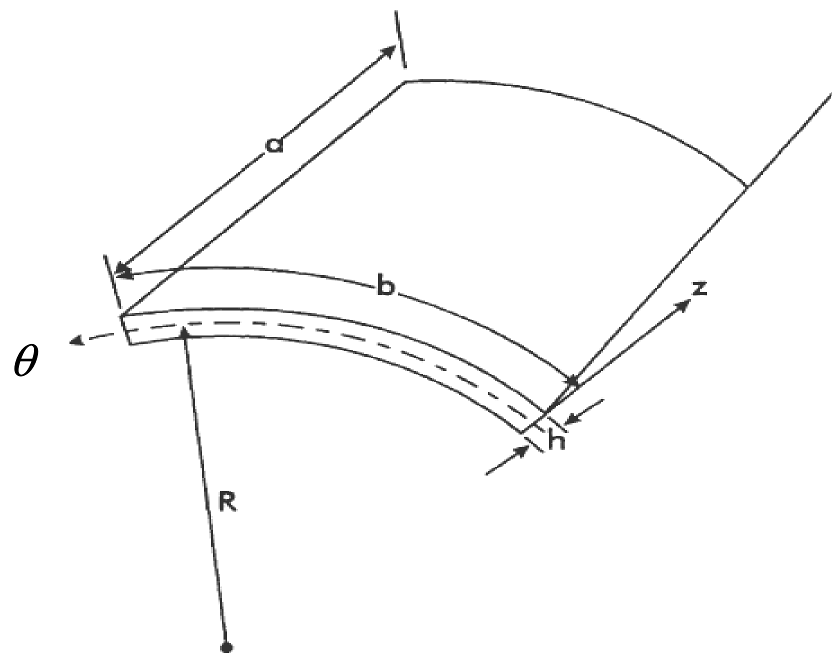

Figure 4.2 Nomenclature for cylindrical shell [22]

The classical theory of elasticity gives the following strain-displacement relations applicable to the geometry shown in figure 4.2, [22].

$$\varepsilon_z = \frac{\partial u}{\partial x},\ \varepsilon_\theta = \frac{1}{\left(1+z/R\right)}\frac{\partial v}{\partial \theta} + \frac{w}{R},\ \varepsilon_z = \frac{\partial w}{\partial z} = 0$$

$$\varepsilon_{\theta z} = \frac{1}{\left(1+z/R\right)}\frac{\partial w}{\partial x} + \frac{\partial v}{\partial z} - \frac{v}{(1+z)R^2} \tag{4.1}$$

$$\gamma_{xz} = \frac{\partial u}{\partial z} + \frac{\partial w}{\partial x},\ \gamma_{x\theta} = \frac{\partial v}{\partial x} + \frac{1}{\left(1+z/R\right)}\frac{\partial u}{\partial \theta}$$

The first order theory assumes the following displacements

$$
\begin{aligned}
u &= u^o(x,\theta) + z\varphi_x(x,\theta) \\
v &= v^o(x,\theta) + z\varphi_s(x,\theta) \\
w &= w^o(x,\theta)
\end{aligned}
\tag{4.2}
$$

where u^o, v^o, w^o are the tangential, axial, and transverse displacements of the mid-surface respectively, and φ_x ,and φ_θ are the rotations of the cross-sections originally formed to x and s axes [22]. Since we assume that the shell is shallow, z/R is small compared to unity. Equations (4.1) and (4.1) and yield

$$
\begin{aligned}
\varepsilon_x &= \varepsilon_x^o + z\kappa_x \\
\varepsilon_\theta &= \varepsilon_\theta^o + z\kappa_\theta \\
\gamma_{x\theta} &= \gamma_{x\theta}^o + z\kappa_{x\theta}
\end{aligned}
\tag{4.3}
$$

Where [ε_x^o] and [κ] are the mid-surface curvatures, respectively, given by [22]

$$
\varepsilon_x^o = \frac{\partial u^o}{\partial x},\ \varepsilon_\theta^o = \frac{\partial v^o}{\partial \theta} + \frac{w}{R},\ \gamma_{x\theta}^o = \frac{\partial u^o}{\partial \theta} + \frac{\partial v^o}{\partial x}
$$

$$
\kappa_x = \frac{\partial \varphi_x}{\partial x},\ \kappa_\theta = \frac{\partial \varphi_x}{\partial \theta},\ \kappa_{x\theta} = \frac{\partial \varphi_x}{\partial \theta} + \frac{\partial \varphi_\theta}{\partial x}
\tag{4.4}
$$

In addition, the interlaminar shear strains are

$$
\gamma_{xz} = \varphi_x + \frac{\partial w}{\partial x},\ \gamma_{\theta z} = \varphi_\theta + \frac{\partial w}{\partial x} - \frac{v}{R}
\tag{4.5}
$$

It is noted that these results are of exactly the same form as for flat, laminated plates of rectangular cross-section with the exception of the w/R term appearing in the mid-surface tangential strains ε_θ^o and –v/R term appearing in the interlaminar shear strains γ_{xz}. Since the analysis assumes that displacements u,v, and w are small compared to the plate thickness h and the radius of the plate R is much larger than h, the additional terms w/R and –v/R in equations (4.1) and (4.5) drop out.

According to classical theory of shells, the membrane stress resultants $N_x, N_\theta, N_{x\theta}$ and the stress couples $M_x, M_\theta, M_{x\theta}$, on region Ω_i, are related to each other as [24]

$$\begin{bmatrix}[N]\\ [M]\end{bmatrix}=\begin{bmatrix}A & B\\ B & D\end{bmatrix}\begin{Bmatrix}\lfloor \varepsilon \rfloor\\ \lfloor \kappa \rfloor\end{Bmatrix}$$

The force and moment resultants [N] and [M] for the shell are [22]

$$\left(N_x, N_\theta, N_{x\theta}\right)=\int_{-\frac{h}{2}}^{\frac{h}{2}}\left(\sigma_x^{(k)}, \sigma_\theta^{(k)}, \tau_{x\theta}^{(k)}\right)dz$$

$$\left(M_x, M_\theta, M_{x\theta}\right)=\int_{-\frac{h}{2}}^{\frac{h}{2}}\left(\sigma_x^{(k)}, \sigma_\theta^{(k)}, \tau_{x\theta}^{(k)}\right)zdz \tag{4.6}$$

Where $\sigma_x^{(k)}, \sigma_\theta^{(k)}$ and $\tau_{x\theta}^{(k)}$ are the in-plane stresses in the k^{th} layer. Integration of the stresses yields the constitutive equations for extension and bending of cylindrical shell [22]

$$\begin{bmatrix}N\\ M\end{bmatrix}=\begin{bmatrix}A & B\\ B & D\end{bmatrix}\begin{Bmatrix}\varepsilon^o\\ \kappa\end{Bmatrix} \tag{4.7}$$

where $[A], [B]$, and $[D]$ are the extensional, coupling and bending stiffness matrices, respectively, defined in reference $[22]$.

$\left[\varepsilon^o\right]=\left[\varepsilon_x^o, \varepsilon_\theta^o, \gamma_{x\theta}^o\right]$ and $\lfloor \kappa \rfloor=\left[\kappa_x, \kappa_\theta, \kappa_{x\theta}\right]$ are defined in equation (4.4).

4.2. Finite Element Modelling

The characteristics of shell element with similar shapes are used to generate a so-called super element for analysis of crack problems for cylindrical shells [23]. The formulation is processed by matrix condensation without involvement of special treatment so that it can deal with various singularity problems in order to present excellent results to crack problems involving cylindrical shell.

For cylindrical shell shown in figure 4.1 a, the wall of this shell is thin, with thickness is less than one-tenth of the radius and it does not change abruptly. The wall is subjected to the stresses that distributed through the thickness uniformly.

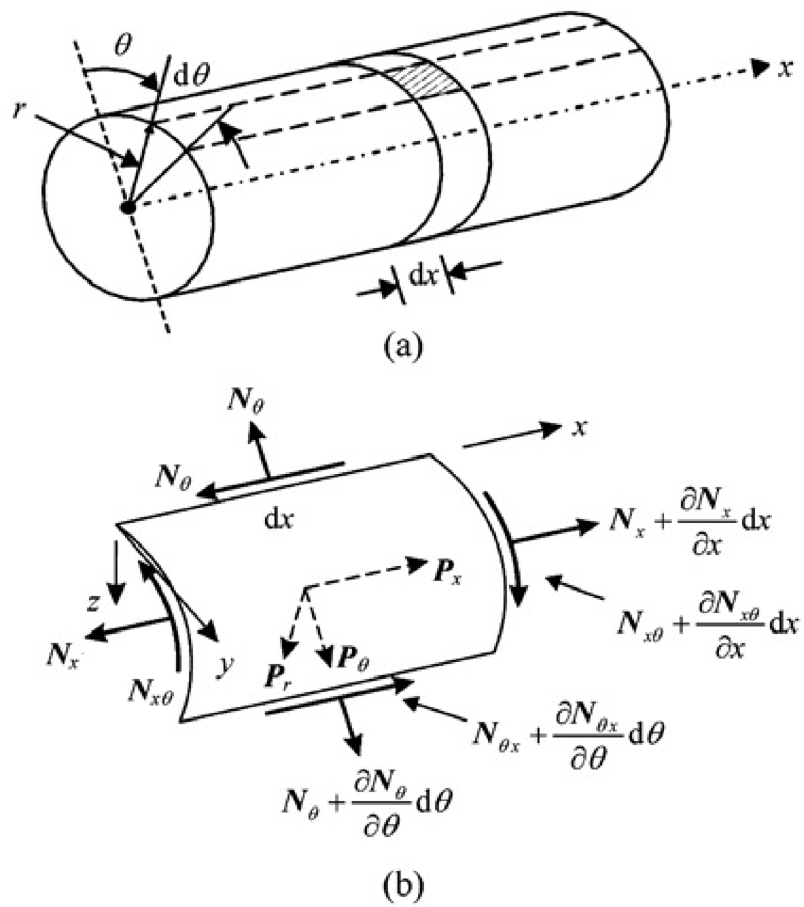

Figure 4.3 - Cylindrical shell and Membrane shell forces (a) Cylindrical shell (b) membrane shell forces [23].

Thus, the membrane theory cited in Sung *et al.* [23], an assumption of the element without flexural rigidity and carrying only the lateral loads by axial and transverse shear loads is applied for the analysis. Based on the assumptions of elastic material and small displacement, it is reasonable to use the potential energy theory to develop a cracked shell element. A free body diagram of membrane element including the forces is shown in Figure.4.3b. The coordinate x and the angle θ were used to describe the position of the shell element. The deformation gradients ($u_{i,1}$), the stress (σ_{ij}) and strain components (ε_{ij}) computed in the shell element are referred to element local coordinates. However, for the energy release rate determination that corresponds to a co-ordinate system orientated with respect to the crack tip co-ordinates. Thus for large deformation, the finite element quantities must be transformed into the crack tip co-ordinates to be able to compute the energy release rate or stress intensity factor [29].

By the assumption of constant thickness shell, the nodal displacements u_i, v_i and w_i shown in the parent element are related to the membrane strains ε_x, ε_θ and $\gamma_{x\theta}$ on the material coordinates as [23]

$$\begin{bmatrix} X \\ Y \\ Z \end{bmatrix} = \sum_{i=1}^{8} N_i(\zeta,\eta) \begin{bmatrix} x_i \\ y_i \\ z_i \end{bmatrix} \tag{4.8}$$

where, $N_i(\xi,\eta)$ is the shape function associated with the parent element. Accordingly, the related displacements are [23]

$$\begin{bmatrix} U \\ V \\ W \end{bmatrix} = \sum_{i=1}^{8} N_i(\xi,\eta) \begin{bmatrix} u_i \\ v_i \\ w_i \end{bmatrix} \tag{4.9}$$

and the three types of strains related to the displacement vector, $\vec{u}$, are $\vec{u} = \begin{bmatrix} u_i \\ v_i \\ w_i \end{bmatrix}$

$$\begin{bmatrix} \varepsilon_x \\ \varepsilon_\theta \\ \gamma_{r\theta} \end{bmatrix} = \begin{bmatrix} \frac{\partial N_i}{\partial x} & 0 & 0 \\ 0 & \frac{1}{r}\frac{\partial N_i}{\partial \theta} & -\frac{N_i}{r} \\ \frac{1}{r}\frac{\partial N_i}{\partial \theta} & \frac{\partial N_i}{\partial x} & 0 \end{bmatrix} \begin{bmatrix} u_i \\ v_i \\ w_i \end{bmatrix} \tag{4.10}$$

Equation (4.10) may be denoted as $\varepsilon = Bu$

The stress-strain (constitutive) relationship is $\sigma = D\varepsilon$, where

$D = \begin{bmatrix} E_{xx} & E_{x\theta} & 0 \\ E_{x\theta} & E_{\theta\theta} & 0 \\ 0 & 0 & G_{x\theta} \end{bmatrix}$ - is the material property matrix

The stiffness **K** and force matrix **Q** are formulated as [23]:

$$K = t\iint B^T DBrdxd\theta \tag{4.11}$$

Eq. (4.11) can be written in a normalized coordinate system (ξ,η) as

$$K = t\int_{-1}^{1}\int_{-1}^{1} B^T DB \det |J| rd\xi d\eta \tag{4.12}$$

$$Q = \iint P^T qrdxd\theta = \int_{-1}^{1}\int_{-1}^{1} P^T q \det |J| rd\xi d\eta \tag{4.13}$$

where, J is the Jacobian matrix and can be written as

$$J=\begin{bmatrix}\dfrac{\partial x}{\partial \xi} & \dfrac{\partial \theta}{\partial \xi}\\ \dfrac{\partial x}{\partial \eta} & \dfrac{\partial \theta}{\partial \eta}\end{bmatrix}=\begin{bmatrix}\cdots\ \dfrac{\partial N_i}{\partial \xi}\cdots\\ \cdots\cdots\ \dfrac{\partial N_i}{\partial \eta}\cdots\cdots\end{bmatrix}\begin{bmatrix}. & .\\ x_i & \theta_i\\ . & .\end{bmatrix} \tag{4.14}$$

In Eqs.(4.11) and (4.12), matrices B and J are functions of ξ and η , the symbols t and r represent the thickness and the radius of the cylindrical shell element respectively.

Stiffness for Similar Shell Elements

For two similar shell elements (1 and 2) with ratio α , the relationships of the coordinates for the corresponding nodes can be represented by

$$\begin{cases} x_i^2=\alpha x_i^1\\ \theta_1^2=\alpha\theta_i^1\end{cases} \tag{4.15}$$

The matrix B in Eq. (4.12) can be decomposed as [23]

$$B=\bar{B}+\bar{\bar{B}}=\begin{bmatrix}\dfrac{\partial N_i}{\partial x} & 0 & 0\\ 0 & \dfrac{1}{r}\dfrac{\partial N_i}{\partial \theta} & 0\\ \dfrac{1}{r}\dfrac{\partial N_i}{\partial \theta} & \dfrac{\partial N_i}{\partial x} & 0\end{bmatrix}+\begin{bmatrix}0 & 0 & 0\\ 0 & 0 & -\dfrac{N_i}{r}\\ 0 & 0 & 0\end{bmatrix} \tag{4.16}$$

Therefore, from Equation (4.15) and (4.16), the matrices B_1 and B_2 for the elements 1 and 2 have the following relationship:

$$\begin{cases}\bar{B}_2=\bar{B}_1/\alpha\\ \bar{\bar{B}}_2=\bar{\bar{B}}_1\end{cases} \tag{4.17}$$

and the relationships for the Jacobian matrix are:

$$\begin{cases}J_2=\alpha J_1\\ J_2^{-1}=J_1^{-1}/\alpha\\ \det|J_2|=\alpha^2\det|J_1|\end{cases} \tag{4.18}$$

By substituting Eq.(4.16) in Eq. (4.12), the stiffness matrix K becomes as

$K=K^{*}+K^{**}+K^{***}$

where

$$K^{*} = t\int_{-1}^{1}\int_{-1}^{1} \bar{B}^{T}\; D\; \bar{B} \det\left|J\right| r d\xi d\eta$$

$$K^{**} = t\int_{-1}^{1}\int_{-1}^{1} (\bar{\bar{B}}^{T}\; D\; \bar{B} + \bar{B}^{T}\; D\; \bar{\bar{B}}) \det\left|J\right| r d\xi d\eta$$

$$K^{***} = t\int_{-1}^{1}\int_{-1}^{1} \bar{\bar{B}}^{T}\; D\; \bar{\bar{B}} \det\left|J\right| r d\xi d\eta$$

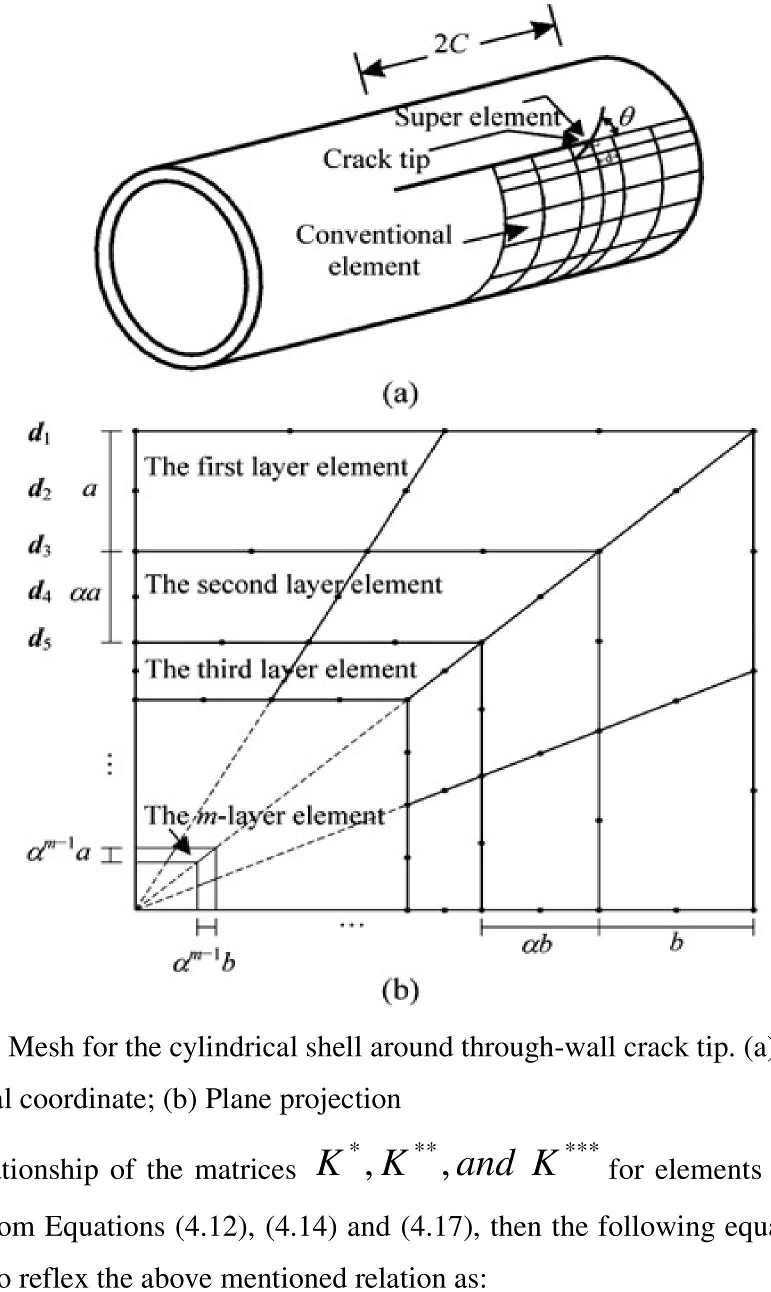

Figure 4.4 Mesh for the cylindrical shell around through-wall crack tip. (a) Cylindrical coordinate; (b) Plane projection

If the relationship of the matrices $K^{*}, K^{**}, and\ K^{***}$ for elements 1 and 2 are derived from Equations (4.12), (4.14) and (4.17), then the following equation can be acquired to reflex the above mentioned relation as:

$$K_2 = K_1^{*} + \alpha K_1^{**} + \alpha^2 K_1^{***} \tag{4.19}$$

Supper Element Formulation

The element mesh around a singularity point is shown in figure 4.2. These elements are similar to each other. The inner-layer element to the adjacent outer-layer element is designated with the ratio α. The stiffness of the outmost element may be expressed as

$$K_1 = K_1^{*} + K_1^{**} + K_1^{***}$$
$$= \begin{bmatrix} K_1^{*} & K_2^{*} & K_3^{*} \\ K_2^{*T} & K_4^{*} & K_5^{*} \\ K_3^{*T} & K_5^{*T} & K_6^{*} \end{bmatrix} + \begin{bmatrix} K_1^{**} & K_2^{**} & K_3^{**} \\ K_2^{**T} & K_4^{**} & K_5^{**} \\ K_3^{**T} & K_5^{**T} & K_6^{**} \end{bmatrix} + \begin{bmatrix} 0 & 0 & 0 \\ 0 & 0 & 0 \\ 0 & 0 & K_6^{***} \end{bmatrix} \tag{4.20}$$

Then, the stiffness matrix for the m-layer element, shown in figure 4.2 (b), is

$$K_m = K_1^{*} + \alpha^{m-1} K_1^{**} + \alpha^{2(m-1)} K_1^{***}$$

This relation indicates that as the layer m-approaches the singularity point, the stiffness matrix for the element varies as per the above relationship derived.

4.3 Anisotropic Stress Functions

The Airy stress function is limited to isotropic problems. For an extension to more complex problems, including anisotropic problems, the stress function $\Phi(x, y)$ can be written as

$$\Phi(x, y) = 2\mathrm{Re}\,[\Phi_1(z_1) + \Phi_2(z_2)] \tag{4.21}$$

where, $\Phi1$ (z_1) and Φ_2 (z_2) are arbitrary functions of $z_1 = x + s_1 y$ and $z_2 = x + s_2 y$, respectively. Combining the definition of stress components from the Airy stress function and satisfying the compatibility equation, the following relation is obtained for anisotropic solids in absence of body forces:

$$C_{22}\frac{\partial^4\Phi}{\partial x^4} - 2C_{26}\frac{\partial^4\Phi}{\partial x^3\partial y} + (2C_{12} + C_{66})\frac{\partial^4\Phi}{\partial x^2\partial y^2} - 2C_{16}\frac{\partial^4\Phi}{\partial x\partial y^3} + C_{22}\frac{\partial^4\Phi}{\partial y^4} = 0 \tag{4.22}$$

which reduces to the following simplified equation for isotropic problems,

$$\frac{\partial^4\Phi}{\partial x^4} + 2\frac{\partial^4\Phi}{\partial x^2\partial y^2} + \frac{\partial^4\Phi}{\partial y^4} = \nabla^2(\nabla^2\Phi) = 0 \tag{4.23}$$

The characteristic equation of the homogenous partial differential equation (4.23) is

$$C_{11}S^4 - 2C_{16}S^3 + (2C_{12} + C_{66})S^2 - 2C_{26}S + C_{22} = 0 \tag{4.24}$$

For an orthotropic material with axes of orthotropy (1,2) coinciding Cartesian (x, y) axes, $c_{16} = c_{26} = 0$, the characteristic Eq. (4.24) is reduced to [10]:

$$S^4 + \left(\frac{E_1}{\mu} - 2v_1 \right) S^2 + \frac{E_1}{E_2} = 0 \qquad (4.25)$$

Finally, the stress components are defined from the second derivatives of the complex stress function $\Phi_i^{''}$

$$\left.\begin{aligned} \sigma_x &= 2\,\mathrm{Re}\left[S_1^{\,2}\, \Phi_1^{''}(z_1) + S_2^2\, \Phi_2^{''}(z_2) \right] \\ \sigma_y &= 2\,\mathrm{Re}\left[\Phi_1^{''}(z_1) + \Phi_2^{''}(z_2) \right] \\ \sigma_{xy} &= -2\,\mathrm{Re}\left[S_1\, \Phi_1^{''}(z_1) + S_2\, \Phi_2^{''}(z_2) \right] \end{aligned}\right\} \qquad (4.26)$$

where and the displacements are obtained from the first derivatives of the complex stress function, $\Phi_i^{'}$:

$$\begin{aligned} u_x &= 2\,\mathrm{Re}\left[P_1\ \Phi_1^{'}(z_1) + P_2\ \Phi_2^{'}(z_2) \right] \\ u_y &= 2\,\mathrm{Re}\left[q_1\ \Phi_1^{'}(z_1) + q_2\, \Phi_2^{'}(z_2) \right] \\ p_i &= C_{11} S_i^2 + C_{12} - C_{16} S_i \quad \text{i=1, 2} \\ q_i &= C_{12} S_i + {C_{22}}/{S_i} - C_{26} \quad \text{i=1, 2} \end{aligned} \qquad (4.27)$$

4.4. Finite Element Method in Anisotropic Fracture Mechanics

Saouma [5] extended the original isotropic maximum circumferential tensile stress theory to anisotropic solids. In this case, the fracture toughness is no longer uniquely defined. Instead, two values of K_{IC}^1 and K_{IC}^2 are required for characterizing the behaviour of crack in a homogenous and transversely isotropic solid with elastic constants E_1, E_2, andμ_{12} (Figure 4.5). For a crack arbitrarily oriented with respect to direction 1, K_{IC}^{θ} would be a function of K_{IC}^1 andK_{IC}^2:

$$K_{IC}^{\theta} = K_{IC}^1 \cos^2\theta + K_{IC}^2 \sin^2\theta \qquad (4.28)$$

In order to avoid performing two separate fracture toughness tests, it is assumed that the ratio of the fracture toughness in both directions is equal to the ratio of the elastic modulus [5]:

$$K_{IC}^2 = K_{IC}^1 \frac{E_1}{E_2} \qquad (4.29)$$

The crack propagation is assumed to be along the direction of the maximum tangential stress σ_θ , while the shear stress is zero:

$$\sigma_\theta = \frac{K_I}{\sqrt{2\pi r}} \mathrm{Re}\left[\frac{s_1 t_1 - s_2 t_2}{s_1 - s_2}\right] + \frac{K_{II}}{\sqrt{2\pi r}} \mathrm{Re}\left[\frac{t_1 - t_2}{s_1 - s_2}\right] \tag{4.30}$$

Where

$$t_1 = (s_2 \sin\theta + \cos\theta)^3$$

$$t_2 = (s_1 \sin\theta + \cos\theta)^3$$

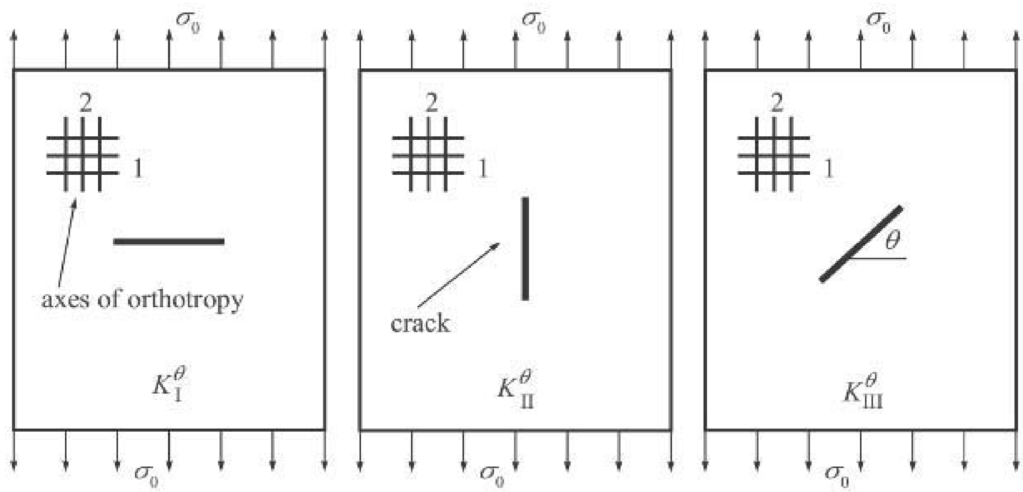

Figure 4.5 Fracture toughness for homogeneous anisotropic solid (Mohammadi, 2008)

4.5 Energy Release Rate and Stress Intensity Factor for Anisotropic Materials

As cited by Mohammadi [10] the concept of energy release rate determination for isotropic materials can be extended to anisotropic materials according to the following relation:

$$\begin{cases} G_I = -\frac{1}{2} K_I C_{22} \,\mathrm{Im}\left[\frac{K_I (s_1 + s_2) + K_{II}}{s_1 s_2}\right] \\ G_{II} = \frac{1}{2} K_{II} C_{11} \,\mathrm{Im}\left[K_{II}(s_1 + s_2) + K_I s_1 s_2\right] \\ G_{III} = \frac{1}{2} K_{III}^2 \left[s_3 c_{66} - c_{56}\right] \frac{1}{c_{66} c_{56}} \end{cases} \tag{4.31}$$

The use of finite element method in fracture mechanics has been quite extensive both in the elastic and elastic-plastic range. A number of special crack tip finite elements have been developed Reddy and Ramamurthy [25], using the displacement method and also the hybrid method. These special crack tip elements lack constant strain and rigid body motion I modes and as a result they do not pass the patch test and necessary requirements for convergence [25].

To overcome these problems, the 8-noded isoparametric elements are used (Figure 4.6). The singularity in these non-singularity elements is achieved by placing the mid-side nodes near the crack tip at the quarter point. It is well known that such elements in their non-singular formulation satisfy the essential convergence criteria as cited in the literature of Reddy and Ramamurthy [25], namely, inter-element compatibility, constant strain modes, continuity of displacements, and rigid body motion modes. These elements also pass the patch test.

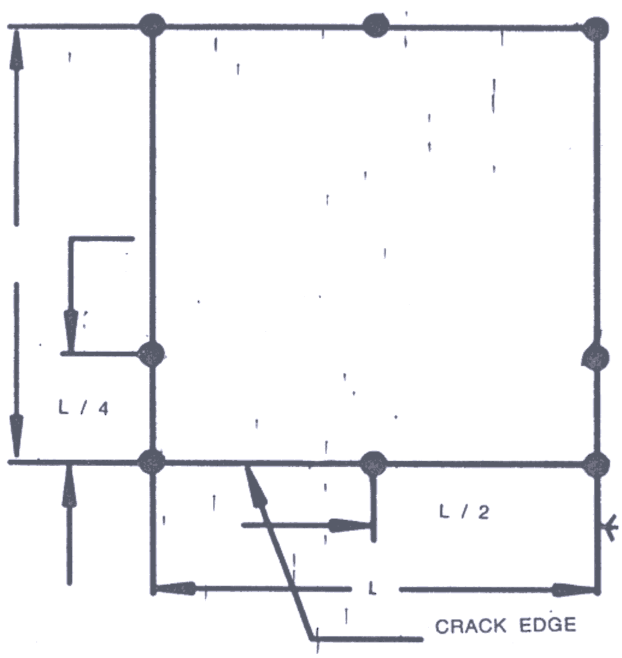

Figure 4.6-8-noded isoparametric element with singularity [23]

Singular Quadratic Isoparametric Elements

The formulation of isoparametric element stiffness is well-documented. The geometry of an 8-noded plane isoparametric element is mapped into the normalised square space (ξ,η) (-1≤ ξ≤ 1, -1≤ η≤ 1) through the following transformations.

$$x = \sum_{i=1}^{8} N_i(\xi,\eta)x_i$$
$$y = \sum_{i=1}^{8} N_i(\xi,\eta)y_i \tag{4.32}$$

$$N_i = \frac{(1+\xi\xi_i)(1+\eta\eta_i)-(1-\xi^2)(1+\eta\eta_i)-(1-\eta^2)[(1+\xi\xi_i)]\xi_i^2\eta_i^2}{4} + (1-\xi^2)(1+\eta\eta_i)(1-\xi^2)\eta_i^2/2 + (1-\eta^2)(1+\xi\xi_i)(1-\eta_i^2)\xi^2/2 \tag{4.33}$$

where N_i are the node shapes that correspond to the node *i*, whose coordinates are (x_i, y_i) in the x-y system and (ξ_i, η_i) in the transformed ξ, η system.

$(\xi, \eta = +1)$ for corner points and zero for mid-side nodes. The displacements are interpolated by:

$$u = \sum_{i=1}^{8} N_i(\xi,\eta)u_i$$
$$v = \sum_{i=1}^{8} N_i(\xi,\eta)v_i \tag{4.34}$$

Strain displacements relationship becomes

$$\{\varepsilon\} = [B]\begin{Bmatrix} u_i \\ v_i \end{Bmatrix} \tag{4.35}$$

where, B is the strain displacement matrix

$$B = \begin{bmatrix} \frac{\partial N_i}{\partial x} & 0 \\ 0 & \frac{\partial N_i}{\partial y} \\ \frac{\partial N_i}{\partial y} & \frac{\partial N_i}{\partial z} \end{bmatrix} \tag{4.36}$$

$$\begin{bmatrix} \frac{\partial N_i}{\partial x} \\ \frac{\partial N_i}{\partial y} \end{bmatrix} = [J^{-1}]\begin{bmatrix} \frac{\partial N_i}{\partial \xi_i} \\ \frac{\partial N_i}{\partial \eta_i} \end{bmatrix} \tag{4.37}$$

The stress is then given by

$$\{\sigma\} = [D]\{\varepsilon\} \tag{4.38}$$

$[D]$-is the stress-strain matrix,

The stiffness matrix then becomes the same form as presented above. To obtain a singular element to be used at the crack tip, the stress equation and the strain equation must be singular. This singularity is achieved by placing the mid-side nodes at the quarter point of the sides. For simplicity, the strength of the singularity is found along the line $\eta = -1$ as Reddy and Ramamurthy [25]. The shape functions along this line are,

$$N_1 = -\frac{1}{2}(1-\xi)$$

$$N_2 = -\frac{1}{2}(1+\xi) \qquad (4.28)$$

$$N_5 = -\frac{1}{2}(1-\xi^2)$$

The strain singularity along the line 1-2 $\eta = -1$ is $1/\sqrt{r}$ which is calculated using equations 4.21 to 4.28 by substituting position of the nodes.

4.6 Cracked Composite Shell Modelling in ANSYS

The composite shell is modelled using ANSYS, which is used for pre and post-processing of the model with FEA as the solver. The model is created in the pre-processing stage of the model and the results are viewed in the post-processing stage. The composite shell is created using linear layered shell 99 elements. The properties of the laminae are given as inputs using ANSYS material library.

The cracks in a shell are generated by cutting out a small strip of negligible thickness (0.25mm) and approximately 8mm long created on the position where the crack is assumed to be generated [18]. The crack is considered to be through crack and may be oriented axially or circumferentially. In principle, cracks in mechanical structure are very random in orientation and shape. It is in most cases propagating from one surface or side to the other. How ever, in order to simplify the analysis to the scope the FEA package such simple cracks as circumferential or axial orientation is assumed for this particular application.

As a practical matter, we consider the material Hercules AS4/3501-6. This material is made of thin carbon fibres (approximately 10µm or 0.001 cm in diameter) which are placed in an epoxy prepreg and pressed into thin sheets, with all the fibers running in one direction. The sheets are then stacked so that in each layer the fibres run perpendicularly to the fibres of the previous layer. The sheets are then heated and pressed together, so that the epoxy forms a continuous matrix that holds the fibers together. The resulting laminate is of the form ... 0°/90°/0°/90° ... (Figure 4.7).

Moreover, each layer is quite thin (approx. 500μm), and a shell of this material, 2.5mm thick, contains 5 layers.

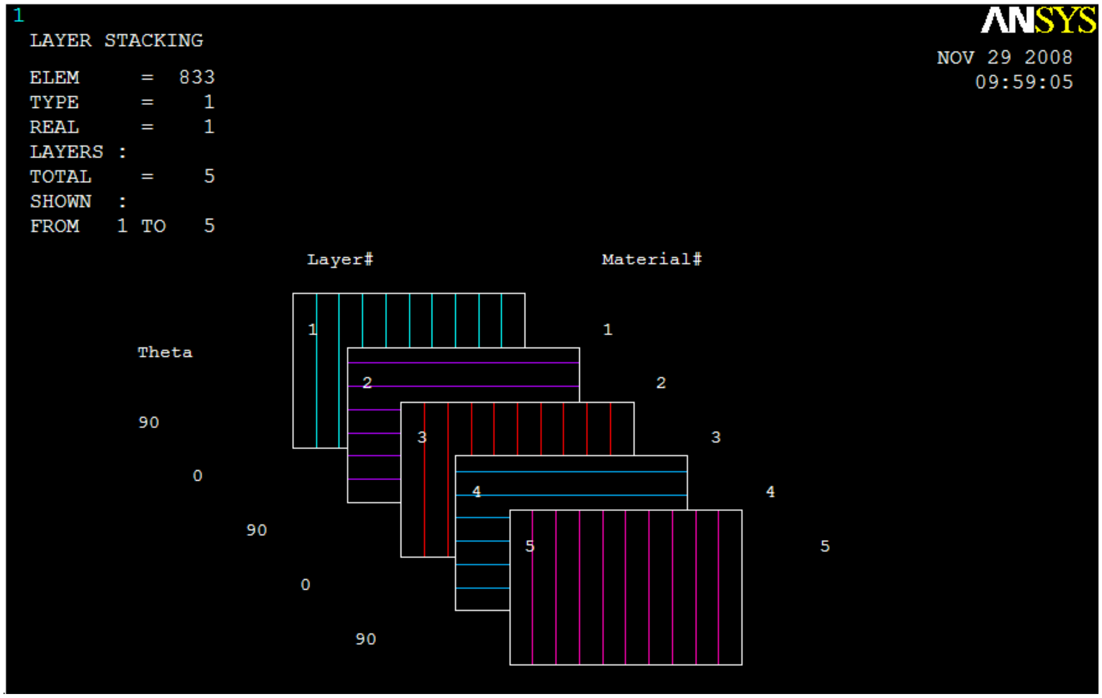

Figure 4.7 The staking sequence of the layers within the laminated shell structure

Let us consider, therefore, modelling of such a composite shell that is made of alternating layers, with layer 1 having fibres which run along the *axial*-direction, and with layer 2 having fibres which run along the *tangential*-direction.

4.6.1 Description of the Parameters of the Model

Crack description:

Width of the crack= 0.25mm .It is generated by cutting out a narrow strip area of 0.25 mm width subtending an angle of 11.25°. Hence, the crack length (a) will be 7.85×10^{-3}m. The crack in this case is oriented tangentially on the periphery of the shell in the tangential direction as shown in figure 4.8.

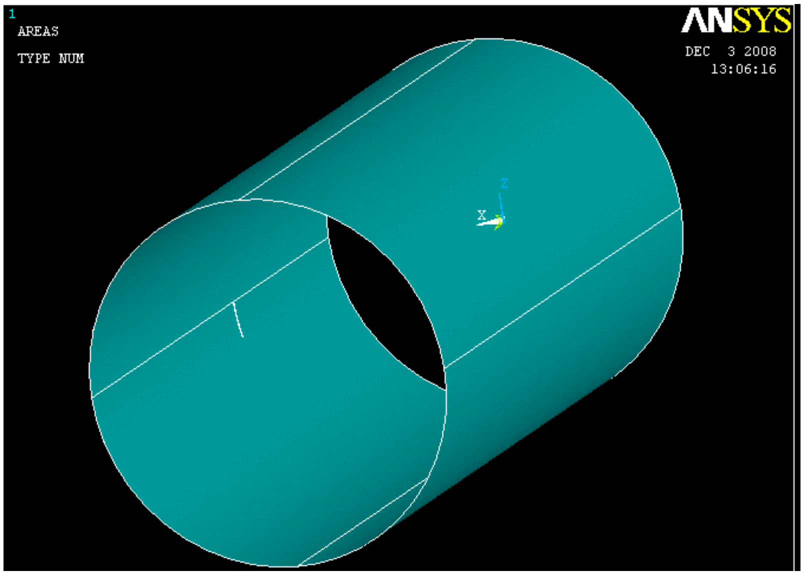

Figure 4.8 Model of composite shell having crack.

Meshing the Model

The model is meshed with automatic mesh generation command “AUTO MESH Generation “. As can be seen from figure 4.9, the model is meshed with more refined elements in the vicinity of the crack and coarsely meshed in areas away from the crack to economize the computation time.

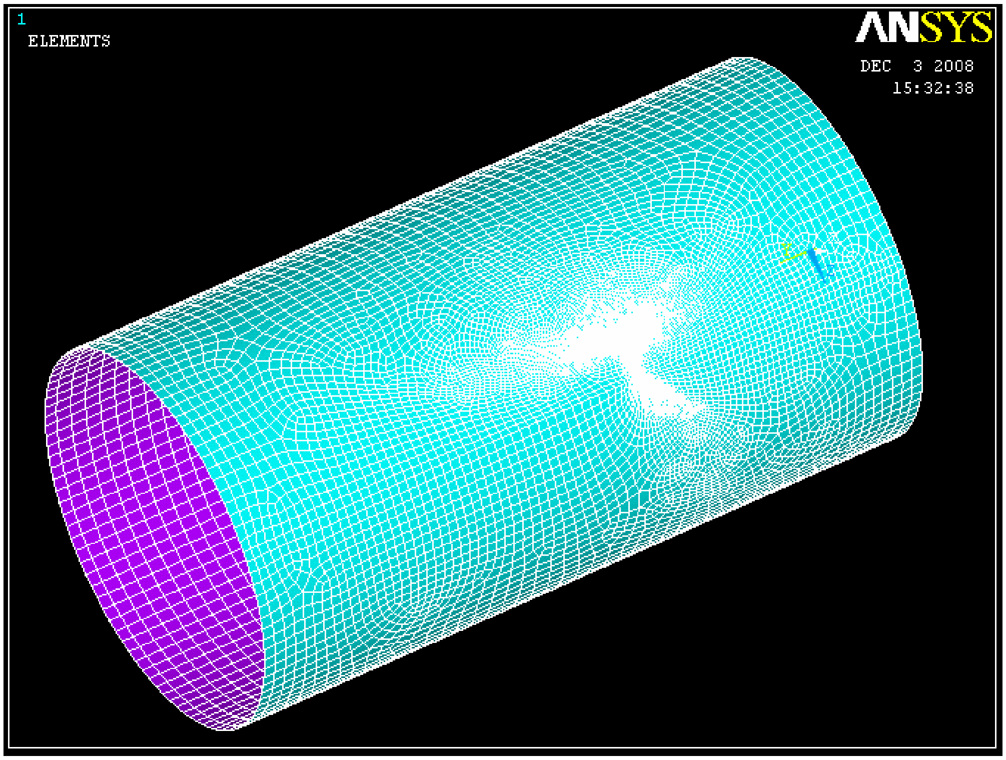

Figure 4.9 Model meshed for analysis

Geometric parameters of the model

Outer diameter= 80mm

Layer thickness= 0.5mm

Inner diameter = 75mm

Length of the cylinder= 150mm

Material of the laminate

The material of the laminate is made of linear elastic orthotropic material with the following properties:

Material= Carbon/Epoxy; $(\sigma^{T}{}_{1})_{ult} = 2000MPa$, $(\sigma_{2}^{T})_{ult} = 52MPa$, $(\tau_{12})_{ult} = 70MPa$

Density = 1.55g/cm^3

E_x = 161GPa

E_y = 9GPa

E_z = 9Gpa

PR_{XY} = 0.26

PR_{YZ} = 0.01

PR_{XZ} = 0.26

G_{xy} = 6.1GPa

G_{yz} = 1GPa

G_{xz} = 6.1GPa

Staking sequence = [90/0/90/0/90]°

4.6.2 Loading and Boundary condition

The shell is constrained at one end with all its degrees of freedom fixed and subjected to a tensile load at the other end as illustrated in figure 5.10.

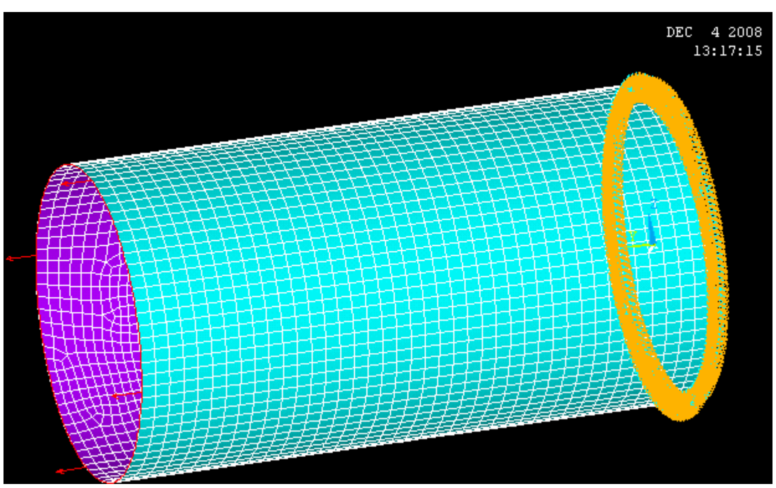

Figure 4.10 Meshed model with boundary condition and load

CHAPTER FIVE
RESULT AND DISCUSSION

5.1 Introduction

The simulation of damage and fracture in structures using Finite Element models can be normally done using the concepts of Fracture Mechanics. The two fundamental aspects of the numerical representation of damage and fracture using finite elements are the kinematic description of the fracture process zone (crack) and the associated constitutive models as presented elsewhere in the previous chapters.

Unlike isotropic materials, the fracture mechanisms of composites are caused as the result of one of the mechanisms: fiber fracture, matrix transverse cracking, fiber pull out or delamination as shown in figure 5.1.

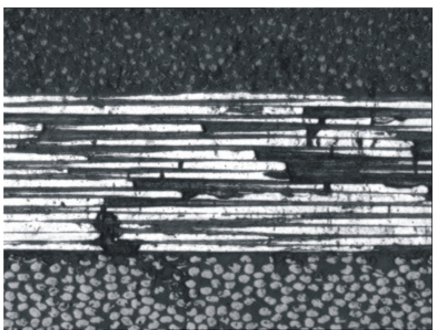

(a) Fibre fracture

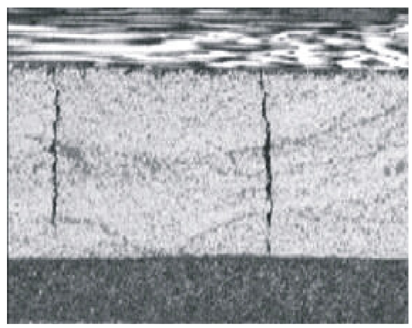

(b) Matrix transverse crack

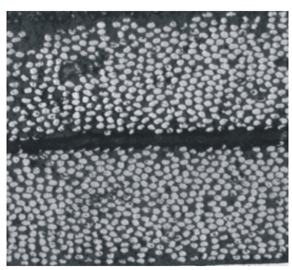

(c) Delamination

Figure 5.1 Fracture mechanisms of composite materials

The Finite Element Models developed to investigate the mode of crack in the cylindrical shell made of composite material using Fracture Mechanics represent the finite element problem of a structure containing a through-crack. Using Linear Elastic Fracture Mechanics (LEFM), crack propagation is predicted by observing the distribution of the stress intensity or strain, which may be used as the description of the components of the energy release rate taken as material properties.

Theoretically, the numerical computation of the stress intensity factors, or of the energy release rate, can be performed using different techniques: J-integral, and the virtual crack closure technique (VCCT). Stability of crack growth can be easily assessed by computing the values of the energy release rate (G) at different crack lengths (a) and calculating the derivative of the energy release rate with respect to the crack length, i.e. if $\partial G / \partial a < 0$, there is stable crack growth.

The motive behind this work is to investigate the mode of variation of the stress at the crack tip and in the vicinity of the crack tip in a fibre reinforced composite shell structure. The stress distribution provides an indication as to where the fracture could initiate. However, it is very difficult to determine the actual crack path through the laminate. In the absence of any experimental data on fibre fracture initiation and propagation during loading, it is presumed that fibre failure occurs due to maximum principal stress exceeding the tensile strength of the fibre; and the failure is initiated in the planes containing the maximum stress or strain as in the figures presented in the following portions. The first failure corresponds to fibre breaking, whereas, the second failure corresponds to a tensile crack of the matrix material. As the damage (crack) moves towards the fibre, the induced maximum tensile principal stresses on the fibre becomes high enough to cause failure of the fibre. The crack of the fibre grows forward but may experience shielding due to the compressive stresses induced in the structure as a result of bending of the fibres in mode I cracking mechanism as shown in figures 5.2, 5.3, 5.3 and 5.5. At the same time the maximum principal stresses in the fibre is also tensile just away from and on both sides of the crack tip. However, these stresses are less than the failure strength of the fibre. It can, therefore, be concluded that a combination of crushing and bending causes the fibre failure. These fibre failures subsequently lead to the formation of a crack advance in the shell structure.

The direction of the Von Misses principal strain/stress in the failed elements varies between 20º to 30º with respect to the fibre axis as in figure 5.7. This implies that the fibre is likely to break along a plane parallel to the fibre transverse axis.

5.2 Model with Tangential Crack

In accordance with the current study, different kinds of crack tip stress distribution are observed:

- Dispersed wing-shaped and scattered stress distribution areas propagating in the direction farther from the crack tip (figure 5.2).

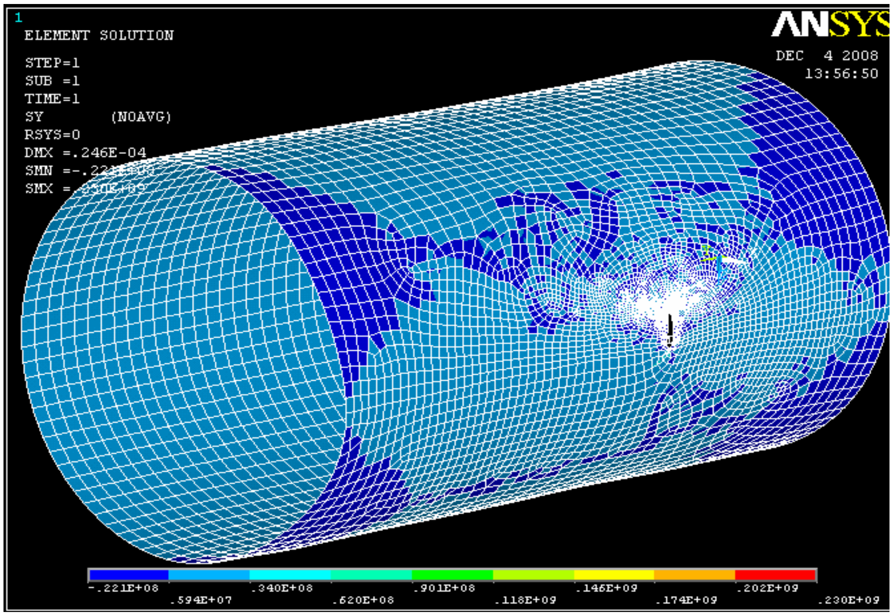

Figure 5.2(a) Crack tip Y-component stress distribution plot

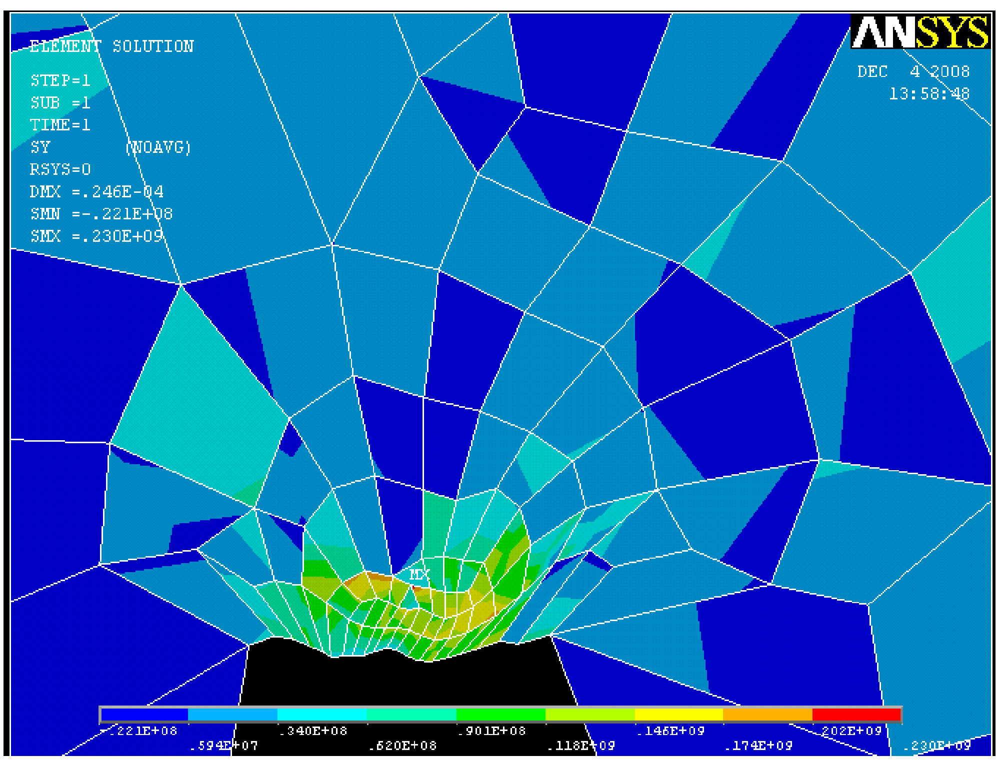

Figure 5.2(b) Crack tip Y-component stress distribution plot in Magnified view

Longitudinal matrix cracks (parallel to the fibres of a layer), going all through the thickness of a layer. The matrix of the material is indented by the bending effect of the fibres contributes to the irregular waviness of the crack tip free edge and forms a stress intensity region shown in figure 5.3 which eventually (at the end of the day) aligns with the weak plane for crack propagation.

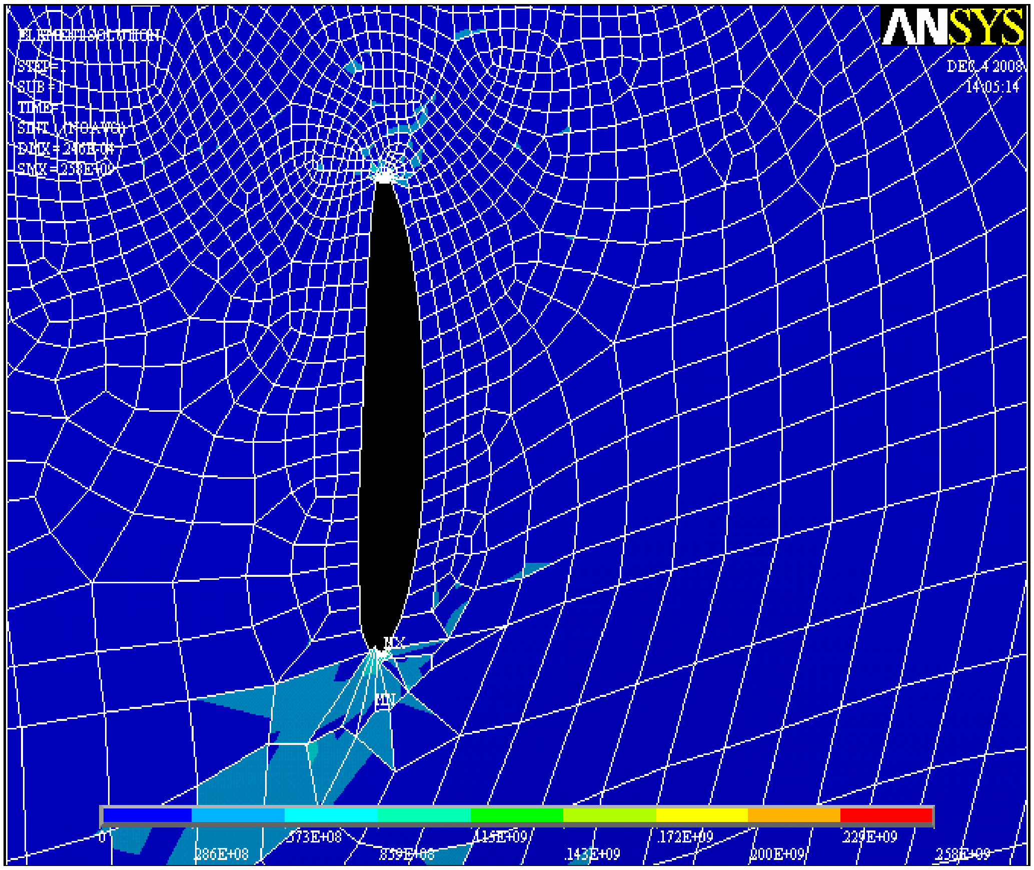

Figure 5.3(a) Stress Intensity distribution ahead of the crack tip plot

The localized maximum Von Misses stress plot presented in figure 5.4 indicates the shielding of the localized damage in the matrix material in front of the crack tip by the immediate fibres and matrix materials. Nonetheless, due to the reinforcement and difference in orientation of the layers of the laminate, different locations in the shell have got different stress and strain intensity levels and show spots of different stress distributions.

At this instant it is reasonable to propose, based on the beam theory, the bending effect of the fibres away from the crack front as the crack initiates. From this proposition, we can take for granted that the adjacent matrix materials to the fibre, on the side away from the crack tip, adjoining with crack will be subjected to compression compared to the matrix material inform of the fibre on the side of the crack for those laminae having fibre orientation parallel to the axis of the shell.

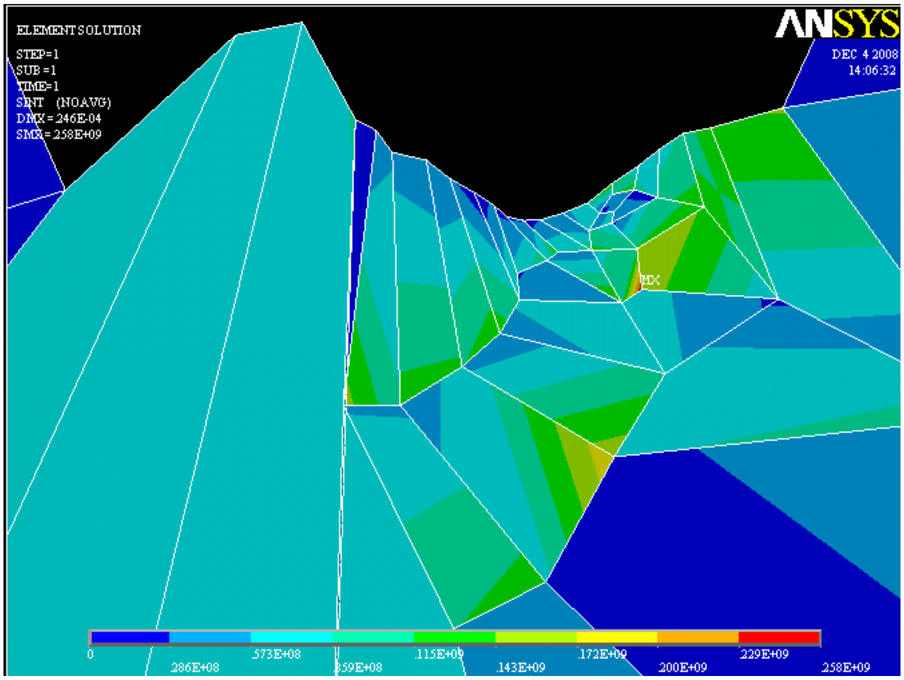

Figure 5.3(b) Amplified stress intensity distribution ahead of the crack tip plot

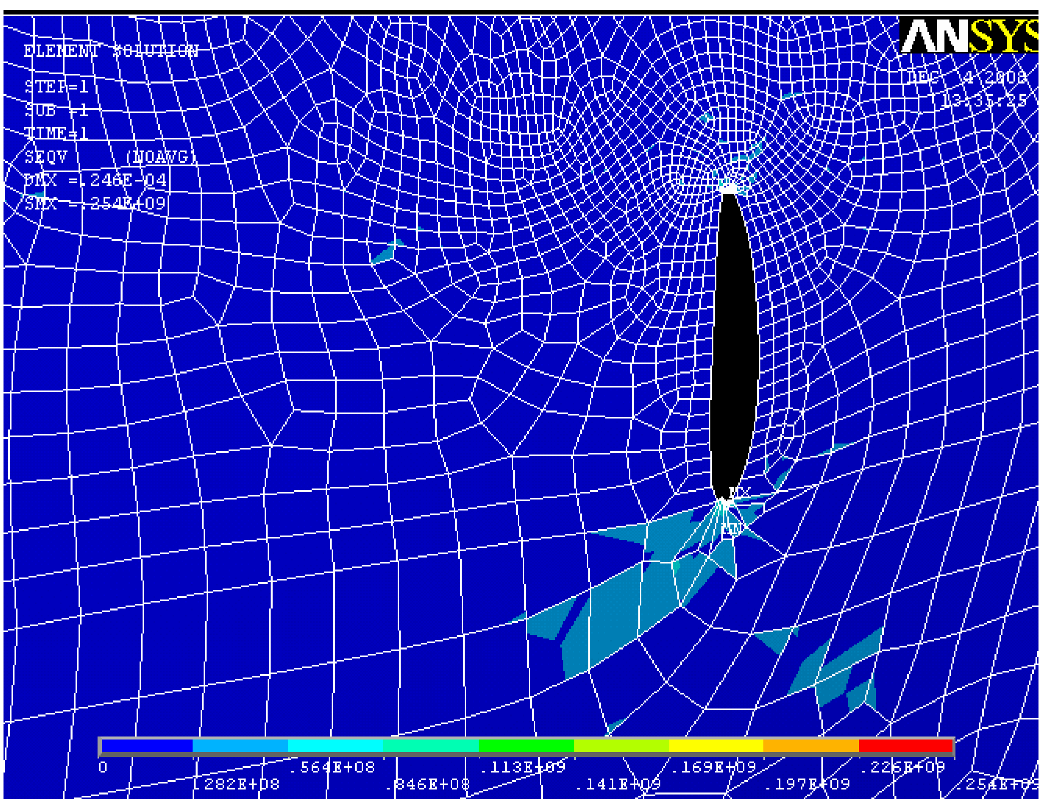

Figure 5.4(a) Crack tip Von Misses stress distribution plot

Nevertheless, the inconsistency of the ruptured fibre material and the matrix material may have an indication of the step by step or successive fracture of the fibre and matrix. Hence, the crack is first initiated in the fibre and ultimately propagates to the matrix when the fibre ruptures. This fibre rupture or break happens as the fibre tends to be pulled out of the matrix under the influence of the tensile loading. The development of irregular contours at the crack tip, shown in figure 5.2 b and 5.3 b, is thus created by the adhesion due to the bonding between the fibre and matrix, and as well the layering made by stacking with fibres of different orientations that has caused the shield of the damage zone at the crack tip. The complex stress conditions created inside the damage zone, which is compressive predominantly, produces protruded irregular contour of the free surface at the crack tip by pushing it towards the free edge.

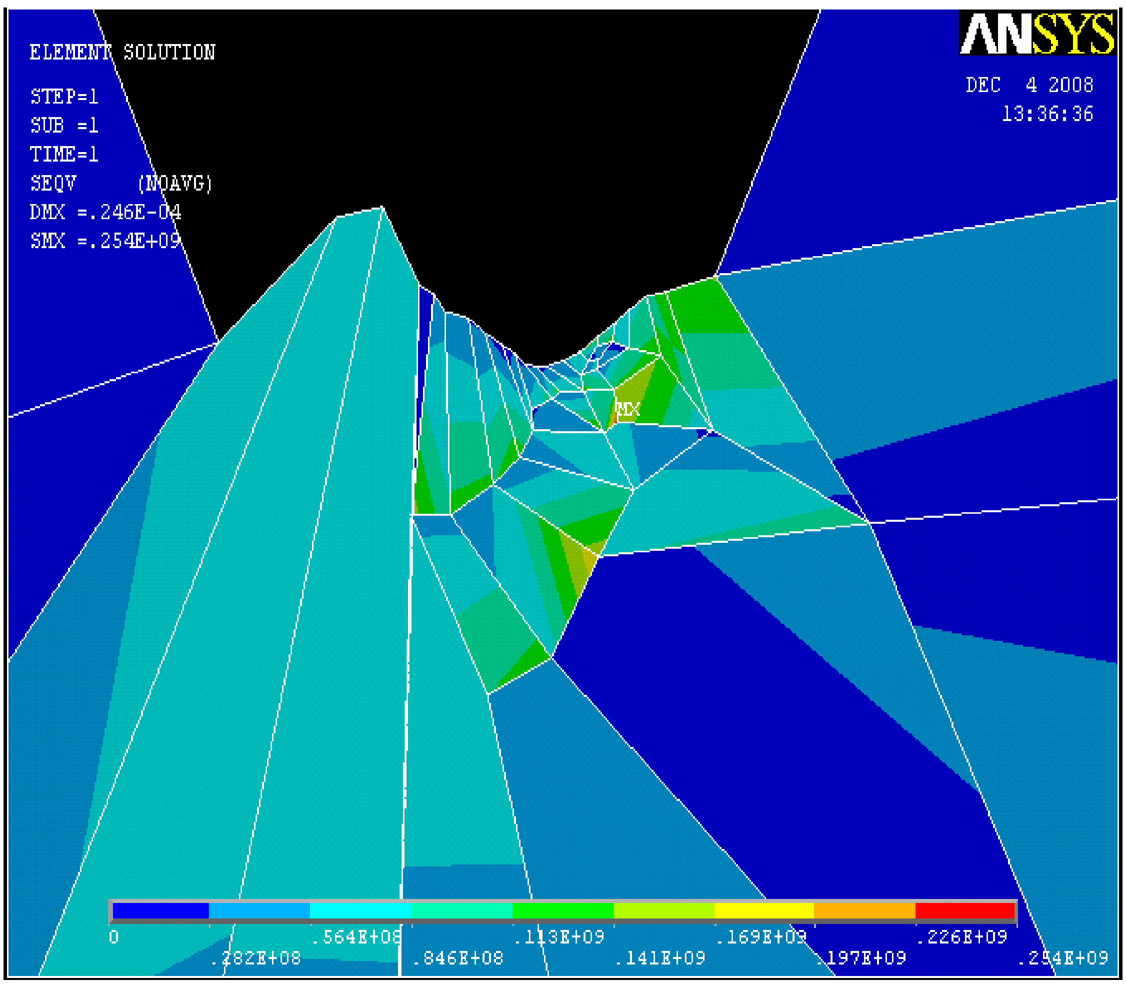

Figure 5.4(b) Crack tip Von Misses stress distribution plot in magnified view

The stress coupling effect in composite materials or the interlaminar adhesion transfers the load applied in the axial direction to the whole body of the shell in radial direction. For similar argument presented before, the pure Z or X-stress components, shown in figure 5.5, have also irregular wave shaped deformation on the free edge of the crack tip and shielded (embedded and covered) critical failure zone due to the indentation effect on the matrix material a head of the crack tip.

Moreover, the interlaminar shear stress induced within the structure is also showing some form of localization and scattered pattern and well coincides with the location of critical stresses and contributes to the crack advance in the structure. The variation style of the shear stress induced in the body is depicted through figures 5.8 to 5.10.

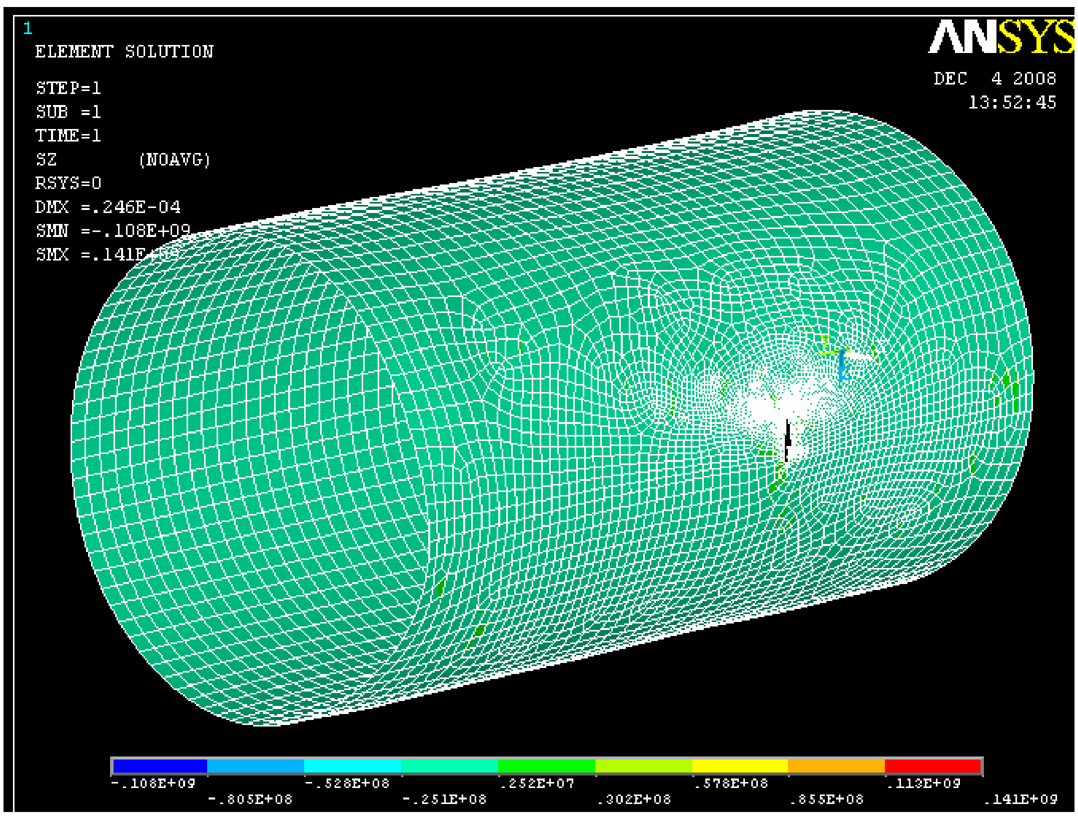

Figure 5.5(a) Crack tip z-component stress distribution plot

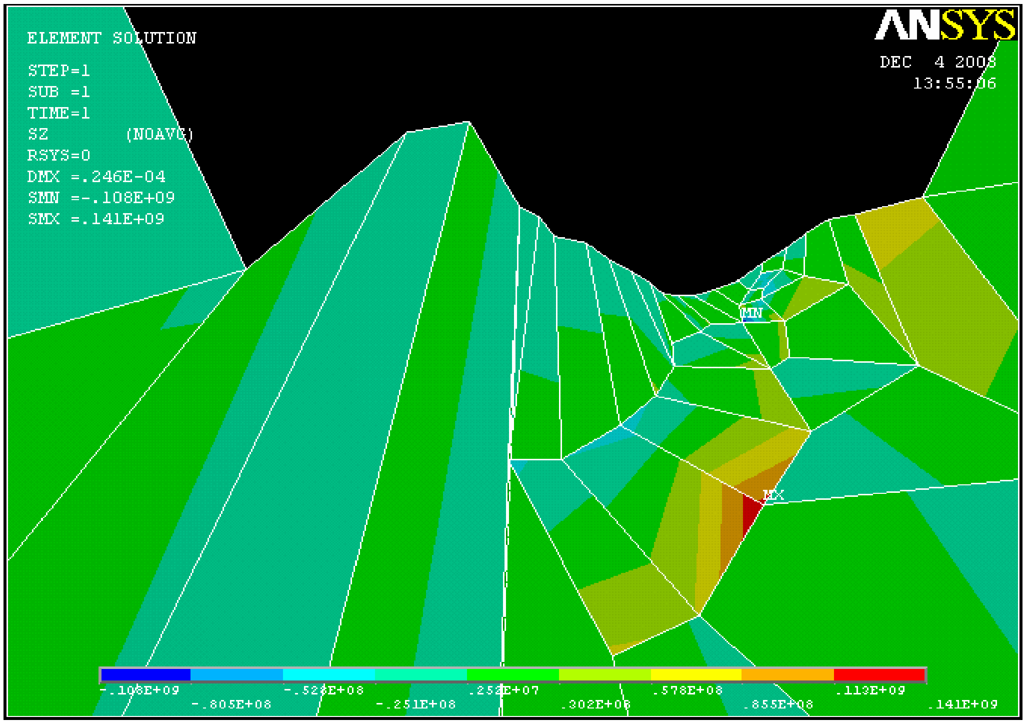

Figure 5.5(b) Crack tip Z-component stress distribution plot in Magnified view

The critical stress or strain region presented in the proceeding figures can be better verified by the stress vector plot, shown in figure 5.6, which shows concentrated stress flow vectors a bit ahead of the crack tip. And this again justifies the argument about shielding of the critically damaged zone a head of the crack front.

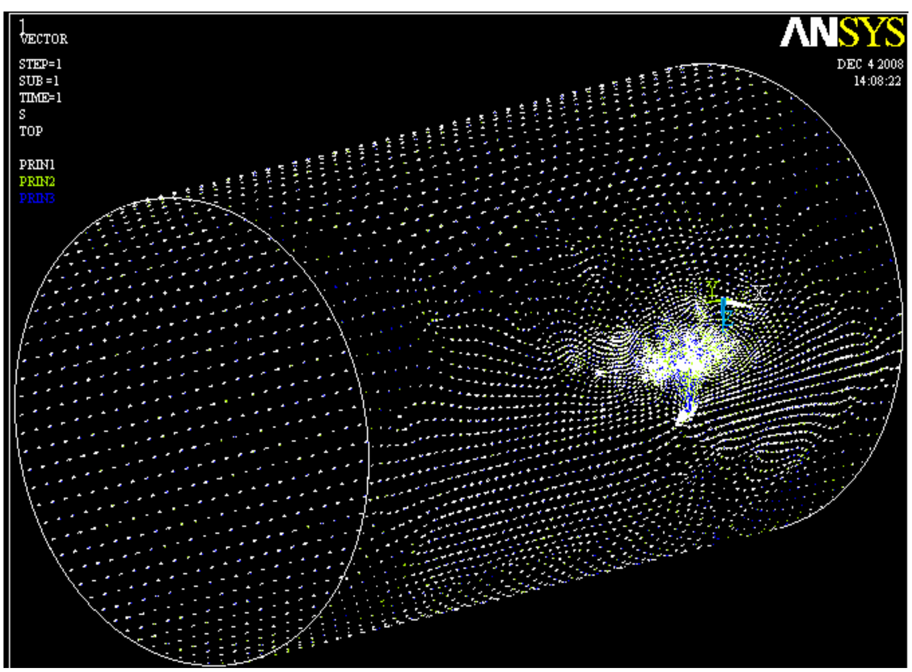

Figure 5.6(a) stress vector plot

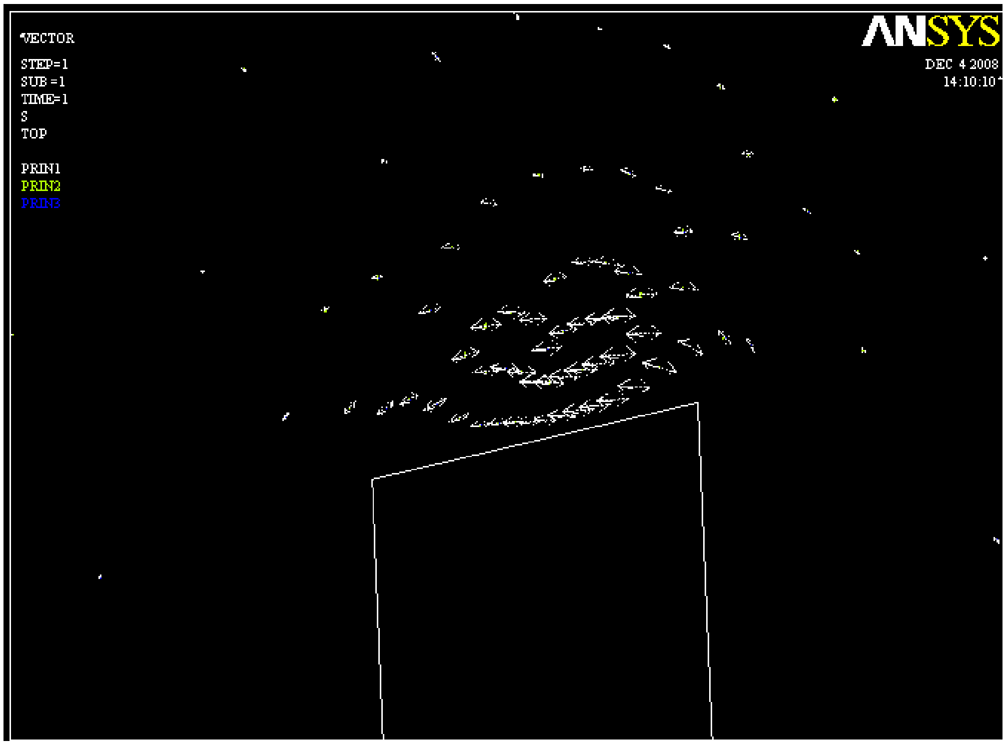

Figure 5.6(b) stress vector plot magnified at the crack tip

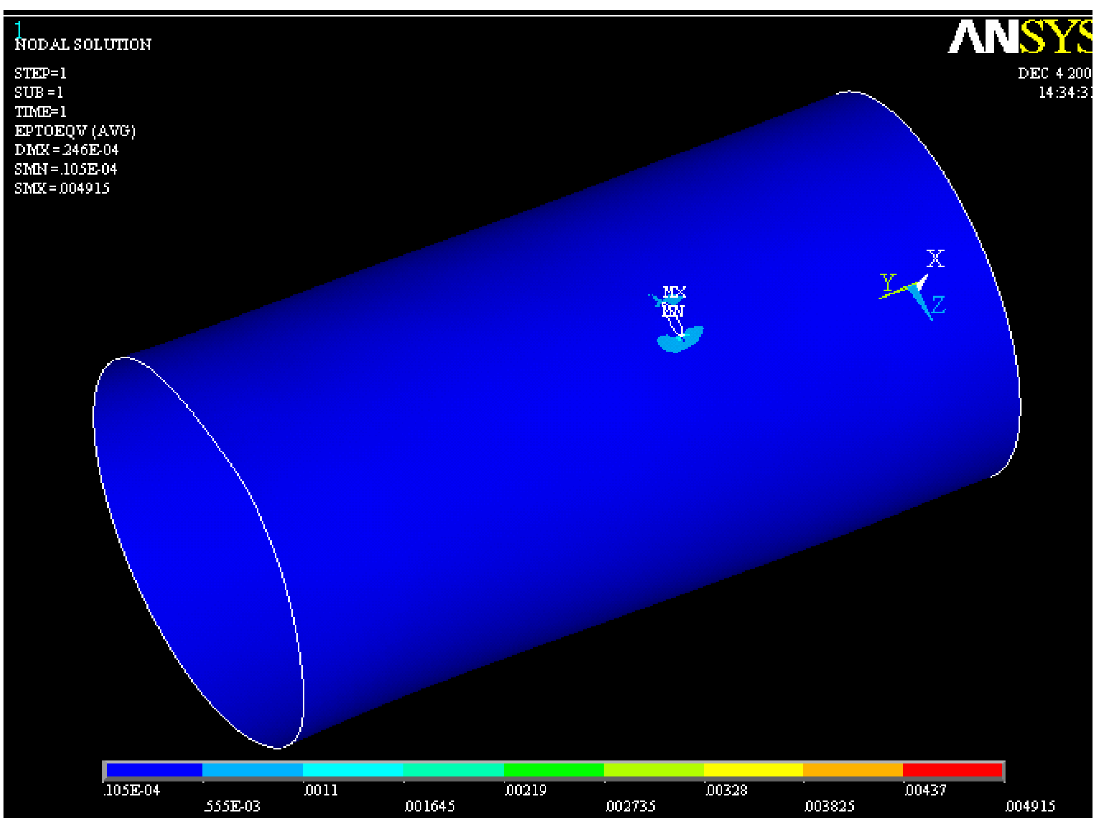

Figure 5.7(a) Total von misses strain plot

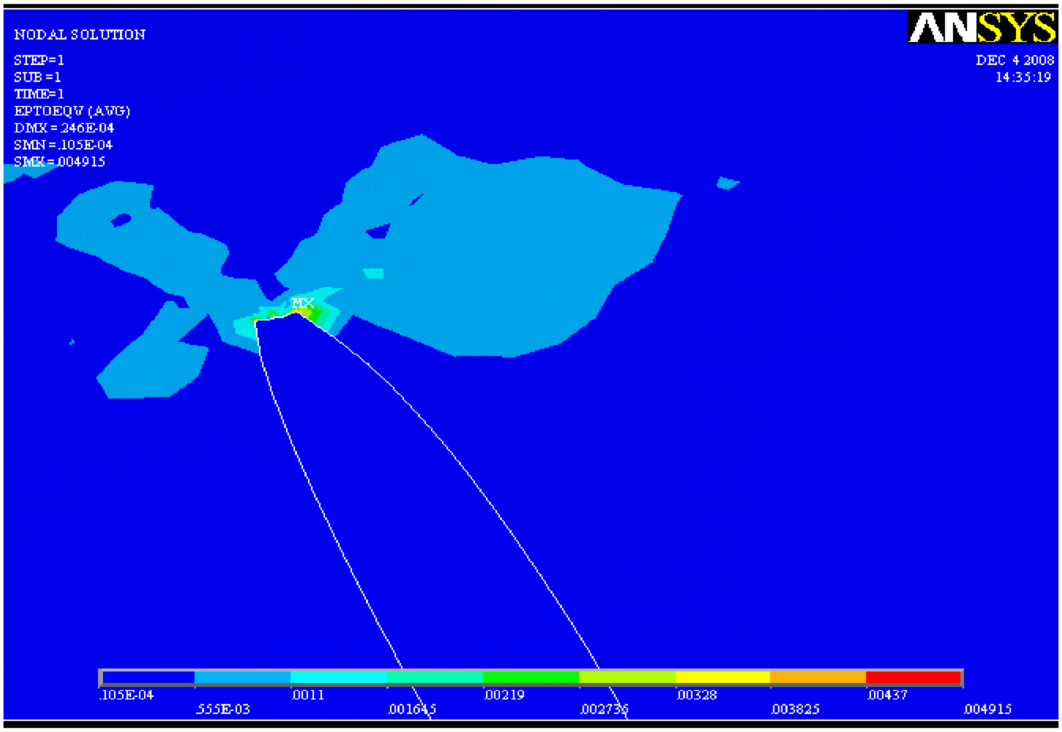

Figure 5.7(b) Magnified total von misses strain plot

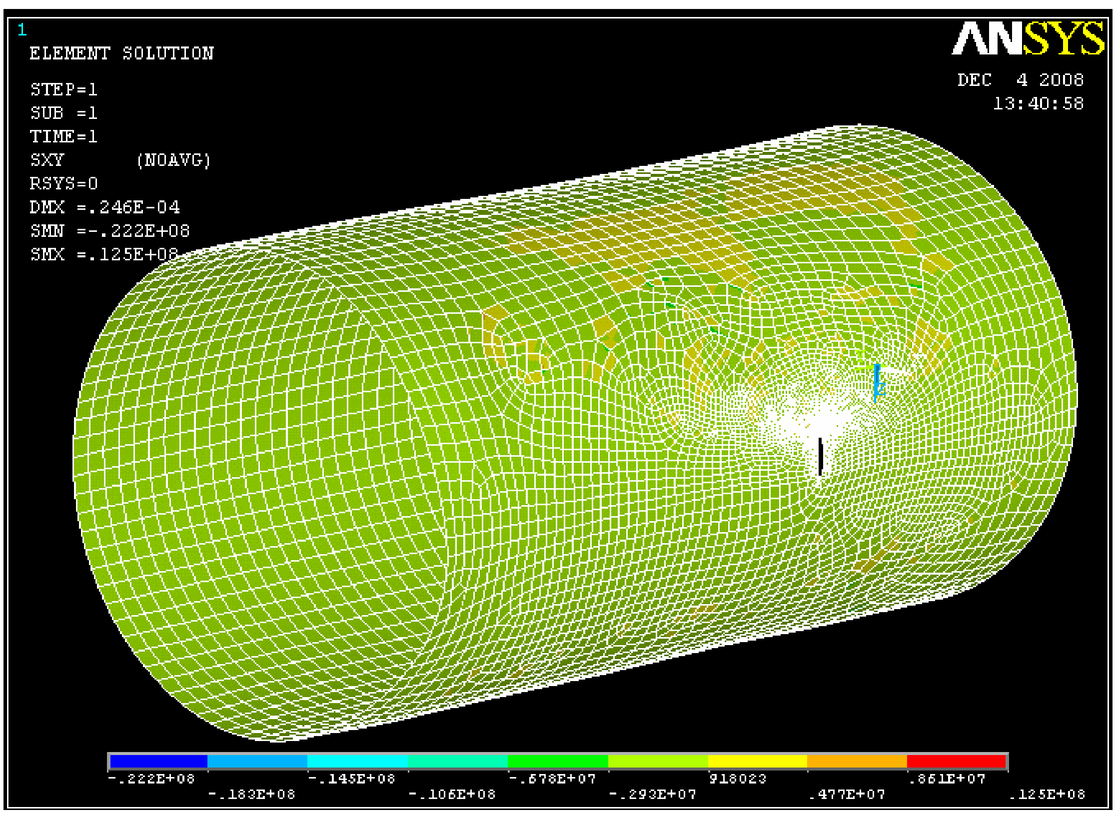

Figure 5.8(a) shear stress distribution on the section perpendicular to the axis of the shell

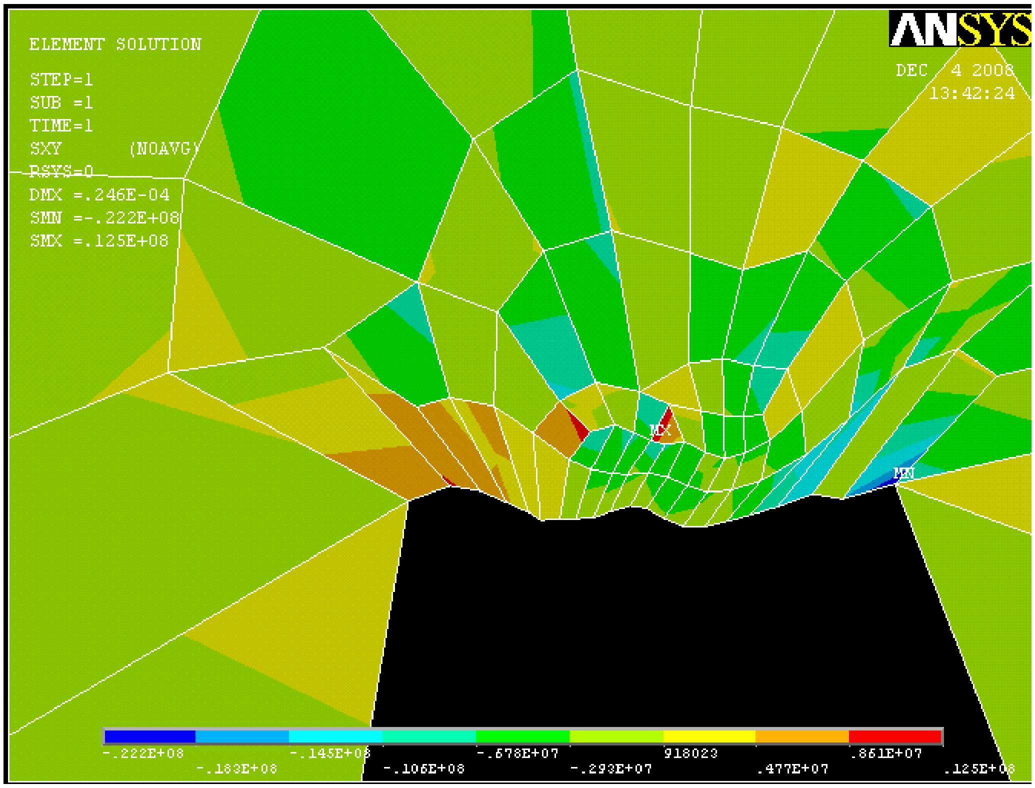

Figure 5.8(b) Magnified shear stress distribution on the section perpendicular to the axis of the shell

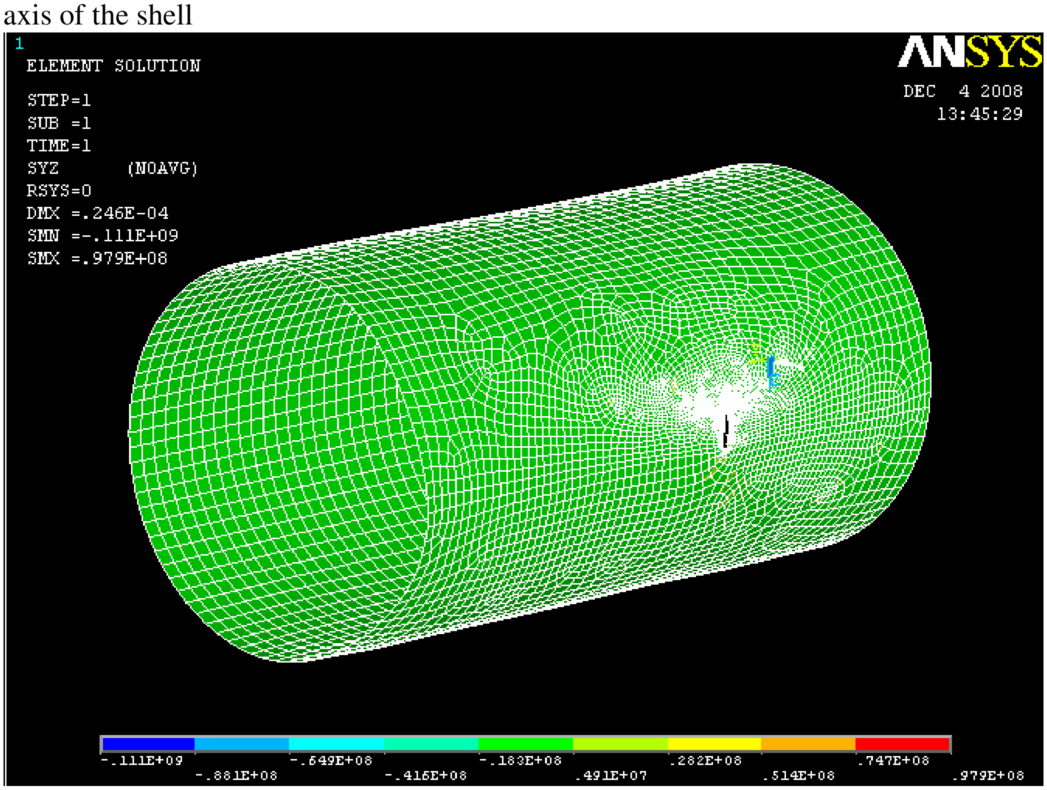

Figure 5.9(a) shear stress distribution in the shell in YZ plane

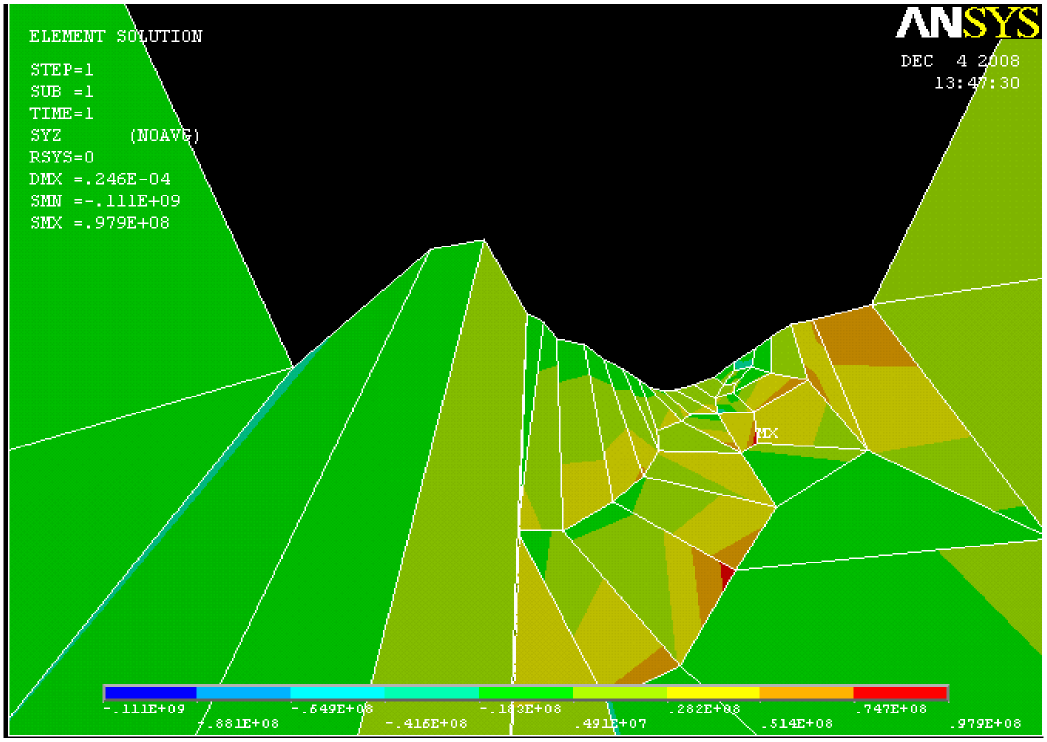

Figure 5.9(b) Magnified shear stress distribution in the shell in YZ plane

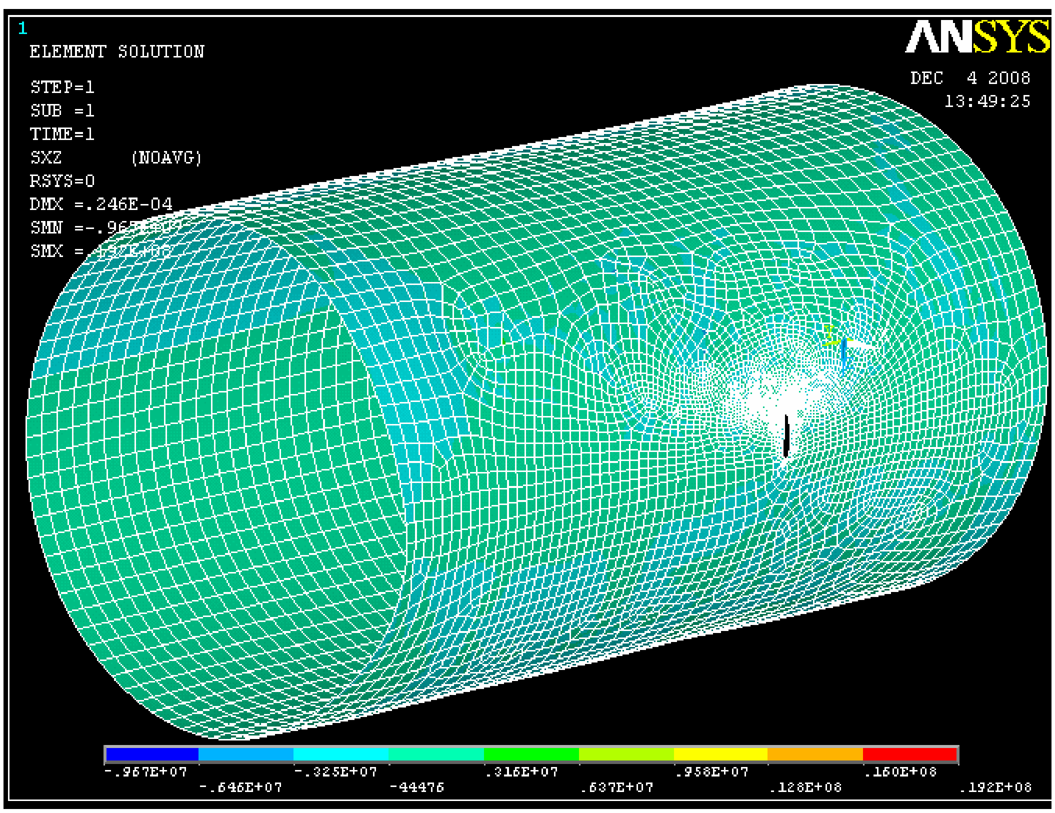

Figure 5.10(a) Shear stress distribution in the shell in XZ plane

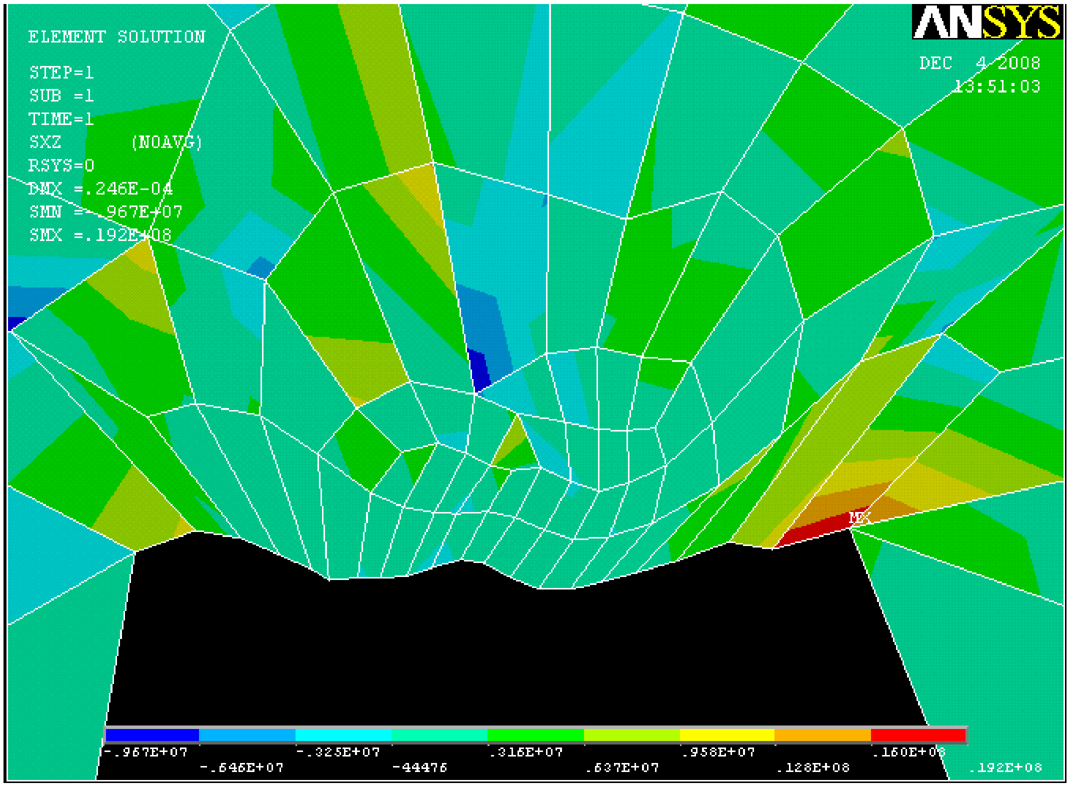

Figure 5.10(b) Magnified shear stress distribution in the shell in XZ plane

The deflection of the composite shell structure under loading towards the cracked side of the shell (figure 5.11) is another output of this analysis which results in the shift in the deflection of the whole shell structure. This implies that, if the shell is to be used as in a dynamic condition rather than stationary condition, it will be subjected to self induced vibration or dynamic loading that may cause fatigue failure of the shell. So, it is imperative that, if crack develops in shell, the shell structure will no more be in balanced condition and it will be under dynamic loading that further makes the condition severe.

Considering again a model with vertical crack, shown in figure 5.12, made of the same material as the previous one and with same geometrical parameter and boundary condition, we can deduce on how stress propagates in the body of the shell structure. In order to make the analysis so reasonable, the meshed shell model presented in figure 5.13 is generated by the ANSYS automatic mesh generation command with very fine elements at the discontinuity points or the crack tip.

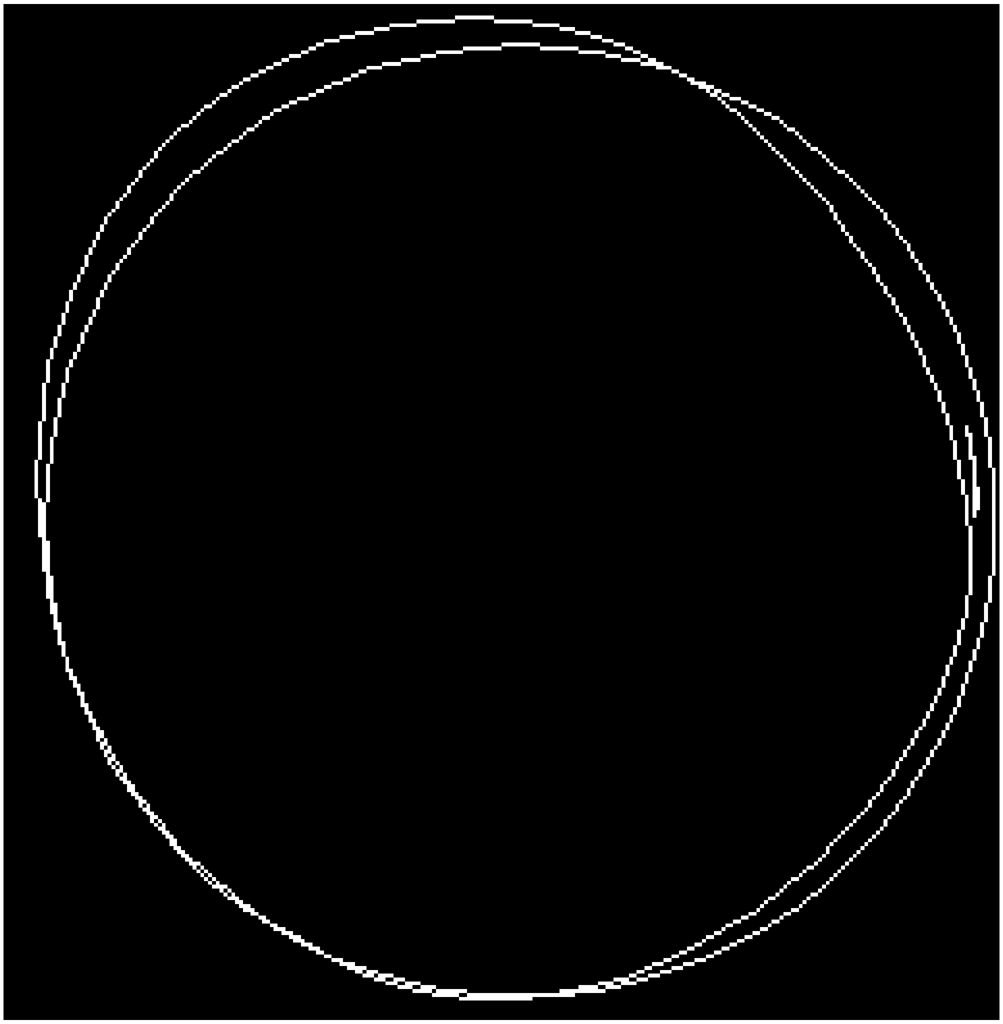

Figure 5.11 Composite shell structure deflected towards the crack

5.3 Model with Axial Crack

A model with the same geometry, boundary condition and material but with the crack axially oriented is developed for the analysis of the stress at the crack tip.

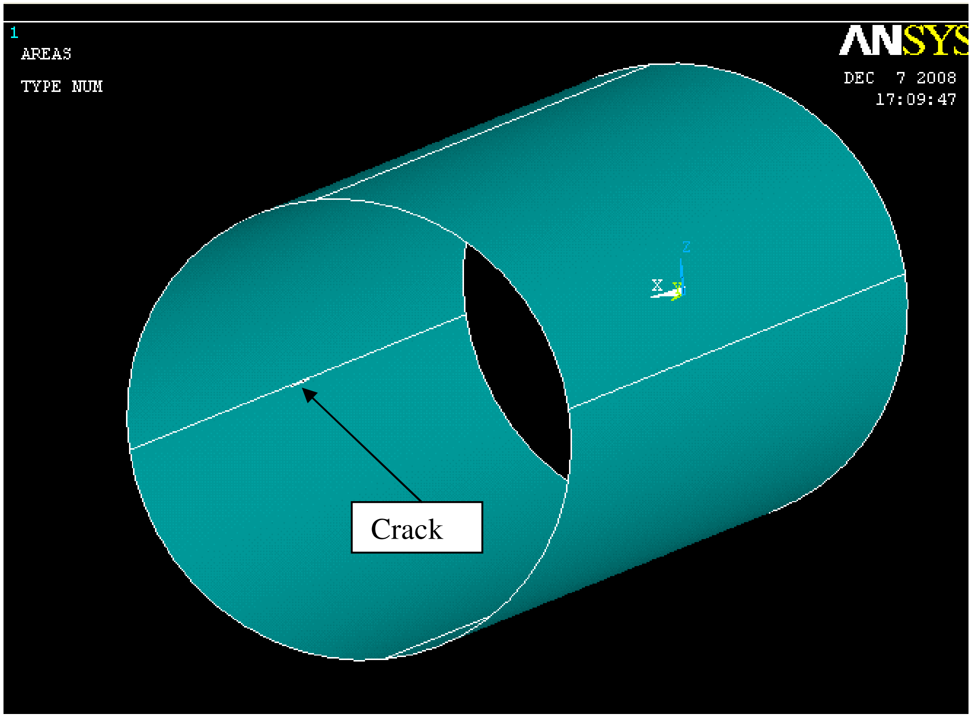

Figure 5.12 Composite shell model with vertical crack

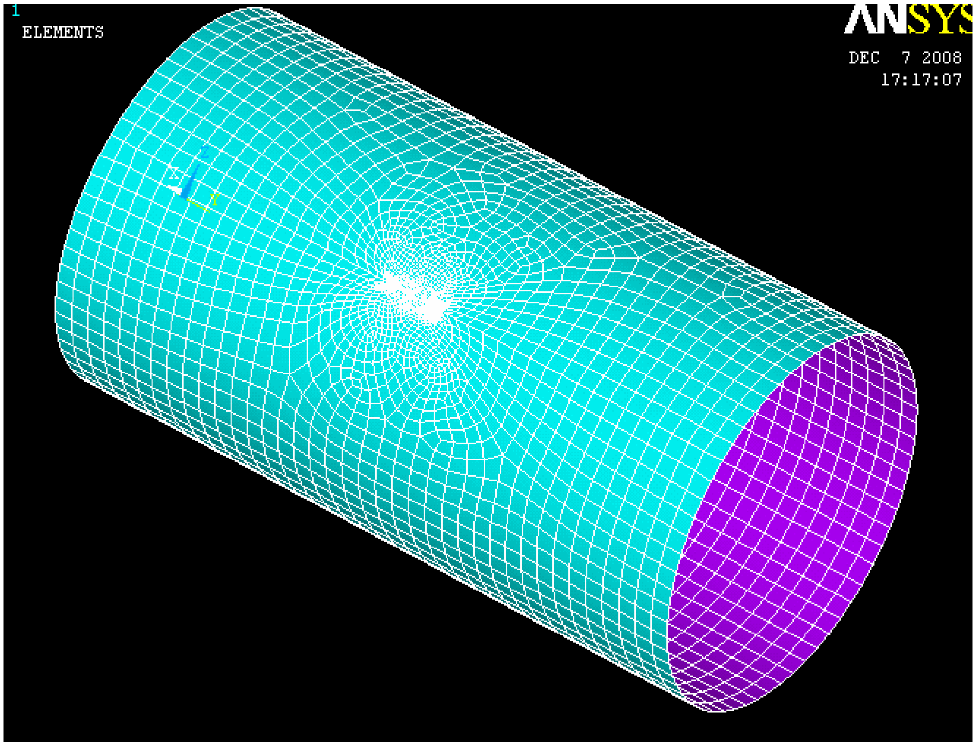

Figure 5.13 Meshed composite shell with vertical crack

The deflection mode for axially cracked shell portrayed in figure 5.14 again describes the formation of weak side of the structure due to the development of flaw or discontinuity. Consequently the shell deflects towards the cracked side when subjected loading and this eventually resulted in the fatigue loading and the crack may be made to propagate dynamically.

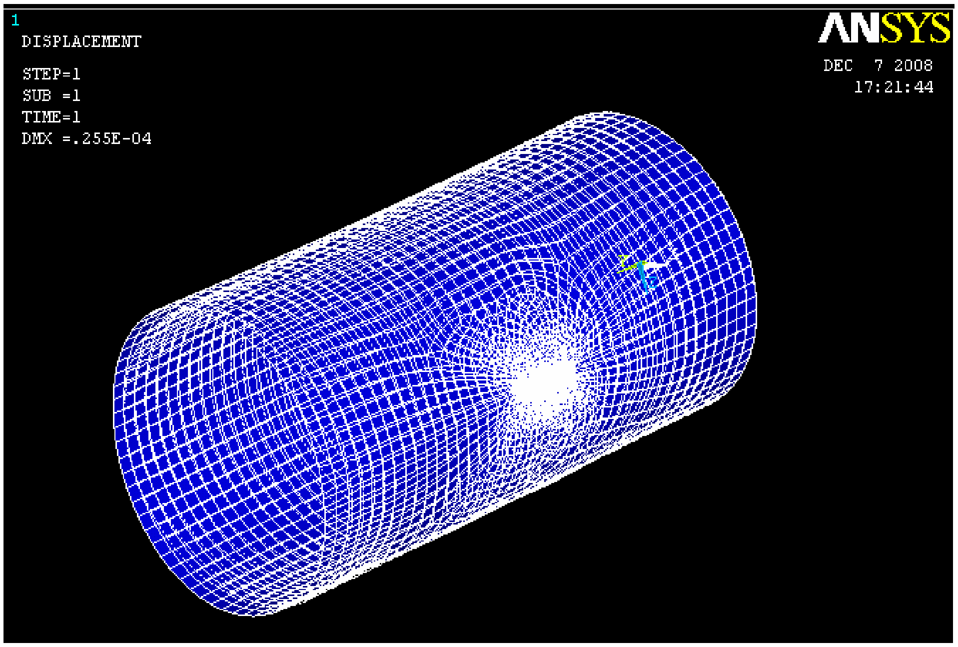

Figure 5.14 a) deformed and undeformed shape of the shell

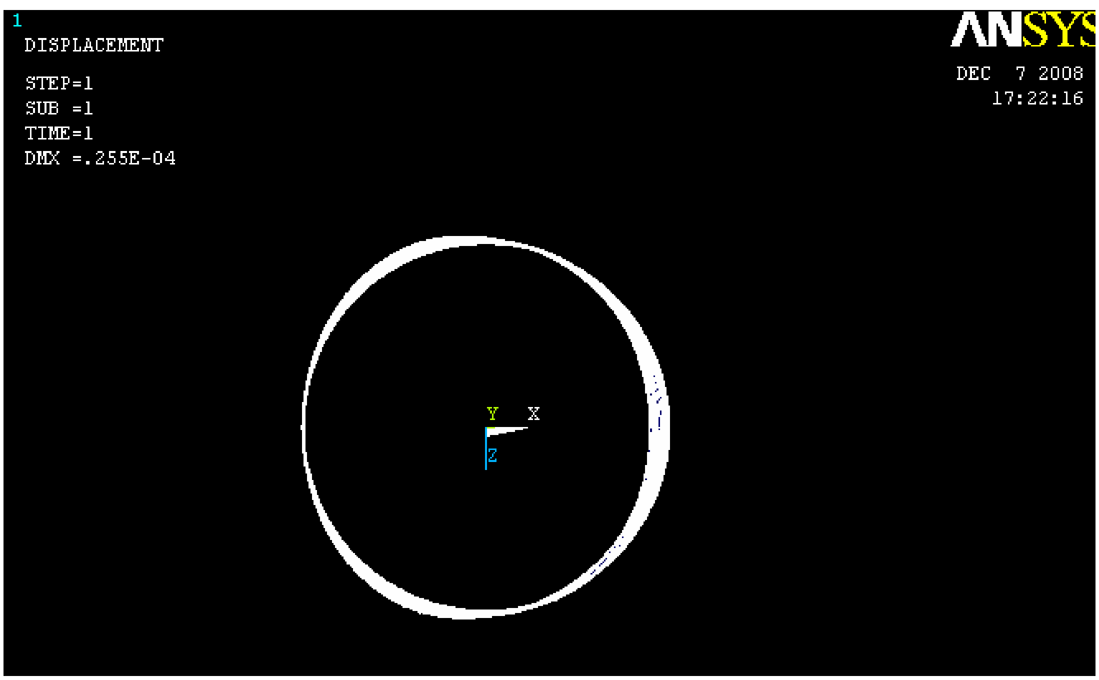

Figure 5.14 b) deformed and undeformed shape of the shell in axial view

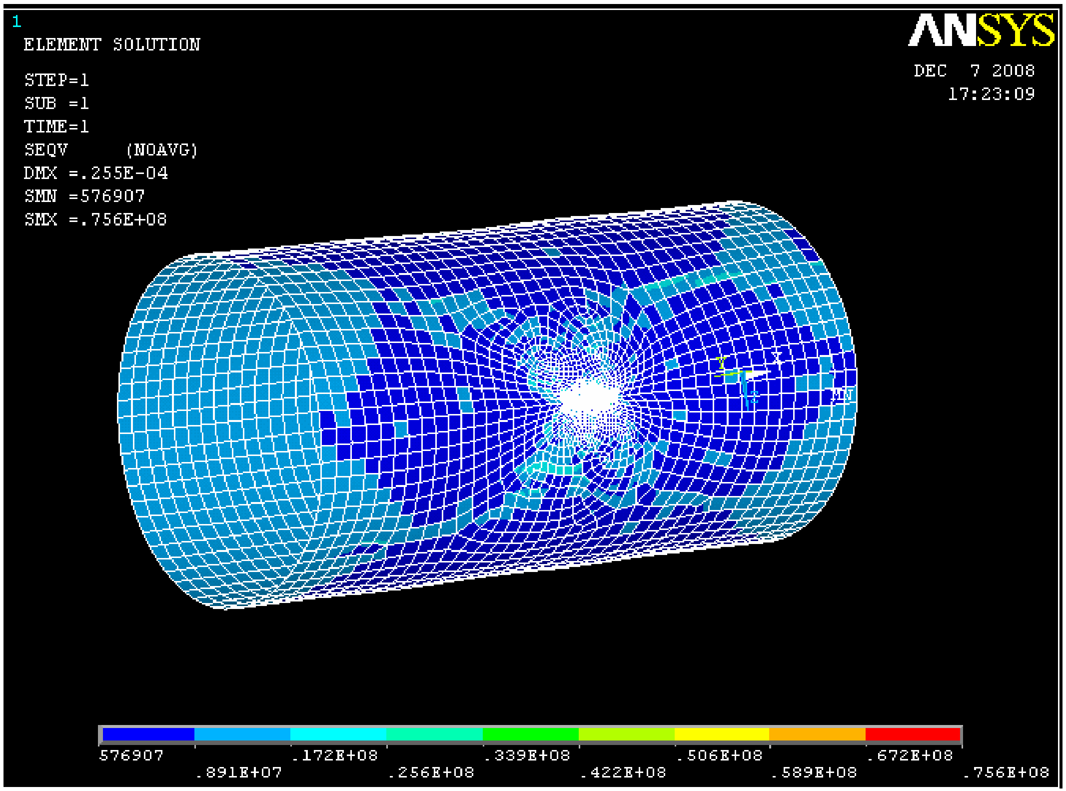

Figure 5.15 a) Von Misses stress distribution for axially cracked shell

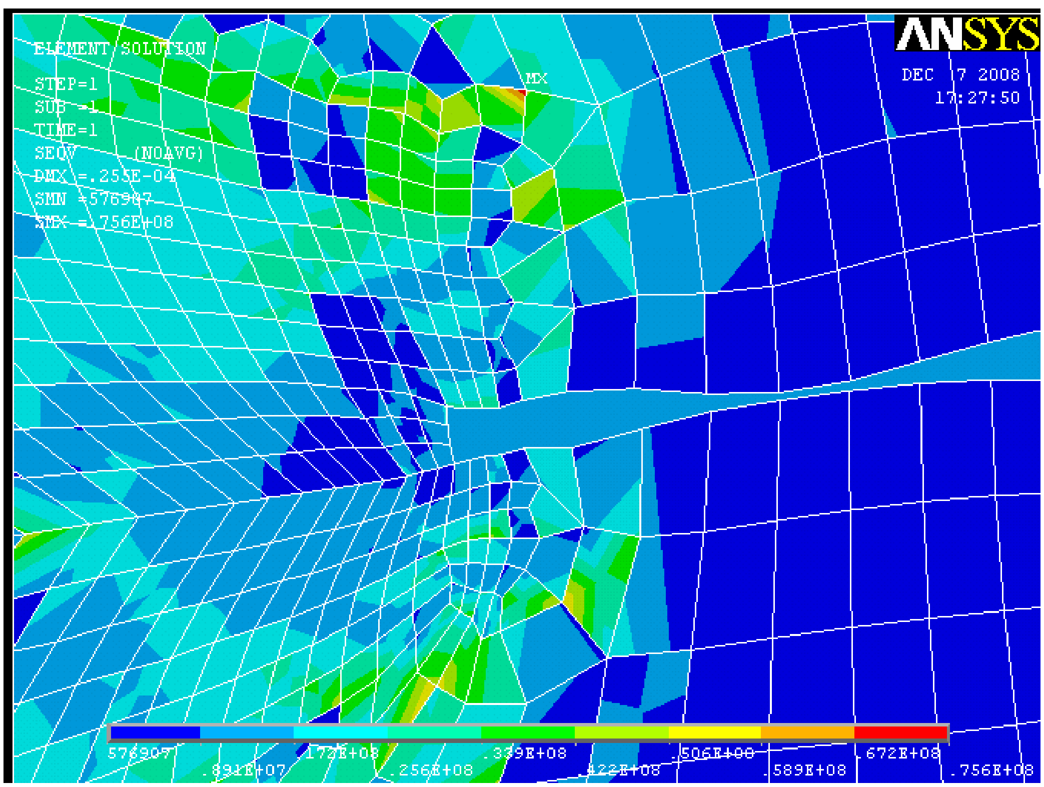

Figure 5.15 b) Von Misses stress distribution for axially cracked shell

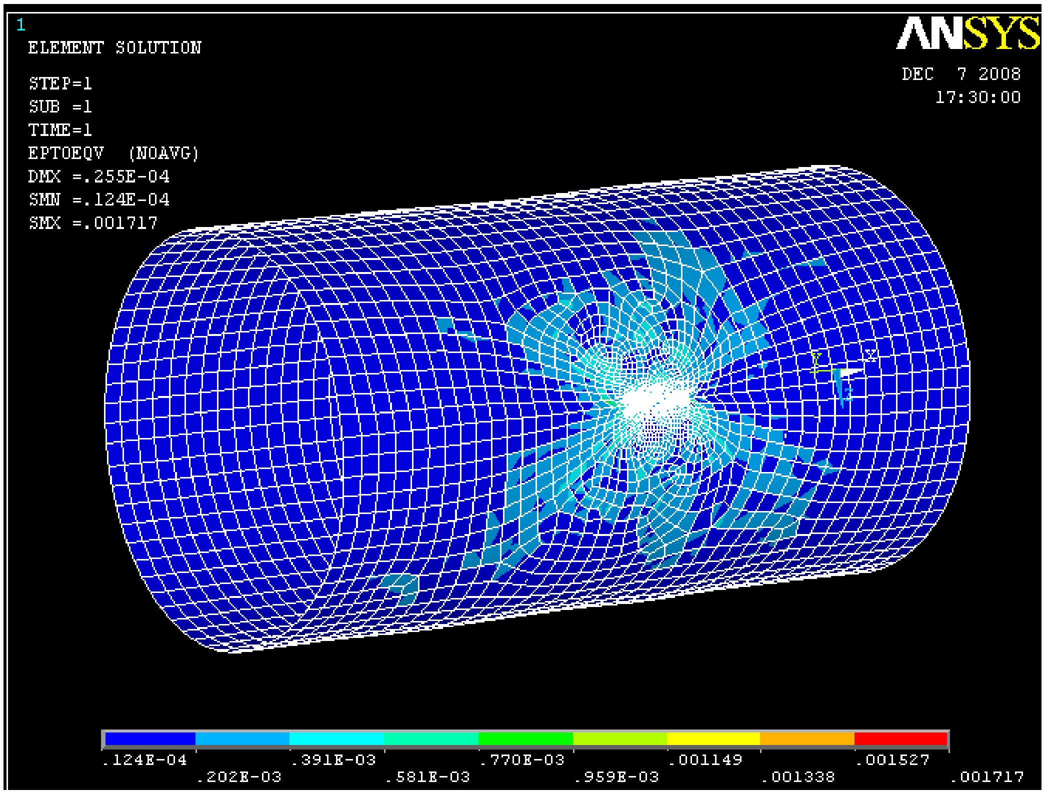

Figure 5.16 a) Von Misses strain distribution for axially cracked shell

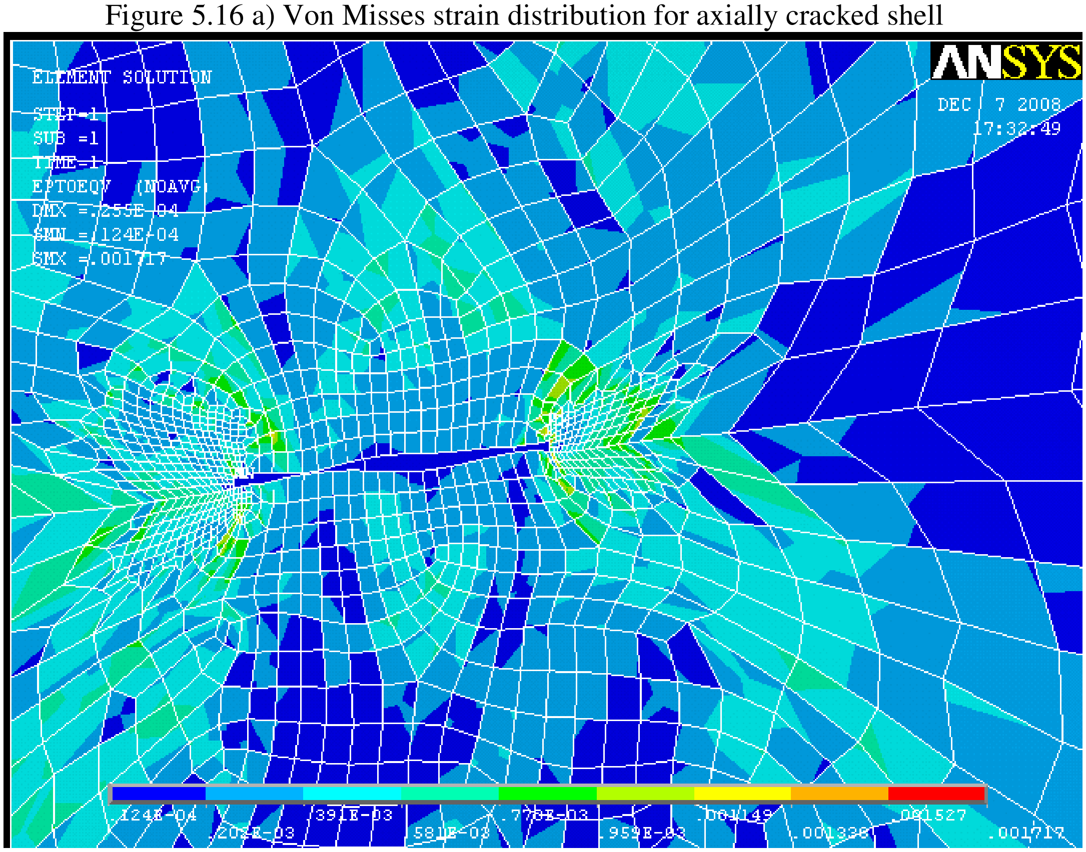

Figure 5.16 b) Full view of Von Misses strain distribution for axially cracked shell

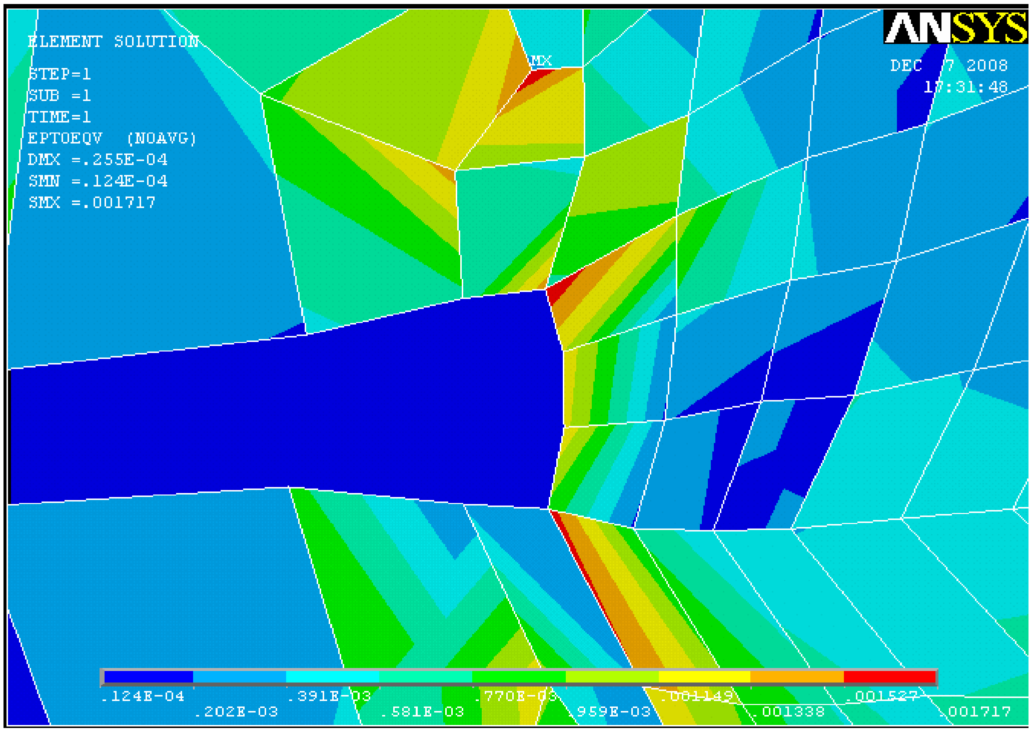

Figure 5.16 c) Magnified Von Misses strain distribution for axially cracked shell

According to figures 5.15 and 5.16, the sliding mode crack (mode II) also highlights the case of tendency of irregular undulation formation on the free edge of the cracked surface and somehow shielding of critically damaged zone that may be on the plane of crack advancement.

In order to conclude on the numerical stress analysis we postulate that crack chronology which will necessarily be an interpretation of the evolution of physical events. That means, we associate the thresholds of energy release rate first crack progress after initiation with the corresponding force level. On the basis of these simulated observations we propose the following chronology for the numerical appearance of crack versus time, whatever the stacking sequence. At F(t) equal to F_{yld} first cracks are initiated in the 0° layer farthest away from the crack tip. When F(t) reaches F_{ult} the 90° layer starts cracking. Hence, the first numerical condition for cracking is an initiation criterion involving transverse bending stress in the fibres and second shear stress, similarly to that found in the literature [27]. The crack (damage) initiation and evolution in the matrix could be modelled based on the yield and ultimate strength of the material respectively. The failure of the fibre was considered based on the maximum principal stress. The interface failure was taken in to account by cohesive zone debonding of the matrix material from the fiber. The interface between the fiber and matrix is simulated by using Cohesive Zone Model (CZM) is a fracture mechanics approach that is used to study the interfacial effects of either dissimilar material or in the same material when these are initially bonded together as indicated by Xu *et al.* [27].

The localized and shielded stress and strain distribution reveals how stress varies in the cracked composite cylindrical shell. Thus, the stress analysis in the vicinity of the crack tip in a composite cylindrical structure reveals the mode of variation that is caused by the combined effects of fiber-matrix debonding, fiber rupture, matrix cracking and delamination between the adjacent layers. Even though the mechanical characterization taking into account these different modes of failure is complex, the finite element analysis performed has given an insight of variation of stress and resistance to crack propagation of composite materials. However, it doesn't mean that the crack introduced as a narrow strip cutout on the simulated model is a perfect representation of the actual crack; rather it is an approximation of an ideal crack that has perfect tangential orientation.

CHAPTER SIX

CONCLUSION AND RECOMMENDATIONS

6.1 Conclusion

Methods and corresponding computer codes for probabilistically assessing composite structure fracture have been discussed. The fracture in composite structures was simulated via a finite package (ANSYS) approach independent of stress intensity factors and fracture toughness parameters. The approach described herein is inclusive in that it integrates composite mechanics (for composite behaviour) with finite-element analysis (for global structural response) and incorporates the assessment of stress analysis at the crack tip during composite structural fracture. Compared to Isotropic materials, Compared to traditional materials (like aluminium for which composites are substitutive), composites have higher resistance to fracture and have unpredicted stress distribution pattern as shown in figure 6.1 and 6.2. Furthermore, the crack tip contouring mode is different for both materials due to the difference in microstructural composition. However, the amount of deflection experienced is more for composites towards the cracked side. The sharp corner also here becomes the critical area for stress initiation. i.e., there is no shielding effect in case of isotropic materials.

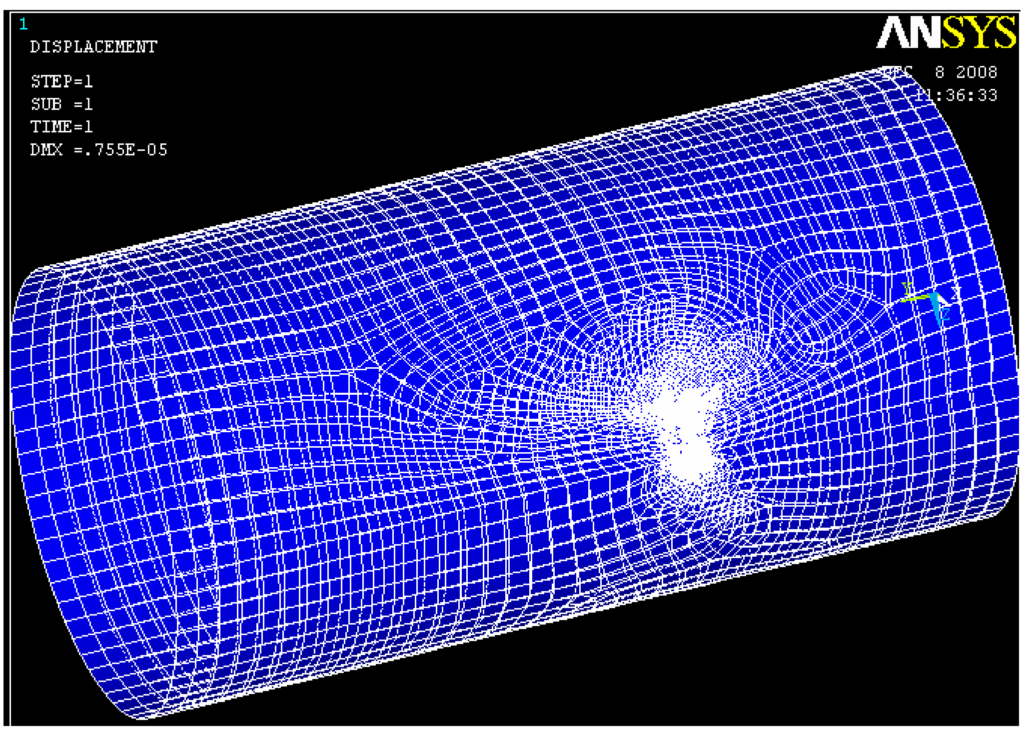

Figure 6.1 a) Axially deformed shape of isotropic cylindrical shell

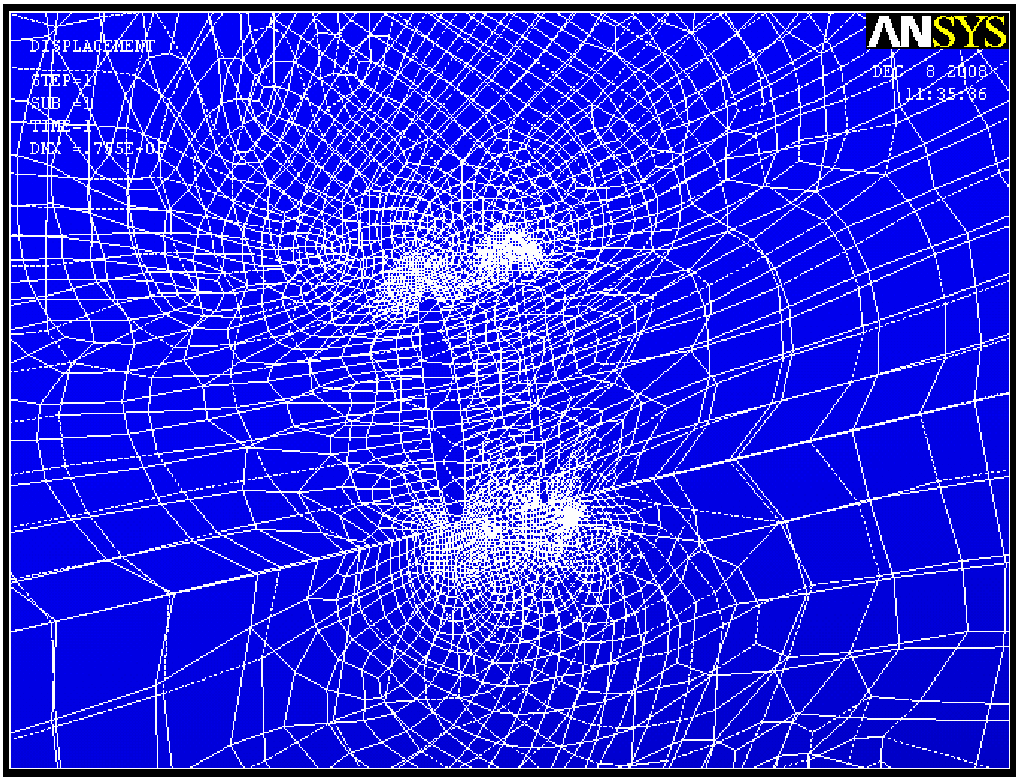

Figure 6.1 b) Deformed shape of isotropic cylindrical shell

Figure 6.1 c) Deformed shape of isotropic cylindrical shell towards crack side

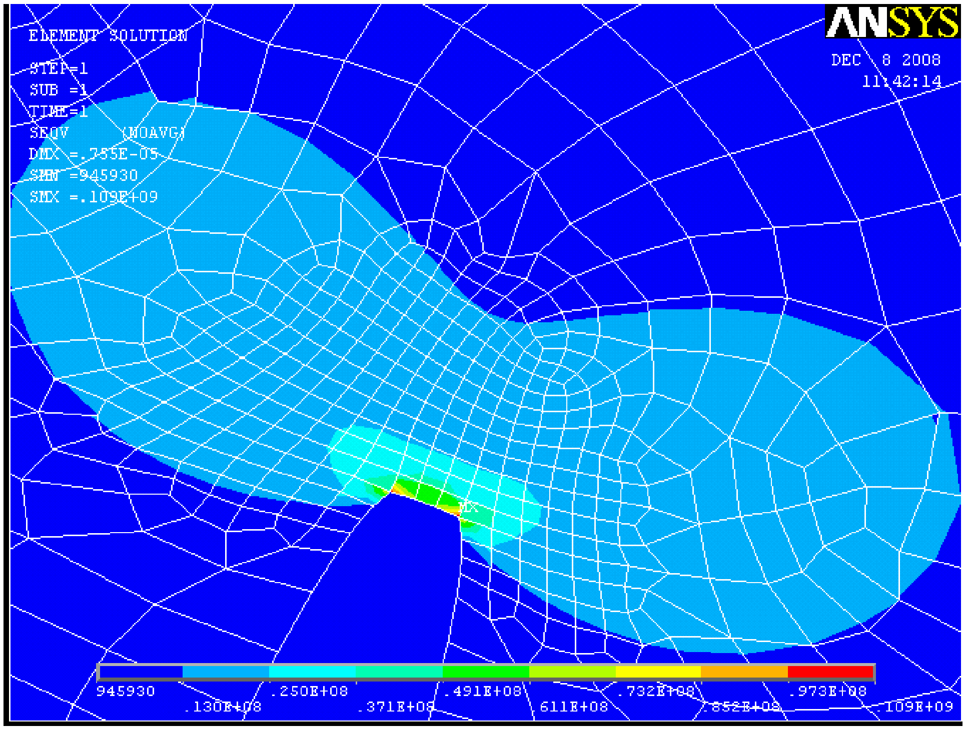

Figure 6.2 a) Von Misses total stress distribution at the crack tip in Isotropic shell

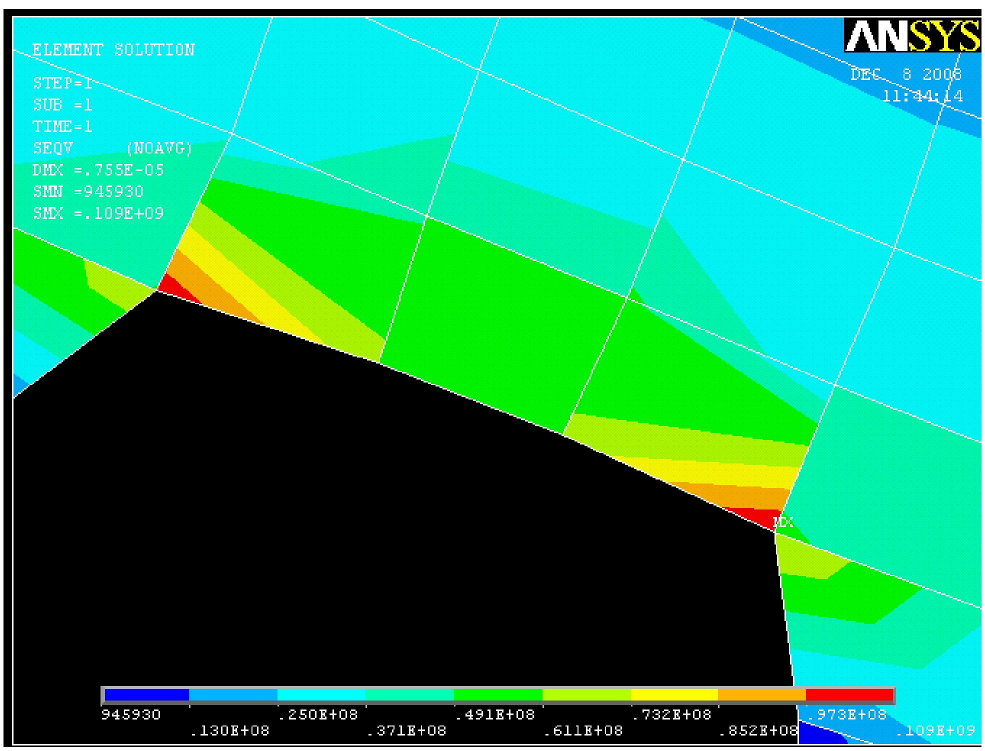

Figure 6.2 b) Magnified Von Misses total stress at the crack tip in isotropic shell

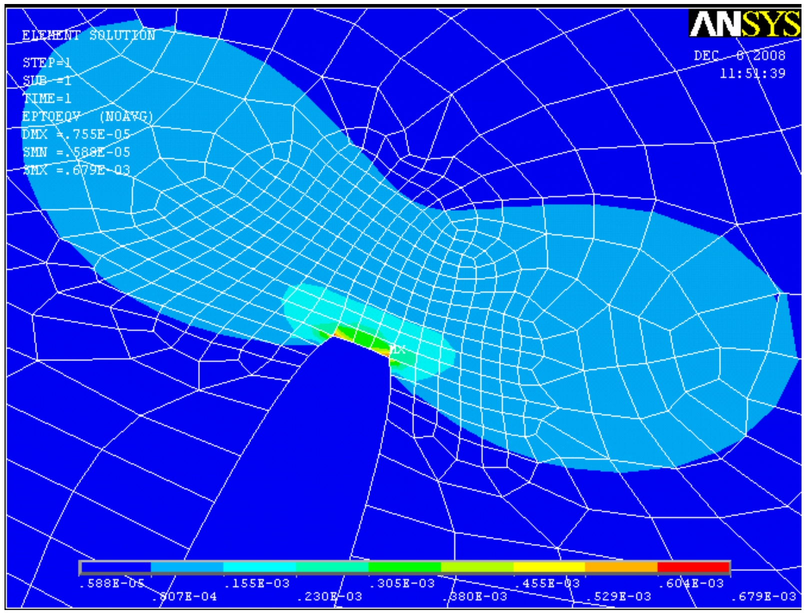

Figure 6.3 Von Misses total strain at the crack tip in isotropic material shell

Moreover, as described elsewhere in this paper, the composite shell structure revealed the advantages of higher specific strength and specific stiffness.

From the results obtained, the following conclusions may be drawn:

1. The composite shell structure has shown strong resistance to crack propagation due to matrix compression and fibre bending in the mode I fracture mechanism.
2. The Von Misses stress and strain distribution is observed at the crack tip with some shielding effect at the crack front.
3. The stress vector plot of the cracked shell subjected to tensile loading indicated shielded vectors at the crack front.
4. The axial stress applied on the fractured shell indicated is found to cause the evolution of the distributed shear stresses in the body of the structure with the critical regions at the sharp corners.
5. The mode of variation of the stress in the fractured composite shell may be used to device the mechanisms to control the load and ply thickness.
6. After damage initiates in the structure and load is applied, unbalanced internal loads are redistributed to the remaining plies and this causes deflection of the shell structure under loading to the cracked side.

7. The cumulative distribution for strain and stresses is most sensitive to the crack region and still composites show much more resistance to crack than isotropic materials due to the fibre blocking of the crack advance.
8. Composites materials have complex fracture behaviour characterization.

In general, this study shows the possible location of failure in the fibre, damage initiation and evolution in matrix material and interfacial debonding between the fibre and matrix. However, in comparison with the traditional materials, composite shell has shown very strong resistance to crack initiation and propagation. Hence, they are very suitable for structures that need very high curiosity of catastrophic failure.

6.2. Recommendation and Future Directions

The use of composites, advanced composites, in modern structural building is becoming predominantly important to assure the reliability of such structures which involve high risk and cost of fabrication. In this paper the stress analysis of composite shell structures with crack is presented by considering a cylindrical shell structure. However, in addition to material non linearity, there could be geometrical non-linearity, which makes the analysis more difficult. Thus, one of the feature continuations of this work could be extending it to geometrically non linear shell structures.

In the current paper the stress analysis is curried out using the finite element method by developing the solid model in ANSYS environment. However, the possibility of developing the stress analysis in the vicinity of the crack by the use of mathematical model of the problem is still what could be conducted ahead. Furthermore, the possibility to have analytical solutions to be compared with the finite element solution is also what should be done in the future.

In this work the crack is modelled as a very small trip cut out of the surface of the shell and the tip has significant variation from the naturally occurring crack. Hence, the researcher proposes the development of a better model in a more versatile software packages which could simulate the reality to be conducted as future work. To further check the reality of the cracked surface waviness, the use very capable software is prominent.

REFERENCES

1. Kaw, A., *Mechanics of Composite Materials*, CRC Press, 1997.
2. Marcel Dekker *Practical Fracture Mechanics in Design*, A series of text books and Reference books in the Ohio state university of Mechanical Engineering, Columbus, Ohio, 2005.
3. Perez, *Fracture Mechanics,* Kluwer Academic Publisher, New York, 2004.
4. Vasiliev, V. and Morozov, E., "*Mechanics and Analysis of Composite Materials"*, Elsevier Science, 2001.
5. Saouma, V. E., "Lecture Notes in Fracture Mechanics", University of Colorado, Boulder, 2000.
6. Xiao H.T., Yue Z.Q., Tham L.G., Lee C.F., "Analysis of Elliptical Cracks Perpendicular to the Interface of Two Joined Transversely Isotropic Solids", *International Journal of Fracture*, **133,** 329–354, 2005.
7. Shang Xin-chun, "An Exact Analysis for Free Vibration of a Composite Shell Structure Hermetic Capsule", *Applied Mathematics and Mechanics*, **22**(9), 1035-1045, 2001.
8. Mahdi, E., Hamouda, A. M.S., Sahari, B. B., Khalid, Y.A., "Effect of Material and Geometry on Crushing Behaviour of Laminated Conical Composite Shells", *Applied Composite Materials*, **9**, 265-290, 2002.
9. Sadd H.M. *Elasticity: Theory, applications, and Numerics*, USA, Elsvier Inc., 2005.
10. Mohammadi S., *Extended Finite Element Method for Fracture Analysis of Structures*, Blackwell, UK, 2008.
11. Pinskunov V.G., Rasskazov A.O., "Evolution of the Theory of Laminated Plates and Shells", *International Applied Mechanics*, **38**, 135-165, 2002.
12. Zenkour, A. M., "Stress Analysis of Axis Symmetric Shear Deformable Cross-Ply Laminated Circular Cylindrical Shells", *Journal of Engineering Mathematics*, **40**: 315-332, 2001.
13. Abrosimov, N. A., "Numerical Modeling of Non-Linear Deformation and Buckling of Composite Plate-Shell Structures Under Pulsed Loading", *Mechanics of Composite Materials*, **35** (6): 495-506, 1999.
14. Lee, Y. S, Lee, J. J, Kang, Y. K, Song, S. Y., "A study on the Structural Analysis of the Steel and GFRP Laminated Composite Cylindrical Shell with a Stiffened Cutout", *Key Engineering Materials,* ***326-328:*** 1837-1840, 2006.

15. Gerasimov, V. P., Gudramovich, V. S., Larionov, I. F., Mulyar, Y. M., Savvin, Y. I., “Ductile Fracture of composite Shells in Axial Compression”, *Institute of Mechanics,* **11**: 58-71, 1979.

16. Ukadgaonker, V.G. and Kakhandki, V., “Stress Analysis for an Orthotropic Plate with an Irregular Shaped Hole for Different In-plane Loading Conditions Part-1”, *Composite structures*, **70**: 255-274, 2005.

17. Folias, E.S., “The Stress Field in a [$0^{\circ}/90^{\circ}$] Laminated Composite Plate Containing a Finite Line Crack”, *International Journal of Fracture*, 114: 203-224, 2002.

18. Sekhar, A. S. and Srinivas, B. N., “Dynamics of Cracked Composite Shafts”, *Journal of Reinforced Plastics and Composites*, **22** (7), 637-653, 2003.

19. Theocaris, P. and Petrou, L., “Stress Distributions and Intensities at Corners of Equilateral Triangular Holes”, *International Journal of Fracture,* **31**: 271–289, 1986.

20. Daoust J. and Hoa S., “An Analytical Solution for Anisotropic Plates Containing Triangular Holes”, *Composite Structures*; **19**:107–130, 1991.

21. Rybicki E. and David S. “Effect of Stacking Sequence and Lay-up Angle on Free Edge Stresses Around a Hole in a Laminated Plate Under Tension”, *Journal of Composite Materials*, **12:**300–313, 1978.

22. Ozdil, F., Carlsson, L. A., Liv, X., ”Characterization of Mode II Delamination Growth in Glass/Epoxy Composite Cylinders”, *Journal of Composite Materials,* **34**, 274-298, 2000.

23. Sung, W., Go, C., Shih, M.,” Finite Element Modeling for Analysis of Cracked Cylindrical Pipes”, *Journal of Zhehiang University of Science A,* **8**, 1373-1379, 2007.

24. Yang J. and Fu Y. “Delamination Growth of Laminated Composite Cylindrical Shells”, Theoretical and Applied Mechanics, **45**:192-203, 2006.

25. Reddy, P.R. and Ramamurthy, G. “Stress-Intensity Factor Using Finite Element Analysis in Rectangular; Orthotropic Composite Annular Disk”, *Journal of Defense Science*, **47**: 55-63, 1978.

26. Collombet, F., Lalbin, X., Charles, J. L., Jeronimidis, G., Lataillade, J. L., “A methodology and Tools for the Study of Composite Structures Under Impact Loading: Application to Long Fiber Laminated Structures”, *Journal of Physics IV,* **3**: 163-168, 1997.

27. Xu, X. P. and Needleman A. “Numerical Simulations of Fast Crack Growth in Brittle Solids”, *Journal of Mechanical Physics of Solids*, **42**(9): 1397-1434, 1994.
28. Lee, D.S., “Nonlinear dynamic buckling of orthotropic cylindrical shells subjected to rapidly applied loads” *Journal of Engineering Mathematics* **38:** 141–154, 2000.
29. Charoenphan, S., Plesha, M. E., Bank, L. C, “Simulation of Crack Growth in Composite Material Shell Structures”, *International Journal for Numerical Methods in Engineering,* **60**:2399–2417, 2004.
30. Sohn, S.W., Kwon, D.A., Hong, S.H.,”A Study on Mode I Interlaminar Fracture Toughness of Foam Core Sandwich Structures”, *International Journal of the Korean Society of Precision Engineering,* **2**:47-53, 2001.